ISSN 1408-7073

RMZ – MATERIALS AND GEOENVIRONMENT

PERIODICAL FOR MINING, METALLURGY AND GEOLOGY

RMZ – MATERIALI IN GEOOKOLJE

REVIJA ZA RUDARSTVO, METALURGIJO IN GEOLOGIJO

RMZ-M&G, Vol. 56, No. 2 pp. 108–253 (2009)

Ljubljana, June 2009

Historical Review

More than 80 years have passed since in 1919 the University Ljubljana in Slovenia was founded. Technical fields were joint in the School of Engineering that included the Geologic and Mining Division while the Metallurgy Division was established in 1939 only. Today the Departments of Geology, Mining and Geotechnology, Materials and Metallurgy are part of the Faculty of Natural Sciences and Engineering, University of Ljubljana.

Before War II the members of the Mining Section together with the Association of Yugoslav Mining and Metallurgy Engineers began to publish the summaries of their research and studies in their technical periodical Rudarski zbornik (Mining Proceedings). Three volumes of Rudarski zbornik (1937, 1938 and 1939) were published. The War interrupted the publication and not until 1952 the first number of the new journal Rudarsko-metalurški zbornik - RMZ (Mining and Metallurgy Quarterly) has been published by the Division of Mining and Metallurgy, University of Ljubljana. Later the journal has been regularly published quarterly by the Departments of Geology, Mining and Geotechnology, Materials and Metallurgy, and the Institute for Mining, Geotechnology and Environment.

On the meeting of the Advisory and the Editorial Board on May 22nd 1998 Rudarsko-metalurški zbornik has been renamed into "RMZ - Materials and Geoenvironment (RMZ -Materiali in Geookolje)" or shortly RMZ - M&G.

RMZ - M&G is managed by an international advisory and editorial board and is exchanged with other world-known periodicals. All the papers are reviewed by the corresponding professionals and experts.

RMZ - M&G is the only scientific and professional periodical in Slovenia, which is published in the same form nearly 50 years. It incorporates the scientific and professional topics in geology, mining, and geotechnology, in materials and in metallurgy.

The wide range of topics inside the geosciences are welcome to be published in the RMZ -Materials and Geoenvironment. Research results in geology, hydrogeology, mining, geotechnology, materials, metallurgy, natural and antropogenic pollution of environment, biogeochemistry are proposed fields of work which the journal will handle. RMZ - M&G is co-issued and co-financed by the Faculty of Natural Sciences and Engineering Ljubljana, and the Institute for Mining, Geotechnology and Environment Ljubljana. In addition it is financially supported also by the Ministry of Higher Education, Science and Technology of Republic of Slovenia.

Editor in chief

Table of Contents – Kazalo

Original Scientific Papers – Izvirni znanstveni članki

Professional Papers – Strokovni članki

Short Papers – Kratki članki

Hardenability prediction based on chemical composition of steel

Napovedovanje prekaljivosti na osnovi kemične sestave jekla

Matjaž Knap[1,*], Jan Falkus[2], Alojz Rozman[3], Jakob Lamut[1]

[1]University of Ljubljana, Faculty of Natural Science and Engineering, Department of Materials and Metallurgy, Aškerčeva 12, SI-1000 Ljubljana, Slovenia
[2]AGH University of Science and Technology, Faculty of Metals Engineering and Industrial Computer Science, Krakow, Poland
[3]Metal Ravne, d. o. o., Ravne na Koroškem, Slovenia

*Corresponding author. E-mail: matjaz.knap@ntf.uni-lj.si

Received: March 26, 2009 **Accepted:** April 22, 2009

Abstract: With use of neural networks the influence of chemical composition of steel on the hardness i.e. hardenability was determined. The chemical composition has varied within for the specified steel prescribed tolerances.
The modeling of influence of chemical composition on Jominy curve was made for three steel grades or steel groups respectively.

Izvleček: Z nevronskimi mrežami smo modelirali vpliv spreminjanja kemične sestave jekla na njegovo trdoto oz. prekaljivost. Kemična sestava se giblje v za določeno jeklo predpisanih tolerancah.
Vpliv spreminjanja kemične sestave na prekaljivost smo modelirali za tri vrste oz. skupine jekel.

Keywords: modeling, neural networks, hardenability, Jominy test
Ključne besede: modeliranje, nevronske mreže, prekaljivost, preizkus Jominy

Introduction

Steel is by production among metals by far in the first place in the world. This is due to its mechanical, physical, chemical and other properties that meet the user's demands in a wide area. One of the parameters affecting the properties of steel is also its chemical composition. For chosen steel grade it is deter-

Original scientific paper

mined with tolerance limits.

Idea to use neural networks for modeling the influence of chemical composition on Jominy curves (hardenability) is not new. VERMEULEN et al.[1] demonstrated that Jominy curve can be modeled if chemical composition of steel is known. They also presented how the neural network parameters influenced the quality of predictions. DOBRZANSKY et al. have published their results from neural network modeling of hardenability[2, 3]. They investigations were focused on constructional steels. Results of their work gave eloquent proof that modeling of Jominy curves on the basis of chemical composition give good results. For mentioned models, i.e. data base, typically relatively small variances in chemical composition occur.

Our department has rich experiences with applying neural networks[4, 5] also with various predictions on basis of chemical composition[6–8].

First results of our Jominy curves modeling on the basis of chemical composition of steel were good[9].

In this study we focused on modeling of hardenability of various steels. Variances in chemical composition within data base were bigger then we found in literature[10].

MATERIALS AND METHODS

Three steel grades were used in the process of hardenability modeling: VCNMO 150, CT207 and 42CrMoS4.

VCNMO150 is a heat treatable, low alloy steel containing nickel, chromium and molybdenum[10]. Steel CT207 is used for highly stressed hardened dies for artificial resin[10]. Steel 42CrMoS4 is used for high and moderately stressed components for automobile industry and mechanical engineering[10]. Typical chemical compositions are presented in Table 1.

Table 1. Typical chemical composition of VCNMO 150, CT207 and 42CrMoS4 in mass fractions, *w*/% [10]

	C	Si	Mn	Cr	Mo	Ni	V	W	others
VCNMO150	0.34	max. 0.40	0.65	1.50	0.23	1.50	-	-	-
CT207	0.21	0.28	0.75	0.85	0.20	1.35	-	-	Cu < 0.25 Al < 0.035
42CrMoS4	0.41	max. 0.40	0.75	1.05	0.28	-	-	-	-

Experimental part

The Jominy test samples have length of 102 mm and a diameter of 25.4 mm. To exclude differences in microstructures due to the preliminary forging, before testing samples were normalized and later austenitised. Austenitising temperature is usually between 800 ºC and 900 ºC. The samples were quickly transferred to the device Jominy where frontend was cooled with controlled jets of water. Cooling the sample from one end simulates the effect of forging of bigger components in the water. After forging and cooling the samples were cleaned. The hardness measurements were made at prescribed intervals along the test samples from the quenched end. The Jominy curves were presented as a function of measured hardness (*HRc*) vs. distance from the quenched end.

Collecting of data base

A database was constructed from measurements of hardness at different distances from cooled surface. The database has contained nearly 20,000 measurements (exactly 19469), but they were not evenly distributed regard to the distance from the surface, as is shown in Figure 1. It can be seen that the maximum number of measurements were carried out up to a distance of 20 mm (about 60 %), as well as can be seen that the number of measurements at a distance greater than 50 mm is negligible (less than 2 %).

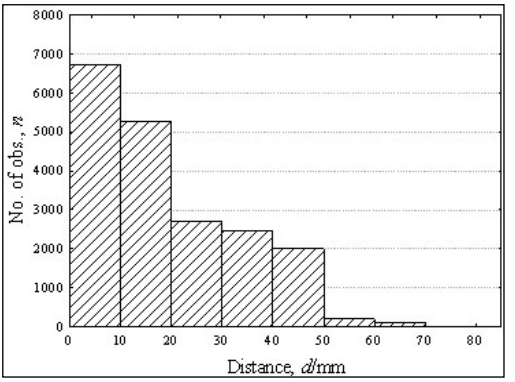

Figure 1. Distribution of measurements regard to the distance from cooled surface

Various steel groups (special steel, alloyed carbon steel and unalloyed carbon steel) were included in data base. It consists of about 50 different steel grades. Less than 10 of them contain more than 10 charges (chemical compositions), about half of them have fewer than 5 entries.

For each of the hardness measurements the chemical composition (25 elements) and distance from the forged surface was attached. These 27 figures formed the so called data vector. The whole database was presented in a matrix consisting of 19,469 lines and 27 columns. From complete data base 11 elements were used for modeling. The selection procedure is presented later. The variations in amount of elements are shown in Figure 2.

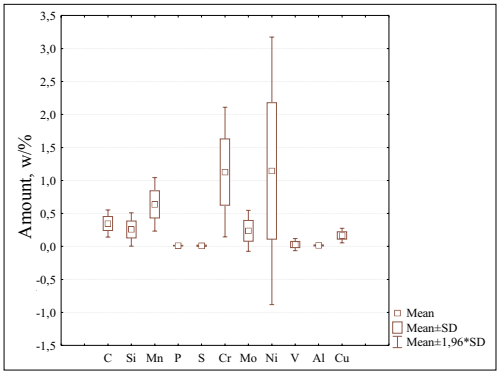

Figure 2. The amount of variation of particular element

Data was randomly divided into training, verification and test data base in the ordinary 2 : 1 : 1 proportion (9735 + 4867 + 4867 model vectors). The distribution in the three groups was automatic and random. The authenticity of the databases is guaranteed, what can be seen from a comparison of correlation coefficients (Table 2).

Table 2. Correlation coefficients for developed neural network model

	training	test	verification
Correlation coefficient	0.9526	0.9424	0.9421

Applied type of neural network

Program Statistica was used for modeling. On the base of our good experiences from previous work[9] multilayer perceptrons type neural network (MLP NN) was used. To obtain good quality of predictions 12 input and 12 neurons in hidden layer were used. Because only one output parameter was calculated also the neural network with one output neuron was applied.

The correlation coefficients for training, test and validation data base are presented in Table **2**. From comparison of those results it can be deducted that applied model is capable to accurate predict the output values and also that overtraining did not occur.

In the process of model development the sensitivity analysis was performed with special module within the program. Based on this analysis we decided that, in addition to distance, only 11 chemical elements will be used. These elements have been found as parameters with maximum correlation with the hardness. Correlation factors of the input parameters are given in Table **3**. The *p* factor indicates the amount of influence and *rang* is classification according to the importance of influence parameters.

Table 3. Factors of influence of the input parameters

	dis.	C	Si	Mn	P	S	Cr	Mo	Ni	V	Al	Cu
p	5.19	6.55	0.08	1.94	1.01	1.05	2.84	1.96	4.60	1.28	1.11	1.06
rang	2	1	9	6	12	11	4	5	3	7	8	10

Results and discussion

Before modeling of the hardness profile basic statistic evaluations of predictions for whole data base were made and results are collected in Table 4 and Table 5.

In those two tables it can be seen that we can expect hardness prediction error smaller than $HRc = 2$. It is also clear that a tiny part of data base cannot fit into developed model.

Table 4. Basic statistic parameters for the absolute error of predictions

No. of predictions	19469
Mean	1.867
Median	1.169
Min.	0.00004
Max.	38.990
25^{th} %	0.529
75^{th} %	2.207

Table 5. Frequency table of absolute error distribution

Range	Cumulative %
0–1	43.96
0–2	71.23
0–5	94.33
0–10	98.20

The results for hardness predictions for three most important chemical elements (Table **3**) – carbon, nickel and chromium are presented on Figure 3, Figure 4 and Figure 5. From higher and lower density of markers on these diagrams is evident that input data was not homogeneously distributed. Also less accurate predictions in boundary areas with no or little records in data base can be observed on these pictures.

Data base contains steel grades with the same amount of carbon but different amount of alloying elements and thus big variances in hardness value. This confirms our hypothesis that more than two input parameters must be taking into consideration if good enough predictions want to be achieved.

Nevertheless, from the pictures it can be seen the general law: carbon increase the hardness of steel and with growing distance from the quenched surface the hardness decreases. This is in agreement with results from literature[2, 3]. On Figure 4 the nickel content influence is presented with surface in the 3D graph. It can be seen that for lower nickel contents the influence of distance from quench surface is noticeable, but at higher nickel values stays almost the same.

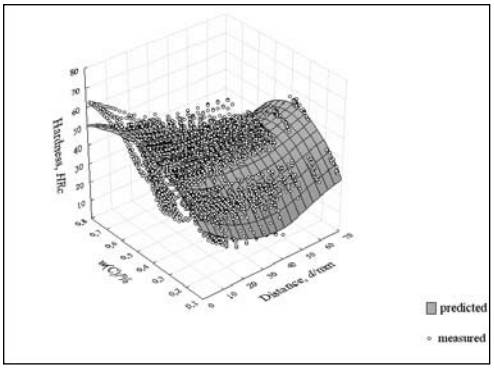

Figure 3. Dependence of hardness (measured – markers and predicted – area) upon amount of carbon and distance

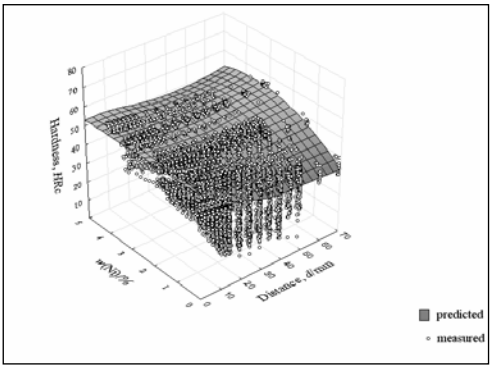

Figure 4. Dependence of hardness (measured – markers and predicted – area) upon amount of nickel and distance

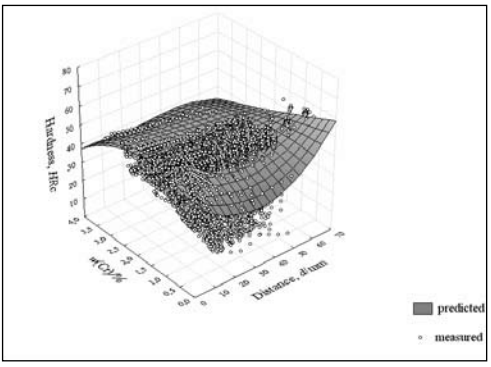

Figure 5. Dependence of hardness (measured – markers and predicted – area) upon amount of chromium and distance

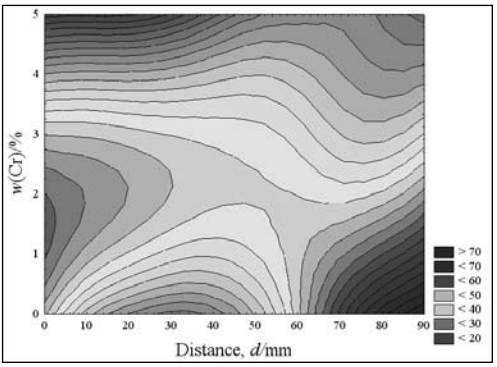

Figure 6. Results from hardness measurements dependent on amount of chromium and distance

On Figure 5 the influence of chromium is presented. It can be seen that the hardness at lower chromium contents near the quenched end decrease with the distance. But at bigger distances from cooled surface even slight increase in hardness can be observed. These unexpected results are due to lack of data but in the agreement with measurements Figure 6. At higher chromium contents the expected drop in hardness at larger distances can be observed.

Effects of charge in chemical composition – variances within one steel grade were studied on case of most influential parameter – carbon.

Table 6. Chemical composition of two VCNMO150 steel samples in mass fractions, *w*/%

	C	Si	Mn	P	Cr	Al	Ni	Mo	Cu
C_{low}	0.320	0.235	0.595	0.013	0.960	0.012	1.485	0.165	0.110
C_{high}	0.430	0.290	0.690	0.021	1.530	0.015	1.720	0.230	0.210

Low alloy steel VCNMO150

For these steel grade 323 different chemical compositions (charges) out of 1508 were used for calculation, what is more than of 1/5 of whole data base. Note; for each chemical composition data up to 15 hardness measurements on different distances from surface is included in data base.

Two chemical compositions used in the process of hardenability prediction are shown in Table 6.

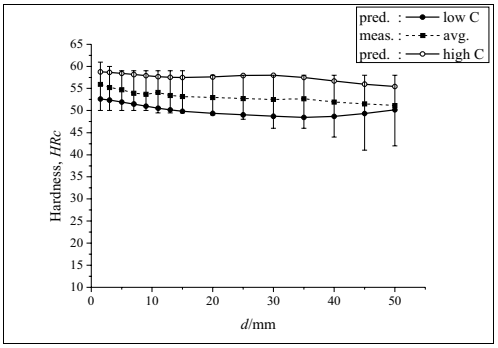

Figure 7. Measured and predicted hardness profile for steel grade VCNMO150

On Figure 7 variations in hardness profile are shown. Both full lines present hardness predictions, one for the sample with high carbon content (white circles) and other predictions for the sample with low carbon (black circles).

Good criteria for variations in measured hardness are points with error bars placed along thin dashed line. They present average value of all measurements at particular distance. The variations of measured hardness at chosen distance were more or less constant on the whole measured area.

From Figure 7 is obvious that effect of chemical composition variations on hardenability for this steel grade can be predicted. Evidently the predicted hardness and trend of hardenability are in good correlation with the results from Jominy test measurements. Differentiation between sample with low and high carbon content and accurate prediction is in this case possible due to broad and accurate data base.

Special structural steel CT207

Data base for CT207 is not comprehensive – it contains only 61 different chemical compositions (charges) out of 1508.

Two chemical compositions for steel grade CT207 with carbon content on upper and bottom border were used for prediction (Table 7). From error bars presented on Figure 8 big differences in measured data can be noticed. On the other hand increase in hardness at distances over 30 mm can be noticed – the line which represents average value of all measurements.

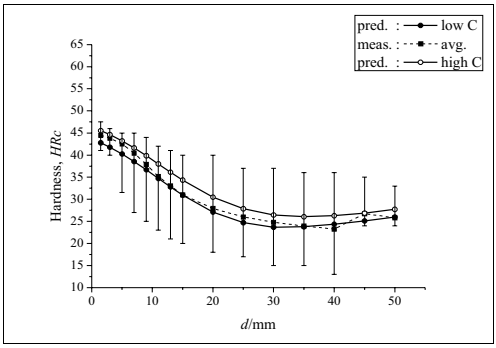

Figure 8. Measured and predicted hardness profile for steel grade CT207

From Figure 8 it is obvious that effect of chemical composition differences on hardenability for steel grade CT207 can be only roughly predicted. Differences in measured hardness are too big and thus generalization occurs. In spite of all that trend of hardenability is in good correlation; also increase in hardness can be predicted.

Special structural steel 42CrMoS4

Data base for 42CrMoS4 is also small – it contains only 66 different charges, what is a little more than 4 % of whole data base. Predictions of hardness profile after Jominy test were made for two test samples with different chemical compositions; one with low and other with high carbon content (Table 8).

Table 7. Chemical composition of two CT207 steel samples in mass fractions, *w*/%

	C	Si	Mn	P	Cr	Al	Ni	Mo	Cu
C_{low}	0.160	0.240	0.580	0.011	0.570	0.017	1.650	0.210	0.150
C_{high}	0.210	0.260	0.610	0.015	0.660	0.027	1.680	0.220	0.220

Table 8. Chemical composition of two 42CrMoS4 steel samples in mass fractions, *w*/%

	C	Si	Mn	P	Cr	Al	Ni	Mo	Cu
C_{low}	0.390	0.230	0.670	0.018	1.080	0.015	0.090	0.180	0.200
C_{high}	0.440	0.280	0.720	0.029	1.140	0.030	0.130	0.230	0.230

Variations in measured hardness near surface are small compared with those measured farther toward specimen center (Figure 9). Near sample surface the measured differences can be practically neglect (*HRc* < 5). At distances 20 mm or more those variations can be almost *HRc* = 20.

It is obvious that such big change in variations cannot be modeled very accurate with the model which was developed for whole data base. In our opinion the predictions which were made for steel grade 42CrMoS_4 can be described as successful. The differences in hardness profile for different steel chemical composition can be observed.

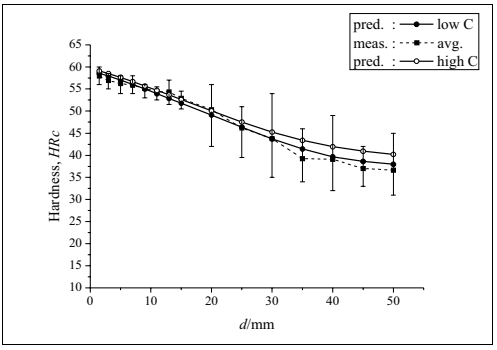

Figure 9. Measured and predicted hardness profile for steel grade 42CrMoS4

Conclusions

It was successfully proved that neural networks are capable to make good and on narrow region focused predictions. In our case even if large and heterogeneous data base was implemented.

If "necessary conditions" are fulfilled very accurate modeling of influences in chemical composition within one steel grade on hardness and hardenability can be made. The "necessary conditions" are: data base must have sufficient data vectors and they have to be representative data for treated steel grade. In the case of VCNMO150 this conditions were completely fulfilled and influence of carbon content on hardenability was successfully demonstrated.

Also for steel grades which have a lesser amount of data modeling of chemical composition influence on hardness can be made. The results are not as accurate but basic law can be deduced. For those steel grades the carbon content influence on the hardness was qualitative successfully predicted; quantitative predictions were less accurate. Basic hardness profile or average value was of course successfully modeled for all the predictions which were made during this research.

References

[1] Vermeulen, W. G. et al. (1996): Prediction of Jominy hardness pro-

files of steels using artificial neural networks. *Journal of Materials Engineering and Performance*; Vol. 5(1), p. 57–63.

[2] Dobrzański, L. A., Sitek, W. (1998): Application of a neural network in modeling of hardenability of constructional steels. *Journal of Materials Processing Technology*; Vol. 78, p. 59–66.

[3] Dobrzański, L. A., Sitek, W. (1999): The modelling of hardenability using neural networks. *Journal of Materials Procesing Technology*; Vol. 93, p. 8–14.

[4] Terčelj, M., Peruš, I., Turk. R. (2003): Suitability of CAE neural networks and FEM for prediction of wear on die radii in hot forging. *Tribology International*; p. 573–583.

[5] Knap, M., Kugler, G., Palkowski, H., Turk, R. (2004): Prediction of material spreading in hot open-die forging. *Steel Research*; Vol. 75, No. 6, p. 405–410.

[6] Turk, R., Peruš, I., Terčelj, M. (2004): New starting points for the prediction of tool wear in hot forging. *International Journal of Machine Tools and Manufacture*; Vol. 44, p. 1319–1331.

[7] Večko Pirtovšek, T., Fazarinc, M., Kugler, G., Terčelj, M. (2008): Increasing of hot deformability of tool steels : preliminary results = Povečanje vroče preoblikovalnosti orodnih jekel : preliminarni rezultati. *RMZ-Materials and Geoenvironment*; Vol. 55, p. 147–162.

[8] Večko pirtovšek, T., Peruš, I., Kugler, G., Terčelj, M. (2009): Towards Improved Reliability of the Analysis of Factors. *ISIJ International*; Vol. 49, No. 3, p. 395–401.

[9] Knap, M., Falkus, J., Rozman, A., Lamut, J. (2008): The prediction of Hardenability using neural networks. *Archives of Metallurgy and Materials*; Vol. 53, No. 3, p. 509–514.

[10] Metal Ravne Steel Selector [online]. Metal Ravne, 5. 1. 2009, [citated: 10. 3. 2009.] http://www.metalravne.com/selector/selector.html.

Waste mould sand-potential low-cost sorbent for nickel and chromium ions from aqueous solution

Potencialni nizkocenovni sorbent za nikljeve in kromove ione iz vodne raztopine odpadnega formarskega peska

Anita Štrkalj[1,*], Jadranka Malina[1], Ankica Rađenović[1]

[1]University of Zagreb, Faculty of Metallurgy, Aleja narodnih heroja 3, 44 000 Sisak, Croatia

*Corresponding author. E-mail: strkalj@simet.hr

Received: January 20, 2009 **Accepted:** February 25, 2009

Abstract: In the present work investigated the sorption of the metal ions on waste mould sand, which is solid residue of gray iron foundry industry. Waste mould sand can be used as a new sorption material for removing some toxic metals from aqueous solution. The system variables studied include initial concentration of Ni(II) and Cr(VI) ions and agitation time. Metal ion sorption was strongly dependent on initial concentration and agitation time. The experimental data fitted well to the Freundlich and Langmuire isotherms.

Izvleček: V članku je raziskana absorpcija kovinskih ionov v odpadnem formarskem pesku, ki je odpadek v livarnah sive litine. Ta odpadni pesek je lahko uporaben kot absorpcijski material za odstranjevanje nekaterih strupenih kovin iz vodne raztopine. Kot preiskane neznanke iz sistema so vključene tudi začetne koncentracije ionov Ni(II) in Cr(VI) in čas mešanja. Absorpcija kovinskih ionov je bila močno odvisna od začetne koncentracije in časa mešanja. Pridobljeni eksperimentalni rezultati se dobro ujemajo s Freundlichovimi in Langmuirovimi izotermami.

Key words: waste mould sand, sorption, nickel ions, chromium ions
Ključne besede: odpadni formarski pesek, sorbcija, nikljevi ioni, kromovi ioni

Original scientific paper

Introduction

People are currently exposed to the hazards of various kinds of metal pollution in wastewater and drinking water. Pollution has a harmful effect on biological systems. Therefore, the elimination of toxic metals from aqueous solutions is important for protection of public health. Heavy metals (Pb, Hg, Cd, Cr, Ni, As, etc.) are very toxic and do not undergo biodegradation[1].

Chromium, which is on the top priority list of toxic pollutants, is present in the electro-plating, metallurgy, and chemical engineering wastewater as Cr(VI) in the form of oxides species, such as chromates (CrO_4^{2-}) and dichromate ($Cr_2O_7^{2}$)[2]. Due to its high solubility, Cr(VI) is the most hazardous, since it can accumulate in the food chain and cause several ailments[3, 4].

Nickel is also a common toxic pollutant. Acute nickel poisoning by inhalation exposure or ingestion of nickel carbonyl or soluble nickel compounds can lead to headache, vertigo, nausea, vomiting, nephrotoxic effects, and pneumonia followed by pulmonary fibrosis [5].

Nickel ions are frequently encountered together in industrial wastewaters (e.g. from mine drainage, plating plants, paint and ink formulation units, porcelain and metal enamellings)[6].

The stricter environmental regulations related to the discharge of heavy metals make it necessary to develop efficient processes for Ni(II) and Cr(VI) ions removal from wastewater. Removal of hazardous metal ions especially in low concentrations from industrial effluent is of great interest due to the large quantity of material processed[7]. The main techniques that have been used for remove heavy metals from water include chemical precipitation, membrane filtration, ion exchange, and sorption on activated carbon[8–13]. However, these methods have limitations such as high operational cost in the case of sorption by activated carbon. Intensive studies have therefore been carried out to develop more effective and inexpensive metal sorbents[14]. Natural materials which are available from industrial waste products or agricultural operations can be used as potential inexpensive sorbents[15].

In foundry industry, millions tones of spent materials are disposed in the world[16]. Over 70 % of the amount of the dumped waste materials consists of sands. For many years, the spent sands generated by foundry industry were successfully used as landfill materials. But disposal by landfill of spent sands is becoming an increasing problem as legislation is getting tighter. Also the disposal costs by current practices increases rapidly[17]. This waste mould sand is composed of fine silica sand,

clay binder, organic carbon, and residual iron particles. Because of their potential sorptive properties, waste mould sand can using as a low cost sorbent[18]. In this work, waste mould sand, was studied as non-conventional and low-cost sorbent for nickel and chromium ions from aqueous solution.

Materials and methods

Waste mould sand which is solid residue from gray iron foundry production was used as sorbent.

For analysis, a representative sample of waste mould sand was obtained by a quartering technique. It was dried at 105 °C for 4 h. The chemical composition of the sample was determined by atomic adsorption spectroscopy AA-6800, Shimadzu. Mineralogical composition was determined by XRD method using a Philips PW 1830.

Batch experiments were performed in order to evaluatie the rate of Ni(II) and Cr(VI) removal in the presence of waste mould sand under different initial Ni(II) and Cr(VI) concentrations. One gram of waste mould sand was placed in contact with 50 mL solutions of different concentrations of the aqueous Ni(II) and Cr(VI) solution for a period of (0.5; 1; 1.5; 2 and 3) h on mechanical shaker. The concentration of free Ni(II) and Cr(VI) ions after sorption was determined spectrophotometrically (model Camspec M-107) using standard procedure[19].

The mass of metal ions solute sorbed per 1 g of sorbent, sorption capacity (q/(mg/g)) was calculated using equation (1):

$$q = \frac{\Delta c}{m} \cdot V \tag{1}$$

where is:
Δc – mass concentration of metal ions, mg/L
V - volume of solution, L
m - sorbent mass, g

The Langmuir and Freundlich isotherms are used to interpret sorption equilibrium data[20]. Their equations are commonly used for describing different sorption systems. The linear equation of Langmuir and Freundlich are represented as follows (equations (2) and (3), respectively):

$$\frac{1}{q_e} = \frac{1}{K_L \cdot q_m \cdot c_e} + \frac{1}{q_m} \tag{2}$$

where is:
q_e - the mass of metal ions solute sorbed per 1 g of sorbent, sorption capacity, mg/g
c_e - the equilibrium concentration of metal ions, mg/L
q_m - saturation sorption capacity of the waste mould sand, mg/g
K_L - Langmuir constant

$$\ln q_e = K_F + \frac{1}{n} \ln c_e \quad (3)$$

where is:
q_e - the mass of metal ions solute sorbed per 1 g of sorbent, sorption capacity, mg/g
c_e – the equilibrium concentrations of metal ions, mg/L
K_F and n - Freundlich constants

The free energy of sorption ($\Delta G°$) can be related to the equilibrium constants K_L/(L/mg) corresponding to the reciprocal of the Langmuir constant q_m, by the van't Hoff equation:

$$\Delta G° = -RTlnK_L \quad (4)$$

The removal efficiency (E, %) was calculated using the following relation:

$$E = \frac{c_0 - c_e}{c_e} \cdot 100 \quad (5)$$

where is:
c_0 – the initial concentrations of metal ions, mg/L
c_e – the equilibrium concentrations of metal ions, mg/L

Results and discussion

Characterization of the waste mould sand

Table 1 and Figure 1 present chemical and mineralogical composition of examined waste mould sand. The waste mould sand is dominated by the mass fraction of SiO_2 (96.1 %).

Table 1. Chemical composition of waste mould sand

Composition	w/%
SiO_2	96.1
Fe	2.57
Al_2O_3	0.85
Ca	0.31
C	0.12
Mg	0.03
Cr	0.009
Mn	0.008

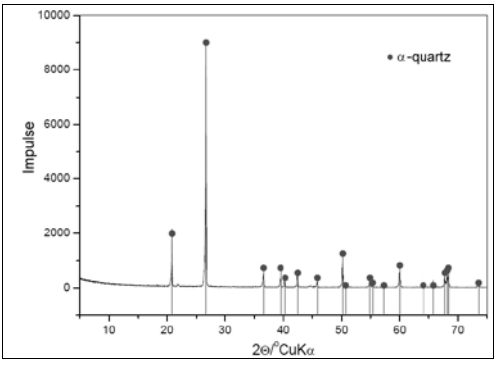

Figure 1. XRD difractogram analysis of waste mould sand

Effect of contact time

The effect of contact time on the uptake of Ni(II) and Cr(VI) ions was studied in single solutions using differential concentrations ((50, 100, 200, 300 and 500) mg/L). The results obtained can be presented as curves $q = f(t)$. Their char-

acteristic form is shown in Figure 2 for initial concentration of 300 mg/L.

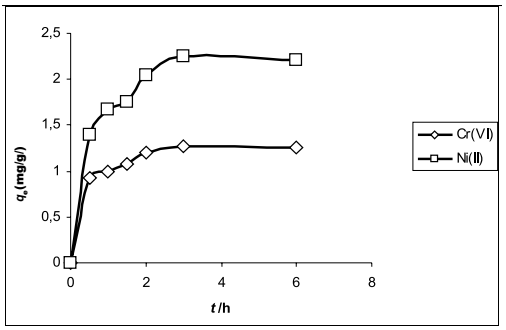

Figure 2. Adsorption capacity, q_e versus contact time for an initial concentration of 300 mg/L

The results show that the removal process was rapid and the equilibrium agitation time for the sorption of Ni(II) and Cr(VI) is 3 h. Such results can be related by theory from which: a) diffusion across the liquid film surrounding the solid particles, b) diffusion within the particle itself assuming a pore diffusion mechanism, and c) physical or chemical sorption at a site[21].

Effect of initial concentration

The effect of initial concentration of Ni(II) and Cr(VI) is shown in Figure 3. Results from this plot indicate that removal efficiency *E* decreases from 18.2 % to 9.4 % for Ni(II) and from 9.6 % to 4.6 % for Cr(VI) as the initial concentration is increased from 50–500 mg/L.

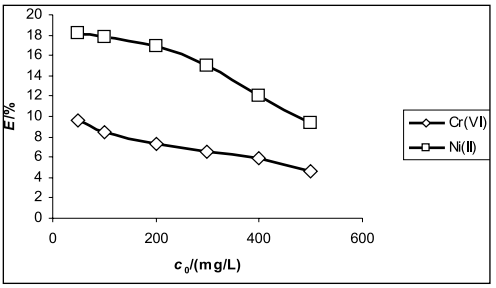

Figure 3. Influence of initial concentration of Ni(II) and Cr(VI) on the fraction of removal metal ions

The percentage of sorption metal ions to the waste mould sand decreased as the initial concentration of metal ions was increased from 50 mg/L to 500 mg/L. This appears to be due to increase in the number of ions competing for the available binding sites in the sorbent.

Sorption isotherms

The sorption isotherms are regular, positive, and concave to the concentration axis. Initial sorption is quite rapid, which is followed by a slow approach to equilibrium at higher metal ion concentrations (Figure 4).

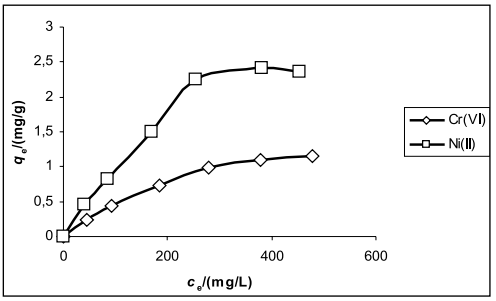

Figure 4. Adsorption capacity, q_e versus equilibrium concentrations of Ni(II) and Cr(VI) ions

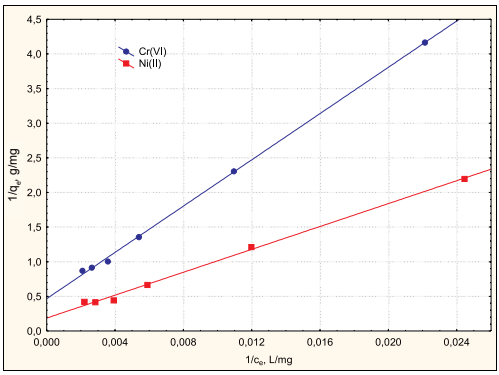

Figure 5. Langmuire isotherms for sorption of Ni(II) and Cr(VI) on 20 °C

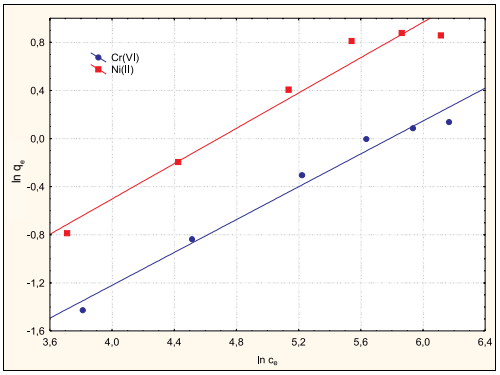

Figure 6. Freundlich isotherms for sorption of Ni(II) and Cr(VI) on 20 °C

Table 2. The values of Langmuir and Freundlich constants and correlation coefficients

	LAI				FAI		
	K_L/(L/mg)	q_m/(mg/g)	R^2	$-\Delta G$/(kJ/mol)	K_F	$1/n$	R^2
Ni(II)	$2.266 \cdot 10^{-3}$	5.340	0.9982	14.83	$32.055 \cdot 10^{-3}$	1.360	0.9651
Cr(VI)	$2.796 \cdot 10^{-3}$	2.141	0.9996	14.32	$19.197 \cdot 10^{-3}$	1.464	0.9899

Figures 5 and 6 show the Langmuire and Freundlich sorption isotherms for Ni(II) and Cr(VI) sorption on waste mould sand. The values of Langmuir and Freundlich constants and correlation coefficients were determined and are shown in Table 2.

The correlation coefficients (R^2) values (Table 2) indicate that, generally, experimental data were better fitted to the Langmuir equation. Langmuir's isotherm model is valid for monolayer sorption onto the homogenous sorbent surface. Once a sorbate molecule occupies a site, no further sorption can take place at that site. The Freundlich expression is an empirical based on sorption on a heterogenous surface[22]. Negative values of $\Delta G°$ indicating that the spontaneous nature of sorption.

CONCLUSION

The equilibrium agitation time for the sorption of Ni(II) and Cr(VI) is 3 h. Results indicate that removal efficiency E decreases as the initial concentration is increased from 50–500 mg/L. The sorption data fit in both Freundlich and Langmuir isotherms. Langmuire iso-

therm model shows a better agreement with equilibrium data. Negative values of $\Delta G°$ indicating that the spontaneous nature of sorption. Waste mould sand indicate better sorption properties for Ni(II) than for Cr(VI) ions. The obtained sorption capacity value is promising in the waste mould sand use as efficient low-cost sorbent in Ni(II) and Cr(VI) removal from solutions.

Acknowledgement

This work was supported by the Ministry of Science, Education and Sports of the Republic of Croatia, under the project 124-1241565-1524.

References

[1] Pehlivan, E., Arslan, G. (2007): Removal of metal ions using lignite in aqueous solution-Low cost biosorbents. *Fuel Processing Technology*; Vol. 88, pp. 99–106.

[2] Babel, S., Kurniawan, T. A. (2004): Cr(VI) removal from synthetic wastewater using coconut shell charcoal and commercial activated carbon modified with oxidizing agents. *Chemosphere*; Vol. 54, pp. 951–996.

[3] Aggarwal, D., Goyal, M., Bansal, R. C. (1999): Adsorption of chromium by activated carbon from aqueous solution. *Carbon*; Vol. 37, pp. 1989–1997.

[4] Lee, T., Lim, H., Lee, Y., Park, J. (2003): Use of waste iron metal for removal of Cr(VI) from water. *Chemosphere*; Vol. 53, pp. 479–485.

[5] Sajwan, K. S., Ornes, W. H., Youngblood, T. V., Alva, A. K. (1996): Uptake of soil applied cadmium, nickel and selenium by bush beans. *Water, Air and Soil Pollution*; Vol. 91, pp. 209–217.

[6] Srivastava, V. C., Mall, I. D., Mishra, I. M. (2008): Competitive adsorption of cadmium (II) and nickel (II) metal ions from aqueous solution onto rice husk ash. *Chemical Engineering and Processing: Process Intensification*; Vol. 48, pp. 370–379.

[7] Liu, S. X., Chen, X., Chen, X. Y., Liu, Z. F., Wang, H. L. (2007): Activated carbon with excellent chromium (VI) adsorption performance prepared by acid-base surface modification. *Journal of Hazardous Materials*; Vol. 141, pp. 315–319.

[8] Gabaldon, G., Marzal, P., Ferrer, A. (1996): Single and competitive adsorption of Cd and Zn onto granular activated carbon. *Water Research*; Vol. 30, pp. 3050–3060.

[9] Kadirvelu, K., Faur-Brasquet, C., Cloirec, P. Le. (2000): Removal of Cu(II), Pb(II) and Ni(II) by adsorption onto activated carbon cloths. *Langmuir*; Vol. 16, pp. 8404–8409.

[10] Mohan, D., Pittman, C. U. (2006): Activated carbons and low cost adsorbents for remediation of tri-and hexavalent chromium from water. *Journal of Hazardous Materials*; Vol. 137B, pp. 762–811.

[11] Mohan, D., Singh, K. P., Singh, V. K. (2006): Trovalent chromium removal from wastewater using low cost acti-

vated carbon derived from agricultural waste material and activated carbon fabric cloth. *Journal of Hazardous Materials*; Vol. 135, pp. 280–295.

[12] Mohan, D., Singh, K. P. (2002): Single-multi component adsorption of cadmium and zinc using activated carbon derived from bagasse-an agricultural waste. *Water Research*; Vol. 36, pp. 2304–2318.

[13] Atkinson, B. W., Bux, F., Kasan, H. C. (1998): Considerations for application of biosorption technology to remediate metal-contaminated industrial effluents. *Water SA*; Vol. 24, pp. 129–135.

[14] Guo, X., Zhang, S., Shan, X. (2007): Adsorption of metal ions on lignin. *Journal of Hazardous Materials*; Vol. 151, pp. 134–142.

[15] Ünlü, N., Ersoz, M. (2007): Removal of heavy metal ions by using dithiocarbamated-sporopollenin. *Separation and Purification Technology*; Vol. 52, pp. 461–469.

[16] Dungan, R. S., Dees, N. H. (2007): The characterization of total and leachable metals in foundry molding sands. *Journal of Environmental Management*; Vol. 90, pp. 1–10.

[17] Jl. S., Wan, L., Fan, Z. (2001): The toxic compounds and leaching characteristics of spent foundry sands. *Water, Air, and Soil Pollution*; Vol. 132, pp. 347–364.

[18] Lee, T., Park, J., Lee, J. (2004): Waste green sands as reactive media for the removal of zinc from water. *Chemosphere*; Vol. 56, pp. 571–581.

[19] Fries, J., Getros, H. (1977): Organic Reagents for Trace Analysis. E. Merck Darmstadt.

[20] Mohapatra, D., Mishra, M. D., Mishra, S. P., Chaudhury, G. R., Das, R. P. (2004): Use of oxide minerals to abdate fluoride from water. *Journal of Colloid Interface Science*; Vol. 275, pp. 355–359.

[21] Zeledon-Toruno, Z., Lao-Luque, C., Sole-Sardans, M. (2005): Nickel and copper removal from aqueous solution by an immature coal (leonardite): effect of pH, contact time and water hardness. *Journal of Chemical Technology and Biotechnology*; Vol. 80, pp. 649–656.

[22] Gopal, V., Elango, K. P. (2007): Equilibrium, kinetic and thermodynamic studies of adsorption of fluoride onto plaste of Paris. *Journal of Hazardous Materials*; Vol. 141, pp. 98–105.

Processing the PK324 Duplex Stainless Steel: Influences on hot deformability of the as-cast microstructure

Izdelava dupleksnega nerjavnega jekla PK324: Vplivi na vročo preoblikovalnost lite mikrostrukture

Tatjana Večko Pirtovšek[1], Peter Fajfar[1,*]

[1]University of Ljubljana, Faculty of Natural Science and Engineering, Department of Materials and Metallurgy, Aškerčeva 12, SI-1000 Ljubljana, Slovenia

*Corresponding author. E-mail: peter.fajfar@ntf.uni-lj.si

Received: April 8, 2009 **Accepted:** May 27, 2009

Abstract: Examination of reasons that cause cracking of the as-cast microstructure of the PK324 duplex stainless steel (DSS) during the hot working process represents an important step to improve the final quality of product. Hot compression tests were applied in the examination and they were combined with the observations in light microscope. Deformation behaviour of initial as-cast samples as well of the samples after ten hours ageing has been studied with the Gleeble 1500D thermo-mechanical simulator. Applied strain rate was in the range of 0.1 s^{-1} to 5 s^{-1}, temperature interval was 900–1300 °C and strains were up to 0.7. Ten hours aged samples exhibited considerably narrower temperature range (interval) of safe hot deformation. Calculated activation energy for the entire range of the hot working process and for peak stresses was 287 kJ/mol.

Izvleček: Za izboljšanje kvalitete končnih izdelkov iz dupleksnega nerjavnega jekla PK324 (DSS) so pomembne preiskave vzrokov za nastanek razpok med vročim preoblikovanjem. Za preiskovalni metodi smo uporabili vroče tlačne preizkuse in optično mikroskopijo. Preizkuse za določevanje preoblikovalnih lastnosti dupleksnega jekla v litem stanju ter v stanju po deseturnem homogenizacijskem žarjenju smo izvajali na simulatorju termomehanskih stanj Gleeble 1500D. Preizkusi so bili izvedeni v območju hitrosti deformacije od 0,1 s^{-1} do 5 s^{-1}, v temperaturnem intervalu 900–1300 °C ter pri

Original scientific paper

stopnji deformacije do 0,7. Temperaturno področje, ki zagotavlja deformacijo brez nastanka razpok, je za žarjene vzorce bistveno ožje kot za lite. Izračunana navidezna aktivacijska energija za vroče preoblikovanje pri največjih napetostih in na celotnem temperaturnem področju je 287 kJ/mol.

Key words: PK324 duplex stainless steel, as-cast microstructure, aging treatment, hot compression

Ključne besede: dupleksno nerjavno jeklo PK324, lita mikrostruktura, žarjena mikrostruktura, vroče stiskanje

INTRODUCTION

Duplex stainless steels (DSS) are constantly gaining their importance due to good combination of their corrosion resistance and of mechanical and physical properties in a wide temperature interval when compared to standard austenitic stainless steels, and they have found their applications in chemical and paper industry, in shipbuilding, as welding materials, in petroleum industry, etc. The obtained properties of super duplex stainless steel result in balanced alloying with the ferrite - (Cr, Mo, Si, etc.) and austenite-forming elements (Ni, Mn, C, N, etc.). Thus steel consists of a two-phase matrix, i.e. of austenite and ferrite, where austenite (γ) contributes toughness while ferrite (α) improves the mechanical and welding characteristics. Their properties have been continually improved by optimization of alloying, hot and cold working, heat treatment, etc.[1–6].

It is well known that hot working of dual-phase steel is a very demanding one since possible problems are usually more intricate in comparison to working single-phase steel especially when the as-cast material is taken in account. Interface boundary sliding (IBS) seems to be the major deformation mechanism in the duplex steel at higher strain rates ($> 1\ s^{-1}$) and relatively low temperatures (about 1000 °C). Precipitation of intermetallic phases (sigma (σ), Cr_2N, Chi phases (χ), etc) in the approximate temperature interval of 500–1050 °C additionally reduces the range of safe hot working therefore the process has to be performed at temperatures above the interval of precipitation of intermetallic phases. Hot working of the as-cast material represents critical step in the production cycle since the as-cast microstructure is very prone to cracking, especially on the ferrite/austenite (α/γ) grain boundaries (it has been observed also on the α/α and γ/γ grain

boundaries) since there eventually impurities and carbides precipitate (usually M_7C_3 and $M_{23}C_6$). Furthermore, both phases have different crystallographic structures and deformation modes, different strengths (austenite is significantly stronger in the range of hot working) and softening mechanisms (and rates too). On the other hand, DSS can exhibit excellent hot plasticity if the microstructure is fine enough[6–16].

The PK324 DSS is usually used as welding material and it belongs to the group of duplex stainless steel, and cracking during the hot working process, especially when cast ingots are worked, is still its disadvantage. This paper represents a contribution to elucidation of reasons for appearance of cracking of the as-cast microstructure in hot working the PK324 DSS.

Applied methods for characterization, testing and materials

An ingot of PK324 DSS weighing 380 kg has been cast in a vacuum electric furnace. Chemical composition of the applied batch is given in Table 1; from the Table is thus visible that the batch contained mass fraction 0.10 % of C, 30.1 % of Cr and 9.5 % of Ni. Test specimens (cylindrical specimens with dimensions $\phi = 10$ mm × 15 mm) were taken from the ingot cross sections and half of them was additionally aged at 1250 °C for 10 h. Both groups of samples were hot compressed (Figure 1a) in the Gleeble 1500D thermo-mechanical simulator at three strain rates (0.1 s^{-1}, 1 s^{-1} and 5 s^{-1}), in the temperature interval of 950–1300 °C and with strains up to 0.7. Cylindrical specimens were heated to the deformation temperature in 5 min. A 5 min holding time, hot compression and gas cooling followed (Figure 1b). (LM) ZEISS JENA VERT microscope was applied in the light microscopy, and Murakami etchant[17] was used in order to colour σ phase grey, α phase brown, carbides red, green and blue, while γ phase remained uncoloured. XRD (X-ray diffraction, Cristalloflex 4 apparatus) was used to determine fractions of phases in the microstructures. All the experiments and testing conditions as well as the applied characterizations in the examinations are presented in Table 2.

The initial as-cast microstructure is presented in Figure 2; the microstructure consisted of γ phase in the interdendritic spaces and of α phase. Amount of ferrite of about 48 %, of austenite of about 52 % were found in the samples taken from the ingot centre, while the amount of sigma phase was below 1 %, and amount of carbides ($M_{23}C_6$ and M_7C_3) at about 0.3 %, measured at the room temperature. Carbides predomi-

nately precipitated on the α/γ boundaries in the interdendritic spaces (due to segregation of C during the solidification) and to a smaller extent also inside the austenite grains but close to the α/γ boundaries while σ phase precipitated in the areas of ferrite. σ phase was at temperatures above 900 °C dissolved in the matrix, thus this phase did not take part in hot deformation in the temperature interval of 900–1300 °C[16].

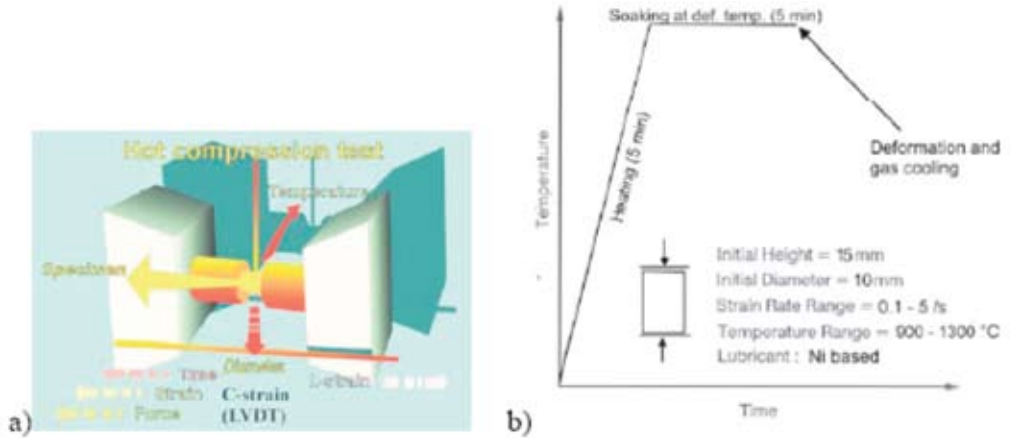

Figure 1. Schematic presentation of the hot compression test with the Gleeble 1500D thermo-mechanical simulator (a), and of thermal cycles used in compression tests (b).

Table 1. Chemical composition of the used batch for experiments, PK324 DSS; *w*/%

C	Si	Cr	Mn	Ni	Mo	S	P	Al	Cu
0.10	0.26	30.1	1.91	9.5	0.04	0.004	0.020	0.007	0.06

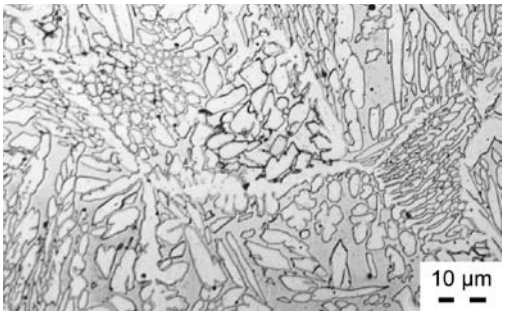

Figure 2. The initial as-cast microstructure of the PK324 DSS, LM.

Table 2. Collected experimental and testing conditions

Initial state	as-cast	
Aging	No	10 h at 1250 °C
Hot compression	Temperature 900–1300 °C, strain rates 0.1 s^{-1}, 1 s^{-1}, 5 s^{-1}	Temperature 900–1300 °C, strain rates 0.1 s^{-1}, 1 s^{-1}, 5 s^{-1}
Cooling	gas	
Characterization	LM, XRD	

Results and discussion

The obtained flow stress curves with the as-cast samples taken from the ingot head and for 0.1 s^{-1} strain rate are presented in Figure 3; steady-state flow was achieved with the initial as-cast material. At higher deformation temperatures, i.e. above 1150 °C, where the fraction of ferrite was considerably higher[16], the flow curves after achieving maximal values retained those levels since dynamic recovery of ferrite occurred during the hot deformation. Ferrite has namely high stacking-fault energy that favours dynamic recovery (DRV). On the other hand, at deformation temperatures below 1150 °C the fraction of austenite was higher in comparison to the upper temperature interval (1150–1250 °C); dynamic recrystallization (DRX) led to reduced values of flow stresses after achieving the peak values. The phenomenon of DRX of austenite was indicated also by shifts of peak values of flow curves to higher strains at decreased deformation temperatures. The shape of flow curves at 1 s^{-1} strain rate was similar to that of curves for 0.1 s^{-1} strain rate while the peaks at the strain rate 5 s^{-1} were not so pronounced since they were more elongated like in hot compression of DSS at higher strain rates[13].

The results about appearance or not appearance of cracks on free surfaces of compressed not aged and 10 h aged

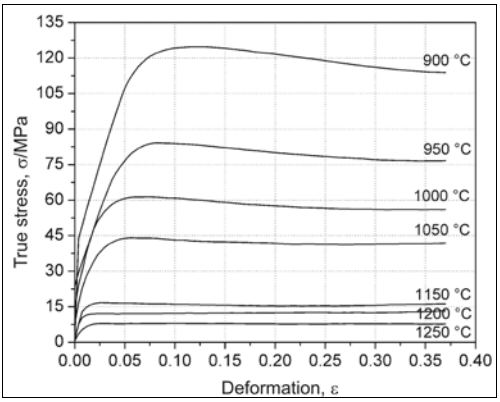

Figure 3. Flow stress curves of the as-cast PK324 DSS at various compression temperatures and at 0.1 s^{-1} strain rate

samples (see Figure 4a–b) are presented in Table 3 for the entire examined temperature interval. The results from the table indicated that good hot deformability was achieved with the non-aged as-cast samples in the temperature range 1150–1250 °C while cracks were observed on deformed specimens bellow mentioned range. This could be attributed to the increased fraction of austenite[16] at temperatures below 1150 °C, to different deformation modes as well as to different strengths of austenite and ferrite, etc. that led to crack formation on the α/γ grain boundaries.

The obtained microstructures of compressed samples at various deformation temperatures are given in Figure 5. The microstructure became finer with the decreased compression temperature since the content of austenite increased; DRX namely took place in

austenite. Formation of austenite on the α/γ and α/α grain boundaries which were sub-boundaries or boundaries of grains began during the hot deformation and the followed cooling. Microstructure of samples being deformed in the 1200–1250 °C temperature range consisted of ferrite and austenite that were in equilibrium at the deformation temperature, of Widmanstätten austenite that was formed during the cooling after the deformation, and of a small amount of carbides on the α/γ grain boundaries (Figure 5a). Equilibrium between ferrite and austenite was achieved at those temperatures almost after ten minutes[16]. Further, dynamic softening process in the mentioned temperature range was very intensive since number of initial spots potentially suitable for precipitation of austenite during the cooling process after the hot deformation was reduced; consequently, austenite precipitated predominately on the α/γ grain boundaries. The obtained microstructures of samples being deformed at lower temperatures (below 1150 °C) (Figure 5b-d) differed from the microstructures of samples that were deformed at temperatures above the mentioned ones. At latter temperatures the softening process was considerably less pronounced, thus many spots potentially suitable for nucleation and consequently also for precipitation of austenite (α → γ) during the cooling process were available.

On the other hand, 10 h aged samples exhibited considerably narrower temperature range of safe hot deformation, i.e. 1200–1250 °C, in comparison to the non-aged samples (1150–1250 °C (Table 3)). This could be attributed to different α→γ transformation kinetics of the not aged and of the 10 h aged samples during the hot deformation. Microstructures of deformed and 10 h aged samples are given in Figure 6a and 6b for the deformation temperatures of 1250 °C and 1150 °C, respectively. Comparison of Figure 5a–b and Figure 6a–b revealed that approximately equal fractions of austenite and ferrite were found in both cases, but the grains in the 10 h aged samples were coarser. On the other hand, approximately 10–25 % higher values of steady-state flow stresses were obtained with the 10 h aged samples in comparison to the not aged samples. This could indicate that higher amount of ferrite was transformed into austenite during the hot deformation and this could be explained in the following way: a higher fraction of ferrite existed in the microstructure of samples being aged for 10 h before the hot deformation, thus higher non-equilibrium ferrite/austenite ratio existed at lower deformation temperatures. Consequently higher transformation (precipitation) rate of austenite took place in the entire ferrite phase and not only on the grain boundaries. Furthermore, the fraction of transformed austenite

was not higher in comparison to that in the not aged samples since there was not enough time for transformation, but austenite probably precipitated in a different way and the difference of its distribution could be observed. Thus the temperature range of safe hot working was narrower with the 10 h aged samples. The results on microanalyses on 10 h aged samples at 1250 °C (before hot compression) indicate that differences in contents of Cr and Ni between α and γ phase seems to decrease, i.e. trying to reach the equilibrium between both phases. Thus the content of Cr decreases and of Ni increases in α while the opposite behaviour for both chemical elements in γ was found (these results will be published in next article). The state of material similar to that obtained after 10 h aging could be obtained also at slow solidification rates of DSS (segregations) that could result in reduced range of safe hot working of as-cast microstructure. For more accurate explanation of these results further examinations should be done.

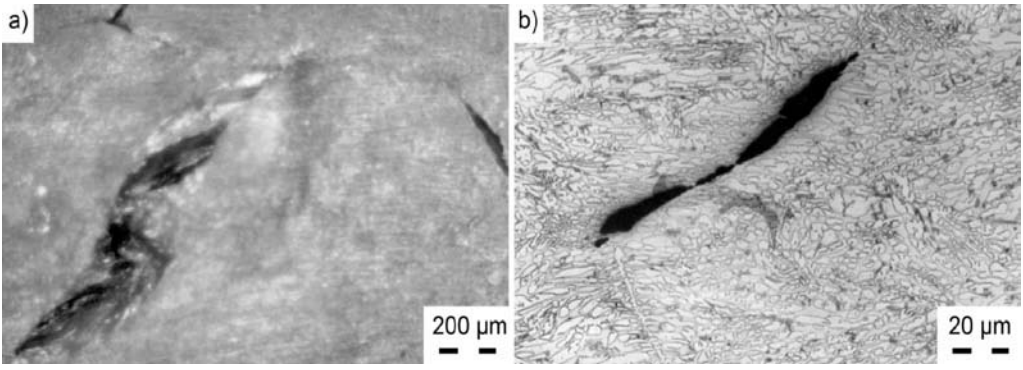

Figure 4. Appearance of cracking phenomenon on compressed samples; macro view (a), and micro view (cracking on grain boundaries) (b)

Table 3. Appearance of surface cracks as a function of compression temperature for as-cast state, not aged, and 10 h aged samples, strain rate 1 s^{-1}.

Deform. temp. *T*/°C		900	950	1000	1050	1100	1150	1200	1250	1300
Cracking	Non-aged	Y	Y	S	S	S	N	N	N	Y
	10 h aged	Y	Y	Y	Y	Y	S	N	N	Y

N - without cracks, Y - deep cracks, S - fine cracks.

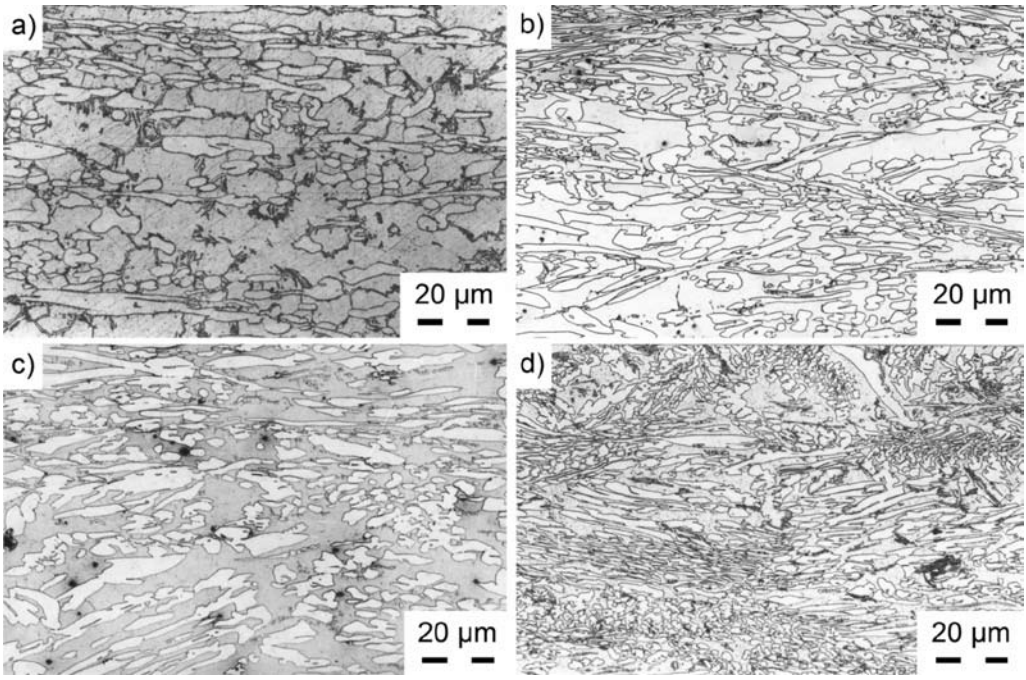

Figure 5. Obtained microstructures at 1 s^{-1} strain rate and at various compression temperatures: 1250 °C (a), 1150 °C (b), 1100 °C (c), and 950 °C (d), non-aged samples, gas cooling

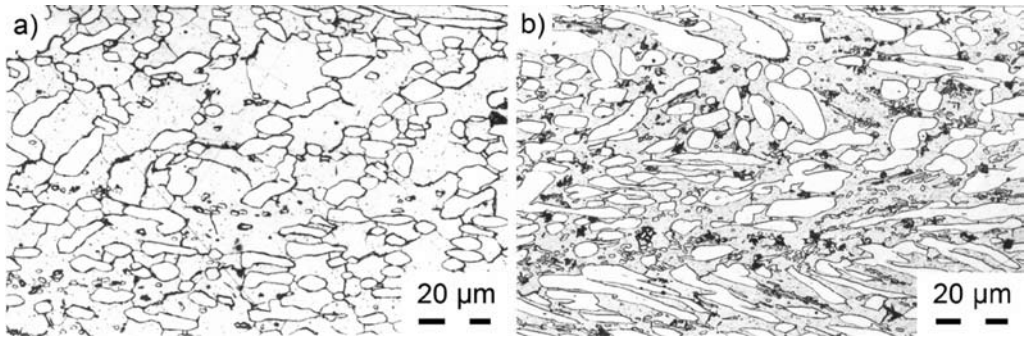

Figure 6. Obtained microstructures at 1 s^{-1} strain rate and at various compression temperatures: 1200 °C (a), 1150 °C (b), samples 10 h aged at 1250 °C, gas cooling

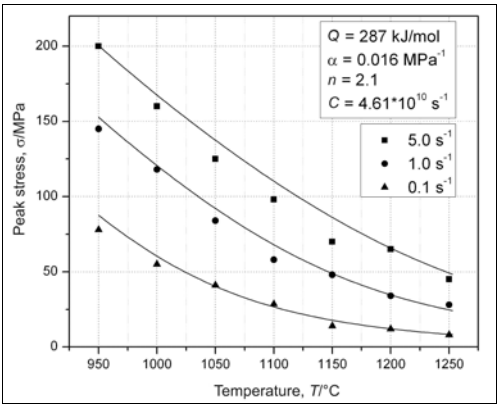

Figure 7. Comparison between the calculated and the measured peak stresses as a function of temperature, not aged, as-cast.

In order to determine activation energies by the procedure given in reference[18], the values of peak stresses for the initial as-cast samples were fitted to the empirical sine-hyperbolic equation:

$$\dot{\varepsilon} = A[\sinh(\alpha\sigma)]^n \exp(-\frac{Q}{RT}) \qquad (1)$$

Q represented the deformation activation energy, R the universal gas constant, and n, α and A materials constants. Activation energy at temperatures of examinations and for the applied strain rate ranges was calculated to be 287 kJ/mol. The comparison between the calculated and the measured values of peak stresses together with the other parameters of the equation (1) is given in Figure 7. The obtained activation energy was somewhat lower than that cited by other authors, e.g. Cabrera et al[9] for 25Cr7NiN3.8Mo DSS (Q = 438 kJ/mol), and Paul et al[15] (Q = 360 kJ/mol). This could be attributed to considerably higher fraction of ferrite in our steel.

Conclusions

Hot deformation behaviour of the PK324 DSS samples, as-cast, and 10 h aged at 1250 °C, was examined at strain rates 0.1–5 s^{-1} and in the 950–1300 °C temperature range. The following conclusions could be made:

- Compression temperature played important role in the deformability of the as-cast microstructure. Appearance of surface cracking in hot compression below 1150 °C and no cracking above that temperature was observed with the not aged samples. Cracking occurred predominately on the α/γ grain boundaries.
- Ten hours aged samples at 1250 °C could be safely deformed only in the temperature range 1200–1250 °C.
- The as-cast microstructure could be broken in the temperature range of 1150–1250 °C, otherwise the workpiece should be reheated to above 1150 °C.
- Calculated activation energy for the hot deformation process and for the peak values of flow stresses was 287 kJ/mol, and it was lower in

comparison to the cited values by other authors since our DSS contained higher fraction of ferrite.

References

[1] Josefsson, B., Nilsson, J. O., Wilson, A. (1992): Phase transformation in duplex steels and relation between continuous cooling and isothermal heat treatment, in: Duplex stainless steels. Ed.: J. Charles and S. Bernhardsson, *Beaune Bourgogne*, France; pp. 28–30.

[2] Nilson, J. O. (1992): Super duplex stainless steels. *Materials Science and Engineering*; Vol. 8, pp. 685–700.

[3] Martins, M., Rodrigues, L. (2008): Effect of aging on impact properties of ASTM A890 Grade 1C super duplex stainless steel. *Materials Characterization*; Nogueira Forti, Vol. 59/2, pp. 162–166.

[4] Charles, J., Bernhardsson, S. (1991): Duplex Stainless Steel. *Les editions de physique les Ulis*; France, pp. 3–48.

[5] F. H. Hayes, M. G. Herherington, R. D. Longbottom, Thermodynamics of duplex stainless steels, Materials Science and Engineering, 6 (1990) 263–272.

[6] C. H. Shek, K. W. Wong, J. K. L. Lai and D. J. Li, Hot tensile properties of 25Cr-8Ni duplex stainless steel containing cellular (σ+γ2) structure after various thermal treatments, Materials Science and Engineering A, 231/(1-2) (1997) 42–47.

[7] Martins, M., Carlos Casteletti, L. (2005): Heat treatment temperature influence on ASTM A890 GR 6A super duplex stainless steel microstructure. *Materials Characterization*; Vol. 55/3, pp. 225–233.

[8] Chi-Shang Huang, Chia-Chang Shih (2005): Effects of nitrogen and high temperature aging on σ phase precipitation of duplex stainless steel. *Materials Science and Engineering*; Vol. 402/(1–2), pp. 66–75.

[9] Cabrera, J. M., Mateo, A., Llanes, L., Prado, J. M., Anglada, M. (2003): Hot deformation of duplex stainless steels. *Journal of Materials Processing Technology*; pp.143–144, pp. 321–325.

[10] Yasuhiro Maehara (1992): Effect of microstructure on hot deformation in duplex stainless steels. *Scripta Metallurgica et Materialia*; Vol. 26/11, pp. 1701–1706.

[11] Momeni, A., Abbasi, S. M., Shokuhfar, A. (2007): Hot compression behaviour of as-cast precipitation-hardening stainless steel. *Journal of Iron and Steel Research International*; Vol. 14/5, pp. 66–70.

[12] Duprez, L., Cooman, B. C., Akdut, N. (2002): Flow Stress and Ductility of Duplex Stainless Steel during High Temperature Torsion Deformation. *Metallurgical and Materials Transactions*; 33A, pp. 1931–1938.

[13] Arboledas, J. M., Martos Tirado, J. L., Sanchez Rodrigues, R. (1996): Optimizing the hot deformability of 2205 duplex stainless steel by thermal/mechanical simulation, Proceedings of Stainless steels. *German Iron and Steel Institute*.

[14] Han, Y. S., Hong, Soon H. (1999): Microstructural changes during superplastic deformation of Fe-24Cr-7Ni-3-Mo-0.14N duplex stainless steel. *Materials Science and Engineering*; Vol. 266, pp. 276–284.

[15] Paul, A., Martos, J. L., Sanchez, R. (1993): Behaviour of 2205 Duplex stainless steel under hot working conditions. *Inovation Stainless steel*; Florence, Italy, 11–14, pp. 3297–3302.

[16] Fazarinc, M., Večko Pirtovšek, T., Bombač, D., Kugler, G., Terčelj, M. (2008): Processing of PK 324 duplex stainless steel: influence of aging temperature and cooling rates on precipitation: preliminary results. *RMZ*; Vol. 55, pp. 420–431.

[17] Klemm, B. (1962): Handbuch der metallographischen Ätzverfahren. Deutsche Verlag für Grundstoffindustrie, Leipzig.

[18] Kugler, G., Knap, M., Palkowski, H., Turk, R. (2004): Estimation of activation energy for calculating the hot workability properties of metals. *Metalurgija*; Vol. 43, pp. 267–272.

Irradiation methods for removal of fluid inclusions from minerals

Iradiacijske metode odstranjevanja tekočinskih vključkov iz mineralov

B. Z. Belashev[1,] *, L. S. Skamnitskaya[1]

[1]Institute of Geology, Karelian Research Centre, Russian Academy of Sciences, Petrozavodsk, Russia

*Corresponding author. E-mail: belashev@krc.karelia.ru

Received: March 11, 2009 **Accepted:** April 8, 2009

Abstract: Methods for removal of fluid inclusions, using gamma quantum and high energy proton irradiation, microwave radiation and electromagnetic impulse treatment, were studied. The effects investigated directly decrease the number of fluid inclusions in minerals and change their temperature spectrum. Radiation methods differ from thermal treatment in that they are not connected with direct heating of a mineral, are less expensive, use background radiation and can be combined with other technologies.

Izvleček: Preučene so bile metode za odstranjevanje tekočinskih vključkov z gama-kvantno in visokoenergijsko protonsko iradiacijo, mikrovalovno radiacijo ter z elektromagnetno impulzno obdelavo. Preučeni efekti neposredno zmanjšujejo število tekočinskih vključkov v mineralih in njihov temperaturni spekter. Radiacijske metode se razlikujejo od termalne obdelave v tem, da niso povezane z neposrednim segrevanjem minerala, so cenejše, uporabljajo radiacijo naravnega ozadja, lahko pa jih tudi kombiniramo z drugimi tehnologijami.

Key words: fluid inclusions, removal of minerals, gamma quantum, high energy proton, microwave radiation, electromagnetic impulses, water extracts

Ključne besede: tekočinski vključki, odstranjevanje mineralov, gama- kvanti, visokoenergijski proton, mikrovalovna radiacija, elektromagnetni impulzi, vodni izvlečki

Original scientific paper

INTRODUCTION

As pure materials are in demand, attempts are made to develop efficient methods to remove impurities from minerals. A common type of inclusions that are hard to remove, that disturb the homogeneity, deteriorate the characteristics and limit the use of minerals are fluid inclusions (ROEDDER, 1984). Such inclusions are removed by heating a mineral to a high temperature that destroys inclusions (DOLGOV, ERMAKOV, 1971; KRAVETS, 1995). As a lot of energy is needed to heat minerals, more economic methods to destroy fluid inclusions are being sought (BELASHEV, SKAMNITSKAYA, LEBEDEVA, OZEROVA, 2001; SKAMNYTSKAYA, KAMENEVA, BELASHEV, 2004).

The paper deals with methods for removal of fluid inclusions from minerals by gamma quantum, high energy particle and microwave irradiation and by treatment with strong electromagnetic impulses.

The mechanism of the effect of radiation on fluid inclusions has not been thoroughly studied. Well-known impacts of radiation on a mineral, such as the formation of colour centres, structural rearrangements, weakening of bonds, redistribution of defects and loosening of a sample (SHEVYAKOVA, LIFSHITZ, POLYASCHENKO, 1980), indirectly contribute to removal of fluid inclusions from a mineral but do not cause their destruction. The study of the effect of various fields on a mineral is expected to cast light on inclusion destruction mechanisms.

The goal of the study is to acknowledge the destructive effect of irradiation on fluid inclusions and to assess its quantitative characteristics.

MATERIAL AND METHODS

The problem was approached by studying initial fluid inclusions in the sample, their disintegration products or inclusions that were not removed by treatment. As the first step it was important to estimate the influence of radiation on all kinds of fluid inclusions in minerals.

Quartz, microcline, plagioclase, kyanite, apatite and tourmaline samples were collected from various deposits in Karelia (DANILEVSKAYA, SKAMNITSKAYA, SHIPTSOV, 2004) and the morphology of fluid inclusions and their spatial distribution in the sample were studied under optic microscope.

At the initial stage of removal of inclusions, the mineral was ground to reveal coarse inclusions and inclusions at grain boundaries. The samples were subjected to gamma quantum irradiation with an energy of 4 MeV on a de-

fectoscopic installation provided by Tyazhbummash Plant (Petrozavodsk). A bundle of protons with an energy of 2 GeV, produced by the Nuclotrone at the Joint Institute of Nuclear Research (Dubna), was also used. The samples were subjected to UHF treatment in a domestic Samsung microwave oven. The minerals were affected by strong electromagnetic impulses with an amplitude of 40–50 kV and a pulse frequency of 125 Hz and 200 Hz on a plant at the Institute for Integrated Development of Mineral Resources (Moscow) designed for disintegration of refractory auriferous raw materials (Skamnitskaya, Kameneva, Belashev, 2004). The efficiency of removal of fluid inclusions was controlled by an acoustic decrepitograph, recording impulses from the disruption of inclusions left after treatment (Belashev, Skamnitskaya, Lebedeva, Ozerova, 2001). It was also controlled by the water extract method used by studying inclusion disintegration products that passed into aqueous solution (Moskalyuk, 1973). The relative error of this method of measurement is 10 %.

Results and discussion

Fluid inclusions, 10–50 μm in size, are distributed in minerals either chaotically or along the internal fractures of grains (Figure 1). The number and composition of fluid inclusions in min-

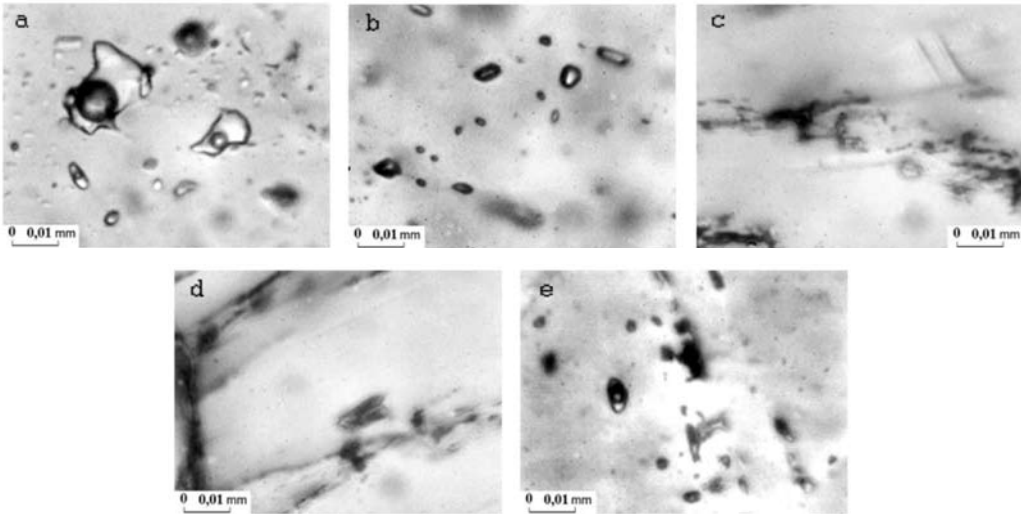

Figure 1. Fluid inclusions in minerals: quartz, Kyrjala deposit, secondary fluid inclusions (a), kyanite, Khizovaara deposit, primary fluid inclusions (b), microcline, Kyrjala deposit, primary fluid inclusions (c), plagioclase, Kyrjala deposit, primary fluid inclusions (d), tourmaline, Kyrjala deposit, primary fluid inclusions (e).

Table 1. Number of fluid inclusions in samples of quartz decrepited in temperature ranges

Temperature ranges, *T*/°C	Sample 9/98, pegmatitic, Kyrjala deposit	Sample 3/94, veined, Khizovaara deposit
	Number of inclusions	
100–200	711	796
200–300	4569	406
300–400	3939	1160
400–500	9159	992

Table 2. Concentration and species composition of initial fluid impurities

Mineral	Extract	Concentration, *c*/(mg/L)										
		pH	Fe	Ca^{2+}	Mg^{2+}	Na^{1+}	K^{1+}	Li^{1+}	HCO_3^-	SO_4^{2-}	Cl^-	$C_{org.}$
Quartz, Kyrjala deposit	1	7.62	0.15	1.4	0.4	2.5	2.4	0.19	16.4	4.4	5.5	2.7
	2	6.97	2.70	1.0	0.2	2.3	0.9	0.08	6.8	5.2	4.6	2.7
Microcline, Kyrjala deposit	1	8.43	0.19	7.4	1.2	05	114	3.9	166	10.0	29.4	0.5
	2	8.43	0.05	7.4	0.5	0.5	55	3.6	138	7.3	6.7	0.5

erals depend on the parameters of mineral-forming solutions and vary with deposit, sector of deposit and temperature range (Table 1). The density of fluid inclusions varied considerably with quartz type (BELASHEV, SKAMNITSKAYA, LEBEDEVA, OZEROVA, 2001).

The sulphate-chloride-bicarbonate composition of fluid inclusions was determined by the water extract method (Table 2). Ion concentration in the inclusions is 1.43 times that in solutions produced by dissolving the minerals. For fluid inclusions in feldspars, a pH of 7.5–8.5 suggests an oxidation-reduction medium. The cations that play the leading role are sodium, potassium and calcium. In microcline, small-sized Na and Ca ions are more easily replaced by H^+ ions than K ions. Impurities in feldspars, such as lithium, magnesium etc., pass into aqueous solution as a result of hydrolysis. Anions are acid residues or the dissolution products of the solid-phase components of fluid inclusions.

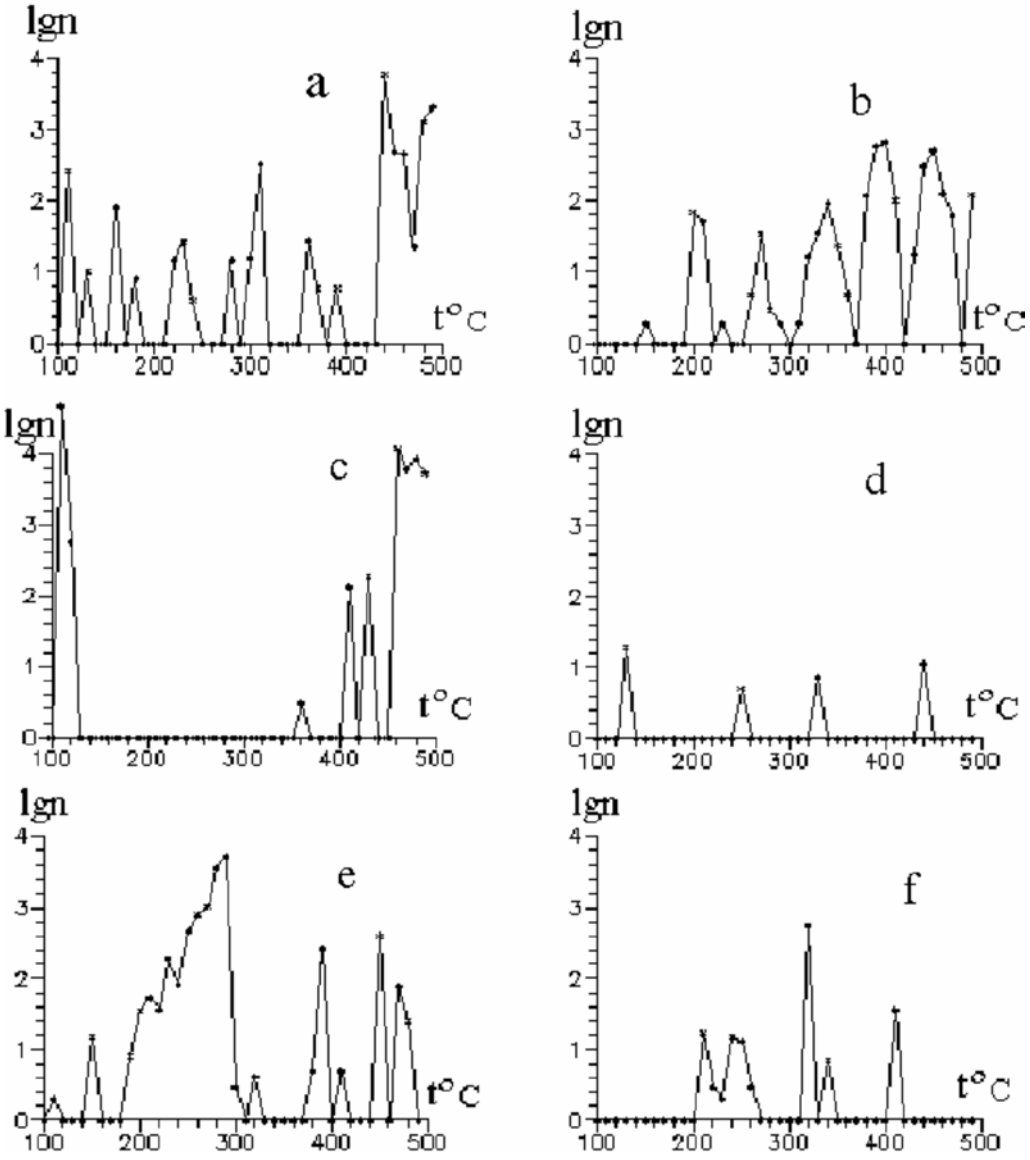

Figure 2. Decreptograms of quartz, microcline and plagioclase of powders from Kyrjala deposit before (a, c, e) and after irradiation (b, d, f) with a bundle of gamma-quanta (E = 4 MeV) for 1 h.

The results of 1 h gamma-quantum irradiation of the minerals are shown in Figure 2. The effect of proton irradiation on fluid inclusions in quartz is

shown in Figure 3. Figure 4 shows the influence of UHF irradiation on quartz samples. The results obtained corroborate the effect of irradiation of minerals on the concentration of fluid inclusions. Figure 2–4 shows that as irradiation dose and mineral treatment time increase, the number of fluid inclusions decreases and their temperature spectrum changes qualitatively: the peaks of the initial decreptograms decrease in amplitude, split up and are shifted to the medium and low temperature range.

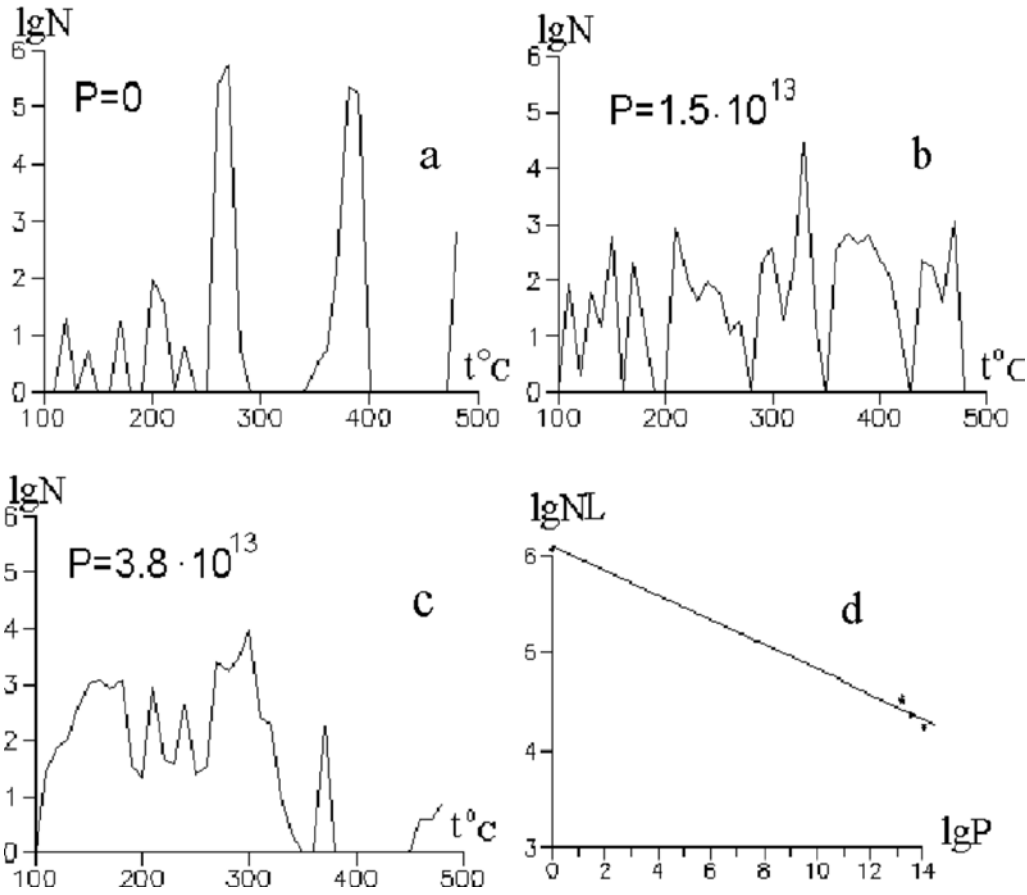

Figure 3. Effect of proton irradiation dose on the number of fluid inclusions in quartz from Kyrjala deposit (a) initial decreptogram not subjected to irradiation; (b, c) decreptograms of quartz subjected to increasing irradiation doses; (d) dependence of the number impulses NL on the decreptogram on the number of protons P that passed through the sample.

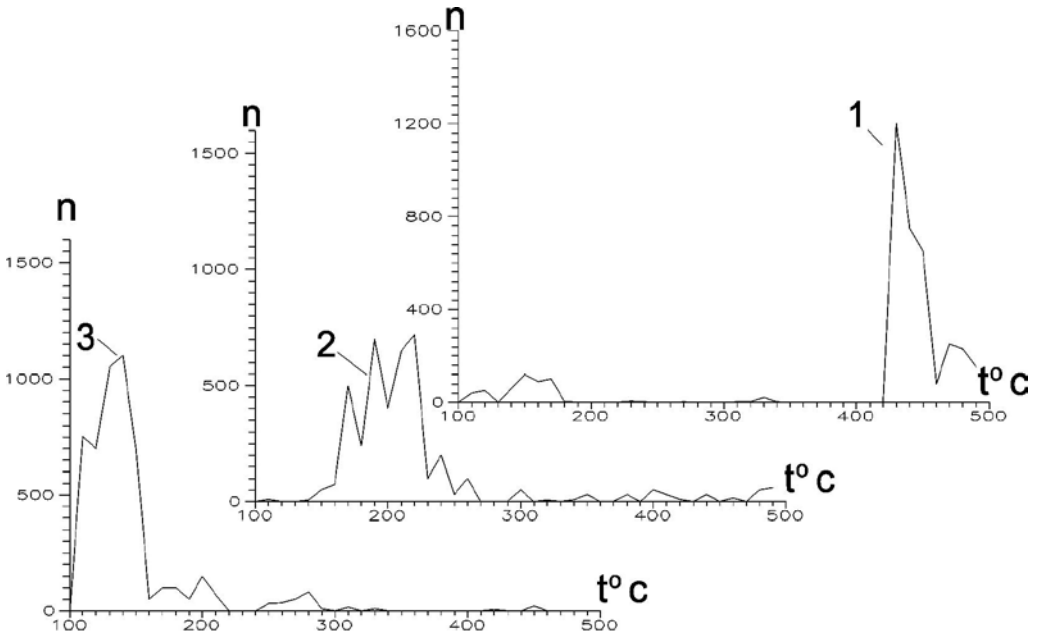

Figure 4. Decreptogram of vein quartz from the Mursula deposit: 1- initial sample, 2 - UHF irradiation for 5 min, 3 - UHF irradiation for 10 min

The compositions of water extracts from the minerals after electromagnetic impulse treatment are shown in Table 3. The regimes used to reveal fluid inclusions vary with mineral. In microcline, treatment with electromagnetic impulses for 60 s reveals a maximum number of inclusions, and the greatest number of HCO^{3-}, SO_4^{2-}, Cl anions pass into water extracts, the number of SO_4^{2-} anions being five times that observed when treatment time is less than 10 s. A maximum number of inclusions is found when treatment time is 15 s for kyanite and 180 s for apatite. The data obtained show that long treatment leads to local heating and destruction of organic impurities and their decreased concentration in water extracts.

The effect on fluid inclusions observed could be explained by mechanisms that act with regard for the composition of inclusions and the characteristics of irradiation. An inclusion is destroyed by a rise in internal pressure caused by ionization and heating of inclusions upon dissipation of particle energy. An inclusion can be heated selectively by protons because of mass equality; they efficiently supply energy and impulse to the water protons of inclusions. UHF irradiation is absorbed in a resonance manner by the rotational fluctuations

Table 3. Composition of extract from minerals after electromagnetic impulse irradiation

Mineral	Treatment time, *t*/s	pH of extract	Concentration, *c*/(mg/L)								
			Ca^{2+}	Mg^{2+}	Na^{1+}	K^{1+}	Li^{1+}	HCO^{3-}	SO_4^{2-}	Cl^-	Corg
Microcline, Kyrjala deposit	0	7.16	1.4	0.3	0.6	0.4	0.03	5.1	0.4	1.2	2.7
	10	7.27	2.2	0.4	0.4	0.9	0.05	7.9	1.8	1.3	10.8
	30	7.28	2.3	0.4	0.4	0.8	0.04	7.9	1.6	1.3	0.5
	60	7.36	3.4	0.6	0.7	1.0	0.06	11.1	2.2	1.5	2.7
	300	7.20	3.3	0.2	0.5	0.9	0.05	7.03	0.6	1.3	2.7
Kyanite, Khizovaara deposit	15	4.65	3.4	0.51	1.4	0.38		0	76.8		35.8
	30	4.57	3.5	0.52	1.4	0.38		0	50.6		22.8
	60	4.50	3.6	0.51	1.4	0.40		0	54.4		6.5
	180	4.52	3.4	0.48	1.4	0.36		0	58.2		21.6
Apatite, Tikshozero deposit	15	5.17	0.92	0.17	0.77	0.23		0	30.9		19.8
	30	5.10	0.92	0.18	0.77	0.24		0	29.1		21.2
	60	5.04	0.84	0.17	0.77	0.22		0	27.2		27.0
	180	5.26	0.92	0.17	0.85	0.26		0	26.2		6.4

of inclusion water molecules. Electromagnetic impulses create in minerals numerous channels that expose fluid inclusions or create high pressure and decompression zones in close proximity to them (CHANTURIA, BUNIN, IVANOVA, SKAMNITSKAYA, PYLOVA, 2004).

Some of the mineral treatment regimes used are far from being optimum. The energy of gamma quanta does not correspond to the energy of their resonance absorption by the water of inclusions. As the ability of protons to cause maximum destruction at the end of their travel in matter is not used, the efficiency of different methods cannot be compared experimentally, and radiation technology should further be improved. An example of UHF irradiation (Figure 4, curve 3) shows that the resonance transmission of field energy to inclusions makes the destruction of high temperature inclusions more efficient. For low temperature peaks, this statement requires additional checking because of masking by an intense peak of adsorbed water.

Conclusions

- Irradiation of minerals and their treatment with electromagnetic impulses at the optimal conditions change the number of fluid inclusions and their temperature distribution, decreasing the number of high temperature fluid inclusions.
- The radiation destruction of fluid inclusions and their treatment with electromagnetic impulses are not connected with direct heating of a mineral, are less expensive, use background irradiation and can be combined with other technologies.
- As dressing continues, the destruction products of fluid inclusions pass into pulp, change its ion composition and affect flotation processes and the composition of return water (Skamnitskaya, Kameneva, 2005).

Acknowledgement

The study was partly supported by RFBR grant 08-01-98804. The authors gratitude to Shimansky S. and Tarkanen I. for management of samples radiation.

References

[1] Roedder, E. (1984): Fluid inclusions. *Reviews In Mineralogy*, Vol. 12, p. 644.

[2] Dolgov, Yu., Yermakov N. (1971): *Thermobarogeochemistry*. Methods To Study Inclusions In Mineral - Forming Media And Their Potential Use, (In Russian), Moscow.

[3] Kravets, B. (1995): Practical Recycling Of Raw Quartz. Izvestie Vuzov. *Gorny Zhurnal* (In Russian), No. 8, p. 160.

[4] Belashev, B., Skamnitskaya, L., Lebedeva, G, Ozerova, G. (2001): Nonconventional Methods For Removal Of Gas-Liquid Inclusions From Quartz. *Geology And Useful Minerals of Karelia* (In Russian), No. 3, p. 131.

[5] Skamnitskaya, L., Kameneva, E., Belashev, B. (2004): Changing The Qualitative Characteristics Of Quartz By Various Power Fields. *Proceedings Of The International Seminar Quartz. Silica*, Syktyvkar, Russia, June (In Russian), p. 52.

[6] Shevyakova, E., Lifshitz, E., Polyashchenko, R. (1980): On The Radiation Resistance Of Natural Minerals Of Various Structural Types. Problems In Atomic Science And Technology. Series: *Radiation Damage Physics And Radiation Study Of Materials* (In Russian), Vol. 50, No. 3, p. 81.

[7] Danilevskaya, L., Skamnitskaya, L., Shchiptsov, V. (2004): *Raw Quartz Materials of Karelia* (In Russian), Petrozavodsk, p. 52.

[8] Moskalyuk, A. (1973): *Determination Of The Composition Of Mineral-Forming Solutions By The Water Extract Method* (In Russian), VSEGEI, St-Petersburg, p. 58.

[9] Chanturia, V., Bunin, I., Ivanova, T., Skamnitskaya, L., Pylova, M. (2004):

The Study Of The Effect Of High Impulses On The Volumetric Properties Of Sulphide-Bearing Products. Modern Methods For Assessment Of The Industrial Properties Of Hardly Dressable And Nonconventional Mineral Products Of Noble Metals And Diamonds And Up-To-Date Reworking Technologies. *Proceedings Of An International Meeting. Plaksin Readings*, Russia, Moscow, October, (In Russian), Moscow, p. 196.

[10] SKAMNITSKAYA, L, KAMENEVA, E. (2005): The Study Of Gas-Liquid Inclusions In Minerals From The Standpoint Of Technological Mineralogy. *Ore Dressing* (In Russian), No. 2, p. 31.

Geochemical and petrogenetic features of schistose rocks of the Okemesi fold belt, Southwestern Nigeria

Geokemične in petrogenetske značilnosti skrilavih kamnin v sistemu gub Okemesi, jugozahodna Nigerija

Olugbenga A. Okunlola & Richardson E. Okoroafor

University of Ibadan, Department of Geology, Ibadan, Nigeria

*Corresponding author. E-mail: o.okunlola@mail.ui.edu.ng

Received: January 13, 2009 **Accepted:** March 18, 2009

Abstract: Schist belts form a dominant component of the Precambrian basement complex of Nigeria. This study of schistose rocks around the Okemesi fold belt, Ife-Ilesha schist belt therefore, is with a view to evaluate their compositional features and petrogenetic affinities and to contribute further to the understanding of the geodynamic evolution of Nigeria's Schist belts.

Three lithologic varieties, namely quartzite, quartz schist and biotite muscovite schist are revealed from systematic mapping and petrographic examinations. Whole rock analytical results of major, trace and rare earth elements of fifteen samples using ICP mass spectrometer method show that the rock units are comparable to those of post Archean pelitic-supracrustal rocks. Variation plots involving Na_2O_3, $Al_2O_{3,}$ and K_2O on one hand and TiO_2 and SiO_2 on the other hand reveal arkosic sedimentary progenitors for the rocks. In addition, La/Th and Th/U ratio suggest that the rocks especially biotite schist is associated with post Archean recycled Upper Crustal sources while Chondrite normalized rare earth signatures of samples further indicate low grade post Archean terrigenous sedimentation of rocks derived from possible mixture of granite- tonalities. Relatively intense weathering and maturity of source rocks is revealed from calculated values of Index of alteration (CIA) and Index of Compositional Variability (ICV). The study further elucidates the possibility of the rocks evolving in a rifted environment of rapid subsidence, followed by closure which led to contemporaneous deformation of the sediments

Original scientific paper

Izvleček: Metamorfni skrilavci so prevladujoča kamnina v predkambrijskem metamorfnem masivu Nigerije. Namen raziskave je določiti sestavo ter nastanek skrilavih kamnin Okemesi pasu, in sicer Ife-Ilesha pasu metamorfnih skrilavcev. Rezultati bodo prispevali k razumevanju geodinamičnega razvoja nigerijskih metamorfnih skrilavcev.

S sistematičnim geološkim kartiranjem in petrografskimi raziskavami smo ugotovili tri litiološke različke – kvarcit, kremenovi skrilavci in biotitno muskovitni blestniki. Z metodo ICP masno spektroskopijo smo določili vsebnost glavnih in slednih prvin ter prvin redkih zemelj v petnajstih vzorcih. Analize so pokazale, da so raziskovani tipi kamnin primerljivi s po-arhajskimi pelitskimi kamninami zgornje skorje. Tako variacijski diagrami Na_2O_3, Al_2O_3, in K_2O kot tudi TiO2 in SiO2 potrjujejo, da je bila izvirna kamnina sedimentna – arkoza.

Razmerji La/Th in Th/U nakazujeta, da so kamnine, zlasti biotitni blestnik, nastale iz po-arhajske reciklirane zgornje skorje. Iz vzorcev hondritsko normaliziranih REE sklepamo, da je bila prvotna kamnina nizko metamorfoziranih arhajskih terigenih sedimentnih kamnin mešanica granitov in tonalitov. Izračunane vrednosti indeksa preperevanja (CIA) in indeksa spremenljivosti sestave (ICV) kažejo na relativno močno preperevanje ter zrelost izvirnih kamnin. V študiji podajamo možnost nastanka kamnin v okolju hitrega pogrezanja razpornega bazena, ki mu je sledilo zapiranje; to je povzročilo sočasno deformacijo sedimentov.

Key words: schist, archean, sedimentary, rifted, compositional
Ključne besede: metamorfni skrilavci, kvarcit, arhaik, sedimentne kamnine, zgornja skorja

INTRODUCTION

Schistose rocks which occur in defined belts are known to be a dominant feature and constitute a distinct component of the western half of the Precambrian Basement Complex of Nigeria. This basement complex itself, apart from the schist belt, is made of the Gneiss- migmatite complex and the Pan African Older Granite rocks. The schist belts are made up of mainly low-medium grade metasediments which are usually associated with minor assemblages of mafic-ultramafic rocks, iron deposits and carbonates (MUOTOH et al., 1988; OKUNLOLA, 2001).

These northerly trending schist belts occur prominently west of 8^0 Meridian (Oyawoye 1964, 1972; Mccurry, 1976). However, it is now known that some extend eastwards of this meridian (Ajibade, 1976; Emeronye, 1988; Eneh et al., 1989; Ekwueme and Shing, 1987). They exhibit distinct petrological and structural features. The belts in the southwest include the Iseyin-Oyan, Igarra, Egbe-Isanlu and Ife-Ilesha schist belts (Rahaman, 1976; Odeyemi, 1977; Elueze, 1981; Annor et al., 1996). The Lokoja-Jakura, Toto-Gadabuike belts (Muotoh et al., 1988; Elueze, 1981; Okunlola, 2001) while the Obudu schist belt is the recently highlighted southeastern belt (Ekwueme & Shing, 1987). So far, there is no complete agreement on delineation, geological nomenclature and geodynamic setting of this major rock unit of the Nigerian Precambrian basement Complex. In this study attempts are made to elucidate the geochemical and petrogenetic features of the schistose rocks around the Okemesi fold belt area, which is a part of the Ife- Ilesha schist belt. The latter has one of the most complex lithological and structural frameworks amongst the Nigeria's metasedimentary belts (Olobaniyi, 2003). The present study, it is hoped will assist in understanding the evolution of this major rock unit of the Precambrian of Nigeria.

Materials and methods

The study involves systematic geological mapping on a scale of 1 : 50 000 collection and thin section study of 15 fresh representative samples of all the lithological units mapped. Four samples each were collected from the quartz schist and biotite muscovite schist and 7 from the quartzite. Variation in sample numbers is largely due to availability of fresh unweathered and uncontaminated samples. For geochemical investigations, collected samples were dried at 60 ^oC, crushed, pulverized and sieved to -80 mesh. A 0.2 g samples aliquot was weighed into a graphite crucible and mixed with 1.5 g of $LiBO_2/LiB_4O_7$ The sample charge was heated in a muffle furnace for 30 min at 980 ^oC. The cooled bead is dissolved in 100 mL of 5 % HNO_3 (ACS grade nitric acid in de-mineralized water). An aliquot of the solution was poured into a propylene test tube. Calibration standards and verification standards are included in the sample sequence. Sample solutions are aspirated into an ICP mass spectrometer (Perkin-Elmer Elan 9000) for the determination of major, minor and rare earth elements at the Acme Laboratories in Vancouver Canada. Quality control protocol incorporates a sample preparation blank (G1) as the first sample in the proce-

dure which is carried through all stages of preparation to analysis. Also, the procedure incorporates a pulp duplicate to monitor analytical precision, a reagent blank to measure background and aliquots of in-house reference material STD SO-18.

RESULTS AND DISCUSSION

Lithological relationship and petrography

The Okemesi Fold Belt lies between Latitudes 7^0 45' and 7^0 52' and Longitudes 4^0 54' and 4^0 50' E and covers an area of 132.25 km^2. It has an antiformal structure comprising massive quartzite, quartz schist, and mica schist with subordinate gneisses and amphibolites (Figure 1). These metasedimentary assemblages has been hitherto referred to as the Effon psammite formation (DE SWARDT, 1953; HUBBARD, et al., 1975).

The quartzite samples are mostly whitish in color but some ferruginized varieties display reddish bands. They are medium to fine-grained, steeply dipping, with an average dip of 54^0 E. They consist mainly of quartz which occurs as irregular fine to medium grained crystals with interlocking grains of muscovite. In thin section, the quartz

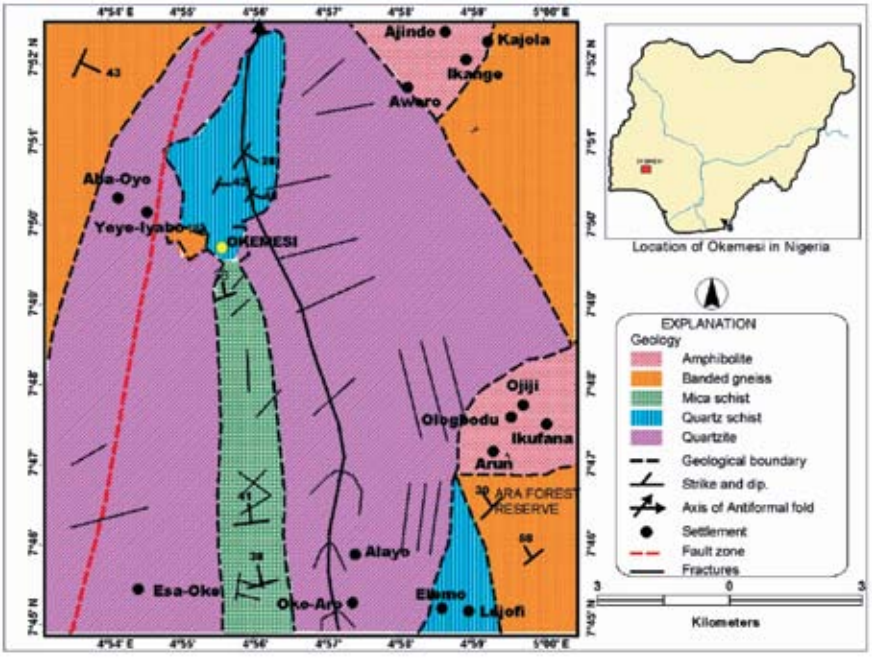

Figure 1. The Geological map of Okemesi fold belt.

grains are colorless to grey in transmitted light. The quartz schist which forms the innermost parts of the Okemesi anticline, occur as low-lying outcrops. They are fine to medium–grained, display incipient schistosity and contain quartz, microcline, muscovite with accessory hematite and zircon. Quartz occurs as randomly oriented crystals. Two generations are evident. The first one is coarser grained, usually anhedral and elongated parallel to the fabric. Some grains exhibit wavy extinction. The finer grained variety occurs as localized granoblastic aggregates and show uniform extinction. This variety may likely be of secondary origin. Microcline which is present in minor amounts as crosshatched twinned elongate fine blasts are located sometimes in intergranular spaces of the interlocking quartz blasts.

The biotite- muscovite schist also occurs in lowland areas between the quartzite ridges and trend generally in the NNE-SSW direction. The foliation on the outcrop is defined by mica streaks, particularly biotite. The schist is generally coarse-grained and contains mainly muscovite, biotite and minor quartz. In thin section, quartz occurs as coarse-grained, stretched, and white to greyish anhedral blasts. Biotite occurs as light brown leaflet sometimes slender and prismatic with occasional stumpy laths and is pleochroic from light brown to reddish brown. Muscovite is subhedral, showing alignment in the foliation plane (Figure 2). Plagioclase is of oligoclase-andesine composition, mostly colourless but in the absence of twinning it is often distinguished from quartz by the alteration to sausurite. Euhedral to subhedral garnet is predominantly almandine with minor amounts of spessartine and grossularite. They sometimes exhibit poikiloblastic texture and are characterized by inclusion of fine quartz and some mica. The schistose rocks occur in association with banded gneiss and amphibolites which occupy mainly the outer portions of the anticline and are more prominent in the eastern side.

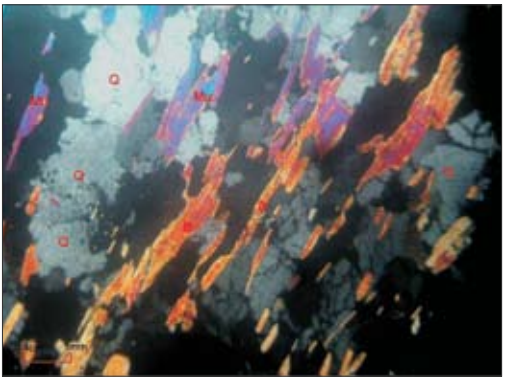

Figure 2. Photomicrograph of biotite-muscovite schist in transmitted light showing Quartz (Q), Biotite (B), and Muscovite (Mu)

The banded gneiss consists of alternating bands of felsic minerals notably

plagioclase feldspars and quartz, and the dark bands consisting of biotite and hornblende. Quartz is present as coarse-grained randomly oriented crystals. The amphibolite which is mostly low lying is laminated in places with leucocratic bands of plagioclase and quartz. Hornblende is the main mineral with minor quartz and plagioclase. Quartz is heterogranoblastic, colourless in transmitted light and in some parts, fractured. The hornblende crystals are pleochroic from brown to light green.

Geochemical features

From the results of the major oxide data (*w*/%), trace and rare earth element (μg/g) composition presented in Tables 1 and 2, the Okemesi metasedimentary rocks are generally siliceous, ($w(SiO_2) > 65$ %) with quartzite being chemically similar to quart-sandstones (BLATT, et. al., 1972). These values are also similar to those for the Jebba quartzite and micaceous quartzite, central Nigeria (OKONKWO, 2006).

Table 1. Major Element Oxides (*w*/%) results of schistose rocks from Okemesi

	1	2	3	4	5	6	7	8	9	10	11	12	13	14	15
SiO_2	88.91	81.11	83.32	84.17	65.31	65.42	65.38	96.97	96.64	94.18	94.10	94.21	96.61	94.21	94.67
Al_2O3	6.52	9.37	8.51	8.21	13.55	13.81	13.82	0.79	1.17	4.11	2.34	1.98	2.31	2.62	2.11
Fe_20_3	0.68	1.29	1.21	1.63	6.30	6.41	6.42	1.22	0.74	0.38	2.1	2.45	0.52	2.41	1.56
MnO	0.0 11	0.02	0.02	0.01	0.01	0.01	0.01	0.01	0.01	0.01	0.01	0.01	0.01	0.01	<0.01
MgO	0.08	0.75	0.71	0.80	2.97	2.64	2.61	0.07	0.12	0.09	0.09	0.06	0.11	0.12	0.11
CaO	0.11	0.410	0.12	0.11	0.11	0.12	0.13	0.12	0.14	0.10	0.09	0.12	0.10	0.11	0.13
Na_2O	0.14	0.68	0.61	0.58	0.14	0.13	0.14	0.01	0.02	0.01	0.04	0.03	0.02	0.02	0.03
K_2O	1.76	3.89	3.11	2.64	1.76	2.1	2.5	0.04	0.21	0.07	0.08	0.06	0.05	0.04	0.07
P_2O_5	0.10	0.22	0.17	0.11	0.10	0.20	0.21	0.03	0.03	0.02	0.03	0.02	0.01	0.01	0.03
$Ti0_2$	0.24	0.23	0.23	0.22	0.24	0.31	0.32	0.05	0.07	0.20	0.16	0.07	0.08	0.07	0.08
Cr_2O_3	0.011	0.012	0.012	0.013	0.011	0.021	0.019	0.046	0.048	0.017	0.020	0.043	0.021	0.042	0.045
LOI	1.2	1.8	1.2	1.3	1.2	1.3	1.3	0.7	0.8	0.8	1.0	1.0	1.0	0.9	1.0
Total	99.75	99.79	99.22	99.99	99.75	99.86	99.81	100.05	99.99	99.98	99.97	99.95	100.83	100.6	99.83

1, 2, 3 and 4 = Quartz Schist
5, 6 and 7 = Biotite-muscovite Schist
8–15 = Quartzite

Table 2. Showing Trace Elements (μg/g) analytical results of rocks from Okemesi

	1	2	3	4	5	6	7	8	9	10	11	12	13	14	15
Sc	13	4	7	6	2	6	4	ND	1	1	1	1	1	ND	1
Be	2	1	2	2	3	2	3	ND	4	2	1	4	2	1	2
V	63	ND	61	61	21	45	40	ND	ND	ND	8	ND	ND	8	8
Ba	93	911	902	880	968	942	902	85	15	60	42	65	62	59	71
Sr	325	201	202	362	64	58	60	12	27	46	32	40	55	31	28
Y	44	47	45	42	33	36	38	32	16	32	22	18	5	10	21
Zr	630	133	589	579	733	829	812	211	318	93	242	200	195	181	262
Co	11	ND	10	10	3	4	4	1	1	1	1	1	1	1	1
Ni	25	20	24	20	20	21	22	20	20	3	4	3	3	3	3
Cu	29	4	4	28	2	3	3.8	6	3	3	4	4	5	4	3
Zn	88	2	81	71	14	30	28	5	5	4	4	5	4	4	3
Ga	20	7	11	10	7	11	10	1	4	4	3	5	5	5	4
As	ND	ND	ND	ND	ND	ND	ND	5	5	ND	ND	3	ND	ND	ND
Rb	127	76	108	109	118	120	119	31	26	35	25	14	31	21	21
Nb	21	11	20	20	6	6.5	6	5	4	5	5	2	3	4	5
Sn	8	11	7	8	2	4	4	1	1	1	1	1	1	1	2
Cs	2	2	2	2	4.5	2	2	ND	2	3	5	6	6	5	4.
Au	ND	ND	ND	ND	1	1	1	ND	ND	ND	ND	ND	ND	ND	ND
Rb/Sr	0.39	0.38	0.54	0.30	1.84	1.98	1.98	2.55	0.96	0.75	0.78	0.34	0.57	0.67	0.76
Sr/Ba	0.35	0.22	0.22	0.41	0.07	0.07	0.07	0.15	1.85	0.78	0.75	0.63	0.89	0.52	0.39

1, 2, 3 and 4 = Quartz Schist
5, 6 and 7 = Biotite-muscovite Schist
8–15 = Quartzite

Average Al_2O_3 content is lowest in the quartzites (1.93 %). The biotite muscovite schist has a much higher average value of Al_2O_3 (13.92 %) than the quartz schist (8.15 %). The same trend is also noticeable in the mean Fe_2O_3 content of the metasediments where the values are less than 7 %. Mean MnO content is generally low (< 0.15 %) in the entire samples. These trends prob-

ably denote an increase in chemically unstable grains (lithic components) with decrease in quartz content. The values are however within the range for metasediments (WEAVER, 1989). Average MgO, CaO, and Na_2O values are generally less than 0.60 % except for the mica schists that have a mean MgO value of 2.74 %. Mean K_2O content is highest in the quartz schist with the quartzites having the lowest value of 0.57 %. The depleted MnO, Na_2O may suggest paucity of movement of metamorphic remobilized fluids during the Pan African or earlier events. Some of Nigeria's schist belt especially the shear zones host auriferous quartz that are presumed to be formed by metamorphic dewatering of the country rocks during the Pan African tectonic phase. (OLOBANIYI, 2003) This result therefore, explains the paucity of auriferous veins as noted in an earlier study around this sector of the Ife-Ilesha Schist belt compared to the more mineralized eastern parts about 80 km from this study area (ELUEZE, 1992) . The values are still within those for metasedimentary rocks (BROWN et al., 1979) and comparable to that of Scottish metapelites (OKONKWO, 1992), Igarra quartz mica schist (OKEKE & MEJU, 1985) and Burum Marble (OKUNLOLA, 2001). Average TiO_2 is highest in the biotite muscovite schist, 0.21 % for the quartz schist and 0.29 % for the mica schist, whereas the quartzite has a mean TiO_2 value 0.10 %. Mean Cr_2O_3 content is generally low in all the samples of both the schists (0.012–0.017 %) and the quartzite (0.035 %). Compared with the post Archean metasediments, the Okemesi rocks are depleted in CaO and Al_2O_3, while they are richer in K_2O when compared with the Archean mudstone (TAYLOR & MCLENNAN, 1985). Also a seemingly positive trend is noticed between the Al_2O_3 and TiO_2 values in the biotite muscovite schist, suggesting that TiO_2 may have been held in the clay mineral lattices. (Figures 3 and 4).This is, unlike the indiscernible or scattered trend in the quartzite and the quartz schist, suggesting that both oxides are contained in the heavy mineral phases. Conversely Zr and Nb in the quartz schist shows a positive trend and this suggest their containment in the heavy mineral phases (Figure 5).

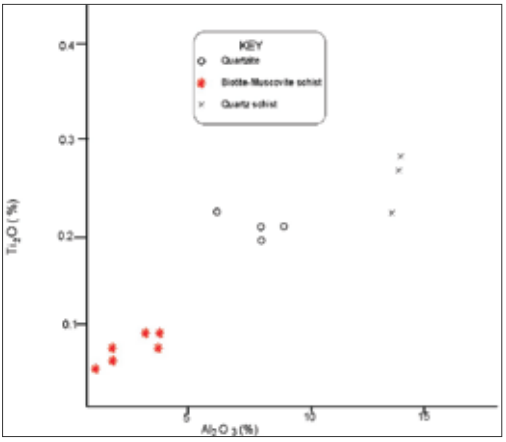

Figure 3. TiO_2 versus Al_2O_3 plot of rocks from Okemesi

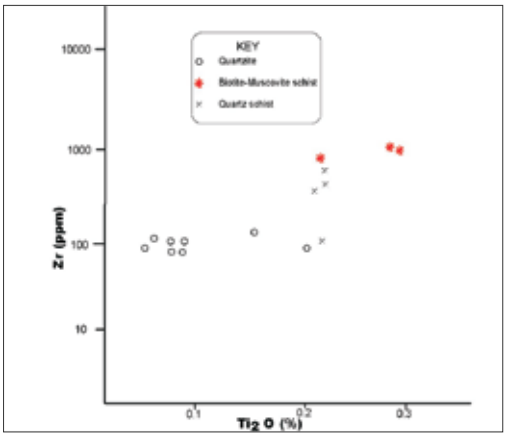

Figure 4. Zr versus TiO_2 plot of rocks from Okemesi

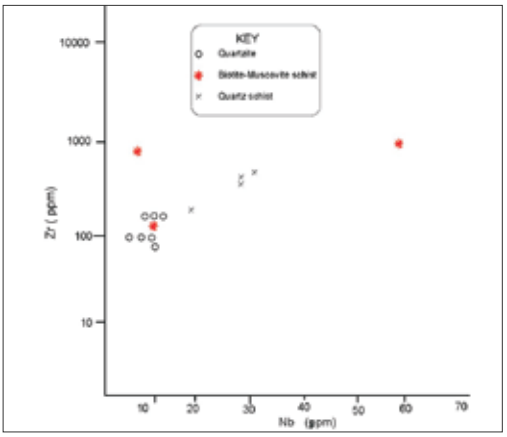

Figure 5. Zr versus Nb plot of rocks from Okemesi

Ba, Sr, Rb and Zr concentrations are more enhanced in the quartz schist than in the quartzite (Table 2) but are well within the range for supracrustal rocks (Brown et al., 1979; Babcock et al, 1979). In particular, the high Zr content may reflect the presence of detrital zircon in the rocks (Elueze, 1981). Zn, Cu and Co content (μg/g) is generally low. The schistose rocks are generally low in Sr/Ba ratios (< 0.4 %). However, Rb/Sr ratio (> 0.4 %) is typical for pelitic metasediments (Van De Kamp, 1968).

The petrogenetic character of the rocks as established on the Na_2O/Al_2O_3 versus K_2O/Al_2O_2 diagram (Garrels & Mackenzie, 1971) (Figure 6) shows that the rocks are largely of sedimentary origin. In the MgO-CaO-Al_2O_3 diagram (Figure 10) (Leyleroup, et al., 1977) the samples plot outside the magmatic field which also supports the sedimentary antecedent of the rocks. These features are similar to those for Ilesha metasediments (Elueze, 1981), Birnin Gwari schist (Ajibade, 1980) and Jebba schists (Okonkwo & Winchester, 1996; Okonkwo, 2006). However, the Na_2O versus K_2O plot (Pettijohn, 1975) (Figure 7) shows possible arkosic affinity of the metasediments, but the discrimination function diagram (Roser & Korsch,1988) (Figure 8) shows that the samples are generally of quartzose sedimentary provenance with the samples plotting deep into the quartzose sedimentary field. The TiO_2-K_2O-P_2O_5 plot (Pearce et al., 1975) (Figure 9) confirms the continental nature of the sediments. On the Al_2O_3–CN–K_2O plot, (Figure 10) the biotite schists and the quartzite plot close to the illite and kaolinite fields while the quartz schist plot close to the average shale. The relatively high content of Ba

in contrast to Rb indicates the contribution of felsic components since Ba indicates K-feldspar-rich source rocks. (OKONKWO, 1992; OKONKWO & WINCHESTER, 1998) In addition, TAYLOR & MCLENNAN, (1985) have indicated the importance of such immobile trace elements as Th and La in provenance determinations of pelitic metasediments because they often reflect those of source rocks. The Th content of Okemesi metasediments (1.4–43.3 μg/g) is comparable to those derived from granitic composition. Also most of the samples analysed have low La/Th and Th/U especially those for the biotite

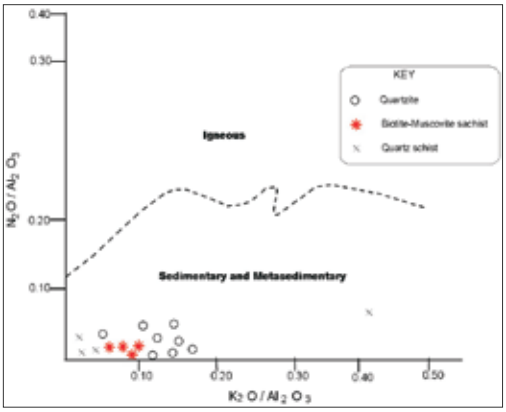

Figure 6. Na_2O/Al_2O_3 against K_2O/Al_2O_3 plot for the Okemesi metasediments (Garrells & MACKENZIE, 1971)

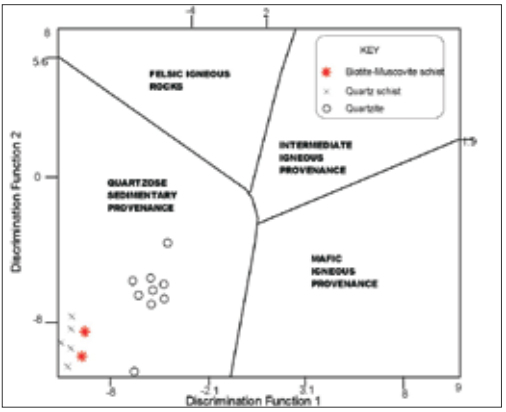

Figure 8. Discrimination Function Diagram of rocks from Okemesi (ROSER & KORSCH, 1988)

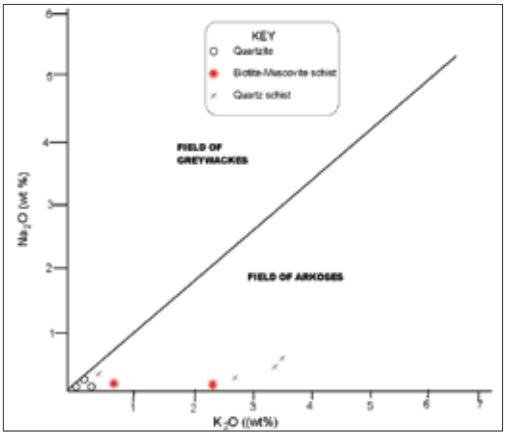

Figure 7. Na_2O versus K_2O plot of rocks from Okemesi (PETTIJOHN, 1975)

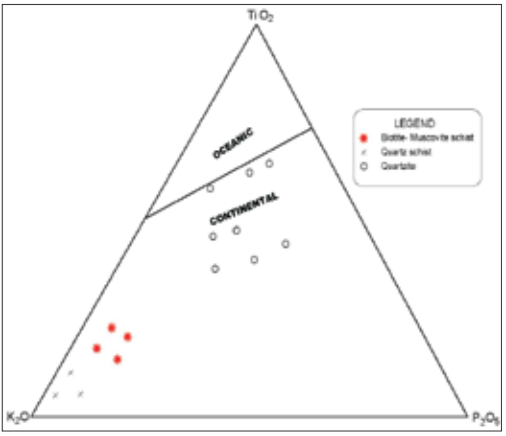

Figure 9. TiO_2-K_2O-P_2O_5 plot of rocks from Okemesi (PEARCE et al., 1975)

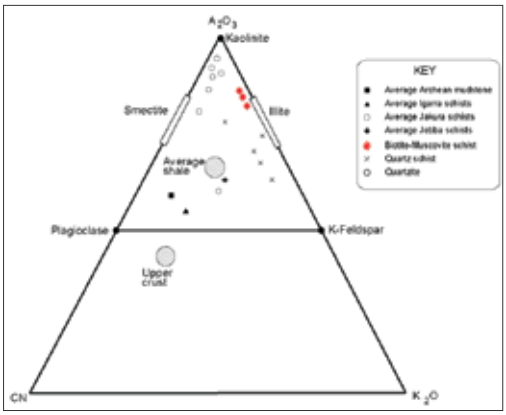

Figure 10. Al_2O_3-CN-K_2O plot for the Okemesi rocks

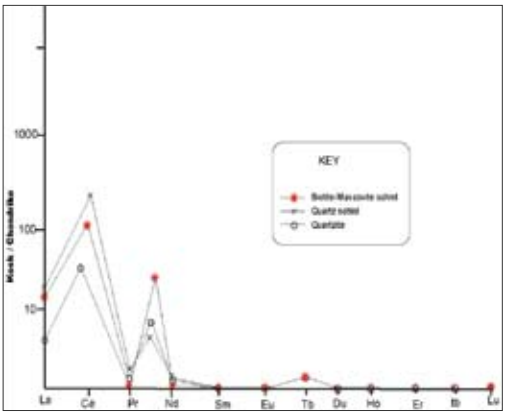

Figure 11. Chondrite normalised REE plot of the Okemesi rocks

muscovite schists. This feature is normally associated with post Archean recycled upper crust sources (Leyleroup et. al., 1977; Taylor et. al., 1986).

The rock samples generally exhibit REE values and patterns typical of low grade Post Archean terrigenous sediments with variable enriched steep LREE and almost flat HREE with no discernible Eu anomaly. (Table 3, Figure 11). La/Yb ratio is also high, resembling the Yellowknife and Pilbara metasediments (Mclennan et al., 1983). These features suggest sediment derivation from a source dominated by felsic igneous rocks (Mclennan & Taylor, 1984). Taylor and co workers, (1986) have also suggested that sediments with steep LREE enrichments and low $Al2_2O_3/Na_2O$ ratio point to derivation from a possible mixture of granite–tonalite rocks to produce the sedimentary protolith.

The results of the Chemical Index of Alteration (CIA) (Nesbitt & Young 1982; Okunlola, 2003) reveal average values of 69.7 %, 85.9 % and 91.2 % for the quartz schist, mica schist and quartzite (Table 4). These values point to relatively intense chemical weathering of the source rocks. The Index of Compositional Variability (ICV) (Cox & Lowe, 1995) which measures the abundance of alumina relative to other constituents of the rock, except SiO_2, show that the quartz schist, biotite-mucovite schist and the quartzite have an average ICV values of 0.68, 0.85 and 0.83 respectively (Table 4). Compositionally immature pelitic rocks have high ICV, whereas mature pelititc rocks with very little non silicates or those rich in kaolinite group clay minerals possess low values (< 0.6) (Elueze & Okunlola, 2003). The calculated ICV value for the quartz schist (0.68) shows the matured nature of the sedimen-

tary protolith prior to metamorphism. Mature to moderately mature pelitic metasediments are characteristic of relatively stable cratonic environments (WEAVER, 1989). This may be marked by sediment recycling or moderate to very intense chemical weathering of first cycle material (BERSHAD, 1966).

In terms of the geodynamic evolution of the rocks in the study area, The Ife-Ilesha schist belt has been thought by earlier workers to be an ensialic basin in an environment of thin and attenuated Crust (AJIBADE, 1976; ELUEZE, 1992; ANNOR, et.al., 1996). Therefore, the occurrence of sub greywacke rocks in the study area as evidenced, suggests a rapidly subsiding depocenter basin, or that there existed much difference in topographic elevation between the sediment source and depocenter. However, since typical deep water sediments and proximal distal-facies variations are absent, there is the possibility that only a moderate depth and width was attained in the basin in the absence of the development of a fully mature ocean. The rapid subsidence of the basin was accompanied contemporaneously with tectonic instability resulting in antiformal deformation and multidirectional fracturing. This may have aided the rapid removal of the sediments before deep weathering and mineralogical maturity was attained. This activity probably accounts for the shallowness of the depth of the basin. Similar characteristics have been noted for the Isanlu schist belt, central Nigeria (OLOBANIYI, 2003). The Nigeria's schist belt is believed to have evolved as a result of an initial continental extensional stage culminating in rift openings and sedimentation with contemporaneous magmatism in the formed basins. These processes were followed by basin closure which led to the deformation of sediments. (AJIBADE, et.al., 1987; ELUEZE, 1992). As seen in this study from petrographic and chemical signature, the Okemesi schistose rocks, which outcrops in the eastern part of the Ife- llesha schist belt,have most probably evolved in a rifted environment of rapid subsidence.

CONCLUSIONS

Systematic geological mapping, petrographic and geochemical evaluation of schistose rocks around the Okemesi fold belt show that the metasedimentary assemblages which form the inner portion of the Okemesi anticline are continental post Archean supracrustals. The sedimentary protolith prior to metamorphism and tectonism have had arkosic affinity and may have also been derived from original source rocks rich in felsic components. However, the discriminant plot of ROSER & KORSCH (1988), suggests contribution from a quartzose sedimentary provenance. Calculations of the Chemical Index of

Alteration (CIA) and Index of Compositional Variability (ICV) show that the schistose rocks are metamorphosed from intensely weathered and mature sediments. Furthermore, the REE signatures confirm the possible contribution of material to the sedimentary protolith from a mixture of granite and tonalite rocks. The rocks are believed to have evolved in a rifted environment accompanied by rapid subsidence.

Acknowledgement

This study has benefited from the assistances of numerous friends and colleagues. The staff of ACME laboratories, Vancouver Canada are specially appreciated for their assistance during the geochemical analysis.

References

[1] Ajibade, A. C. (1976): Provisional Classification and Correlation of the schist belt of Northwestern Nigeria. *Geology of Nigeria*; Kogbe C. A., (ed). Elizabethan Pub. Co., Lagos, pp. 85–90.

[2] Ajibade, A. C. (1980): *Geotectonic evolution of Zunguru Region, Nigeria*. Unpbl PhD Thesis, University of Wales Aberyswyth, 421p.

[3] Annor, A. E., Olobaniyi, S. B. & Muche, A. (1996): A note on the geology of Isanlu in the Egbe-Isanlu schist belt, S.W. Nigeria. *J. Min. Geol.*; Vol. 32(2), pp.47–51.

[4] Blatt, H., Middleton, C. & Murray, R. (1972): *Origin of sedimentary rocks*. Prentice-Hall Inc. Englewood Cliffs, New Jersey. 643p.

[5] Bershad, I. (1966): *The effect of a variation in precipitation on the nature of clay mineral formation in soils from acid and basic igneous rocks*. Proceedings, International; Clay Conference; pp. 167–173.

[6] Brown, E. H., Babcock, R. S. & Clark, M. D. (1979): *Geology of Precambrian rocks of Grand Canyon in Petrology and structurew of Vishu Complex*. Prec. Res. 8, pp219–241.

[7] Cox, R & Lowe, D. R. (1995): Controls on sediment composition on a regional scale. *Conceptual view*; J Sed. Res. A. 65: pp. 1–12.

[8] De Swardt, A. M. J. (1953): The Geology of Country around Ilesha. *Geological Survey of Nigeria*; Bulletin, Vol. 23, 54p.

[9] Ekwueme, B. N. & Shing, R., (1987): Occurrence, Geochemistry and Geochronology of mafic-Ultramafic rock in the Obudu Plateau S.E. Nigeria in Srivasta R.K. and Chadta, R. (eds) Magmatism relation to diverse tectonic settings.

[10] Elueze, A. A (1981): Dynamic metamorphism and oxidation of amphibolites, Tegina area, north western Nigeria. P*recambrian Res*.; Vol. 14, pp. 368–379.

[11] Elueze A. A. (1992): Rift System for Proterozoic schist belt in Nigeria. *Tectonophysics*; Vol. 209, pp 167–169.

[12] ELUEZE, A. A., & OKUNLOLA, A. O. (2003) : Petrochemical and petrogenetic characteristics of Metasedimentary Rocks of Lokoja-Jakura Schist belt, Central Nigeria. *Journal of Mining and Geology*; Vol. 39(11), pp. 21–27.

[13] ELUEZE, A. A & OKUNLOLA, O. A. (2003): Petrochemical and Petrogenetic characteristics of metasedimentary rocks of Lokoja-Jakura schist belt, Central Nigeria. *Journal of Mining and Geol.*; Vol. 39 (1), pp 21–27.

[14] EMERONYE, B. F. (1988): Appraisal of manganese mineralization around Ikpeshi, Bendel State, Nigeria. Abstract of seminar GS.N. 5p.

[15] ENEH, K. E., MBONU, W. C. & AJIBADE A. C. (1989): The Nigerian metasedimentary belts. Facts, fallacies and New Frontiers. In: Oluyide P.O (ed) *Precambrian geology of Nigeria Geol.*; Surv. Nigeria. 201p.

[16] GARRELS, R. M. & MACKENZIE F. F. (1971): Evolution of Sedimentary Rocks. W M Norton and Co., New York, 394 p.

[17] HUBBARD, F. H., 1975: Precambrian crustal development in Western Nigeria: Indications from the Iwo region. *Geology Society of America Bulletin*; Vol. 86, p. 548–55.

[18] LEYLEROUP, A., DUPPY, C. & ANDRIANMBOLONA, R. (1977): Chemical Composition and consequence of Evolution of the French Massive Central Precambrian crust. *Mineral Petrol*; Vol. 62, pp. 283–300.

[19] MCCURRY, P. (1976): The Geology of the Precambrian to Lower Paleozoic rocks of Northern Nigeria – a review In: C.A.Kogbe (Editor). *Geology of Nigeria*; *Elizabethan Publ.*, Lagos, pp. 15–39.

[20] MCLENNAN, S. M., TAYLOR, S. R. (1984): Archean sedimentary rocks and their relation to the composition of the Archean continental crust. *Archean Geochemistry* (eds. A. KRONER, G. N. HANSN and A.M. GOODWIN), pp. 47–72, Springer-Verlag, Berlin, Heidelberg.

[21] MCLENNAN, S. M., TAYLOR, S. R. & ERIKSSON K. A. (1983): Geochemistry of Archean shales from the Pilbara Supergroup, Western Australia. *Geochim. Acta*; Vol. 47, 1211–1222.

[22] MUOTOH, E. O. G., OLUYIDE, P. O., OKORO, A. U. & MOGBO, O. E.(1998): The Muro Hills baded iron formation G.S.N. Annotated technical reports; 1358. pp. 15–25.

[23] NESBITT, H. W. & YOUNG, G. M. (1982): Early Proterozoic Climates and Plate Motions Infered from Major Element Chemistry of Lutites. *Nature 199*; pp. 715–717.

[24] ODEYEMI, I. B (1977): The basement rocks of Bendel state of Nigeria. Unpublished Ph. D. Thesis. University of Ibadan.

[25] OKEKE, P. O. & MEJU, M. A. (1985): Chemical evidence for the sedimentary origin of Igarra Supracrustal rocks S.W. Nigeria. *Jour. Min. and Geol.*; Vol. 22 (1 and 2), pp. 97–104.

[26] OKUNLOLA, O. A. (2001): Geological and Compositional Investigation of Precambrian Marble Bodies and associated Rocks in the Burum and Jakura

areas, Nigeria. Ph.d Thesis, University of Ibadan, Nigeria, 193p.

[27] Okonkwo, C. T (1992): Structural geology of basement rocks of Jebba area, Nigeria. *Journal of Mining and Geology*; Vol. 28(2), pp. 203–209.

[28] Okonkwo, C. T. (2006): Chemical Evidence for the Sedimentary Origin of Igarra Supracrustal Rocks S.W. Nigeria. *Journal of Mining and Geology*; Vol. 22, pp 97–104.

[29] Okonkwo. C. T. & Winchester. J. A. (1996): Geochemistry and Geotectonic Setting of Precambrian Amphibolites and Granititc Gneisses in the Jebba Area, Southwestern Nigeria. *Jour. Min. Geol.*; Vol. 32(1), pp 11–18.

[30] Okonkwo, C. T. & Winchester, J. A. (1998): Petrochemisry and petrogenesis of migmatitic gneisses and metagreywackes in Jebba area southwestern Nigeria. J*ournal of Mining and Geology*; Vol. 36 (1), pp 1–8.

[31] Olobaniyi, S. O. (2003) Geochemistry of semi politic schist of Isanlu area, Southwestern Nigeria: Implication for the geodynamic evolution of the Egbe-Isanlu Schist belt. *Global Journal of Geological Sciences*; Vol. 1, No. 2, pp. 113–127.

[32] Oyawoye, M. O., (1964). The petrology of a potassic syenite at Shaki, Western Nigeria: Contrib. *Min. Petrol.*; Vol. 16.

[33] Oyawoye, M. O. (1972): The Basement Complex of Nigeria, in, Dessauvagie T.F.J. and Whiteman A. J. (Eds) Africa Geology, University of Ibadan, pp 66–82.

[34] Pearce, .M., Gorman, B. E. & Birkett, T. C. (1975): The Relationship between Major Element Chemistry and Tectonic Environment of basic and intermediate Volcanic Rocks. *Earth. Sci. Lett.*; Vol. 36, pp 121–132.

[35] Pettijohn, T. J. (1975): Sedimentary Rocks. Harper and brothers, New York, 718 pp.

[36] Rahaman, M. A. 1976: Review of the Basement Geology of Southwestern Nigeria. In: Kogbe,C. A. (Ed.). *Geology of Nigeria*, an Elizabethan Publishing Company, Lagos, 41–57.

[37] Roser, B. P., & Korsch, R. J. (1988): Provenanace Signatures of sandstone-mudstone Suites determined using discriminant Function Analysis of Major Element Data. *Chem. Geol.*; Vol. 67, pp. 119–139.

[38] Tarney, J. (1977): Petrology, mineralogy and geochemistry of the Falkland Plateau basement rocks. Site 30, deep sea drilling project, Initial Report, 36, pp. 893–920.

[39] Taylor, S. R & Mclennan, S. M. (1985): The continental crust: Its composition and Evolution. Oxford, 311p.

[40] Taylor, S. R., Roberta, L. R., McLannan, S. M. & Eriksson, K. A. (1986): Rare Earth Element patterns in Archean high-grade metasediments and their tectonic significance.*Geochimica e:Cosmochimica Acta.* Vol. 50, pp. 2267–2279.Blackwell.

[41] Weaver, C. E. (1989): Clays, muds and shales. *Elsevier*; Amsterdam, 820p.

Lower Jurassic carbonate succession between Predole and Mlačevo, Central Slovenia

Spodnjejursko karbonatno zaporedje med Predolami in Mlačevim, osrednja Slovenija

Stevo Dozet[1]

[1]Geološki zavod Slovenije, Dimičeva ulica 14, SI-1000 Ljubljana, Slovenija

*Corresponding author. E-mail: stevo.dozet@geo-zs.si

Received: March 4, 2009 **Accepted:** April 8, 2009

Abstract: The paper deals with Lower and Middle Jurassic carbonate succession sotheasterly of Ljubljana in the area belonging to the northern margin of the Dinaric Carbonate Platform. The Lower Jurassic carbonate succession between Predole and Mlačevo is composed of five lithostratigraphic units that in view of biostratigrafy belong to the cenocona *Palaeodasycladus mediterraneus* (Pia). In the topmost part of the Lower Jurassic stratigraphic sequence there is an unfossiliferous interval zone of the platy Spotty Limestones. The considered rocks are developed in a shallow-water carbonate facies lying conformably upon the Norian-Rhaetian variously grey bedded dolomite in Lofer development, the Main Dolomite respectively. The passage of the micritic Lower into oolitic Middle Jurassic limestones is gradual. In the Lower Jurassic carbonate sequence, where limestones strongly prevail over dolomites, occur thinner and thicker sedimentary rhythms of subtidal and intertidal environments. The first and especially the last unit of the Lower Jurassic carbonate succession between Predole and Mlačevo are poor in fossils. In central more or less fossiliferous unit play most important role alga *Palaeodasycladus,* benthic foraminifer *Orbitopsella*, lithiotid bivalves and corals. Important are also megalodontid bivalves that appear already in the Rhaetian and Lowermost Jurassic part of the Mesozoic stratigraphic sequence. Lithiotid and megalodontid bivalves occur in the form of

Original scientific paper

lumachelles composing biostromes, whereas the corals build minor mud mounds. Nonfossiliferous dark platy Spotty Limestones were deposited in restricted parts of shelf, where there were no favourable conditions for greater diversity of organisms. In geotectonic regard is the investigated area a part of External Dinarides.

Povzetek: Članek obravnava spodnje in srednjejursko karbonatno zaporedje plasti jugovzhodno od Ljubljane na ozemlju, ki pripada severnemu robu Dinarske karbonatne platforme. Spodnjejursko karbonatno zaporedje med Predolami in Mlačevim je sestavljeno iz petih litostratigrafskih enot, ki biostratigrafsko pripadajo cenoconi *Palaeodasycladus mediterraneus* (Pia). Prav na vrhu je nefosiliferna intervalna cona ploščastih marogastih apnencev. Obravnavane kamnine so razvite v plitvovodnem karbonatnem faciesu. Leže konkordantno na norijsko-retijskem, različno sivem plastnatem dolomitu v loferskem razvoju oziroma na Glavnem dolomitu. Prehod mikritnih spodnjejurskih v oolitne srednjejurske apnence je postopen. V karbonatni spodnjejurski skladovnici, v kateri močno prevladujejo apnenci nad dolomitom, se pojavljajo tanjši in debelejši ritmi sedimentov podplimskega in medplimskega okolja. Prva in še zlasti zadnja enota spodnjejurskega karbonatnega zaporedja med Predolami in Mlačevim sta revni s fosili, v osrednjih fosilifernih plasteh pa igrajo pomembno vlogo alga *Palaeodasycladus*, bentična foraminifera *Orbitopsella* in litiotidne školjke. Zelo opazne so tudi megalodontidne školjke, ki se pojavljajo že v retijskem in spodnjejurskem delu mezozojske skladovnice. Litiotidne in megalodontidne školjke se pojavljajo v obliki lumakel ozorima horizontov, korale pa ponekod tvorijo manjše kopaste grebene. S fosili revni, temni, ploščasti marogasti apnenci so nastajali v zatišnih delih šelfa, kjer ni bilo ugodnih pogojev za večjo raznolikost organizmov. V geotektonskem pogledu je raziskano ozemlje del Zunanjih Dinaridov.

Key words: stratigraphy, shallow marine carbonate rocks, litho- and biostratigraphic subdivision, Lower and Middle Jurassic, External Dinarides, Slovenia

Ključne besede: stratigrafija, plitvomorske karbonatne kamnine, lito- in biostratigrafska razdelitev, spodnja in srednja jura, Zunanji Dinaridi, Slovenija

Introduction

In this article are applied data obtained during geological mapping for elaboration of Geological Map of Slovenia on the scale of 1:50 000 on the Map Sheet Grosuplje performed in the years 2005 to 2007 by Stevo Dozet.

With our research work we intend to define, above all, the stratigraphy of the Lower Jurassic sedimentary succession and to carry out lithostratigraphic and biostratigraphic subdivision in formations, unit, cenocones and subcones, what will be useful for elaboration of the geologic formation-map of this ter-

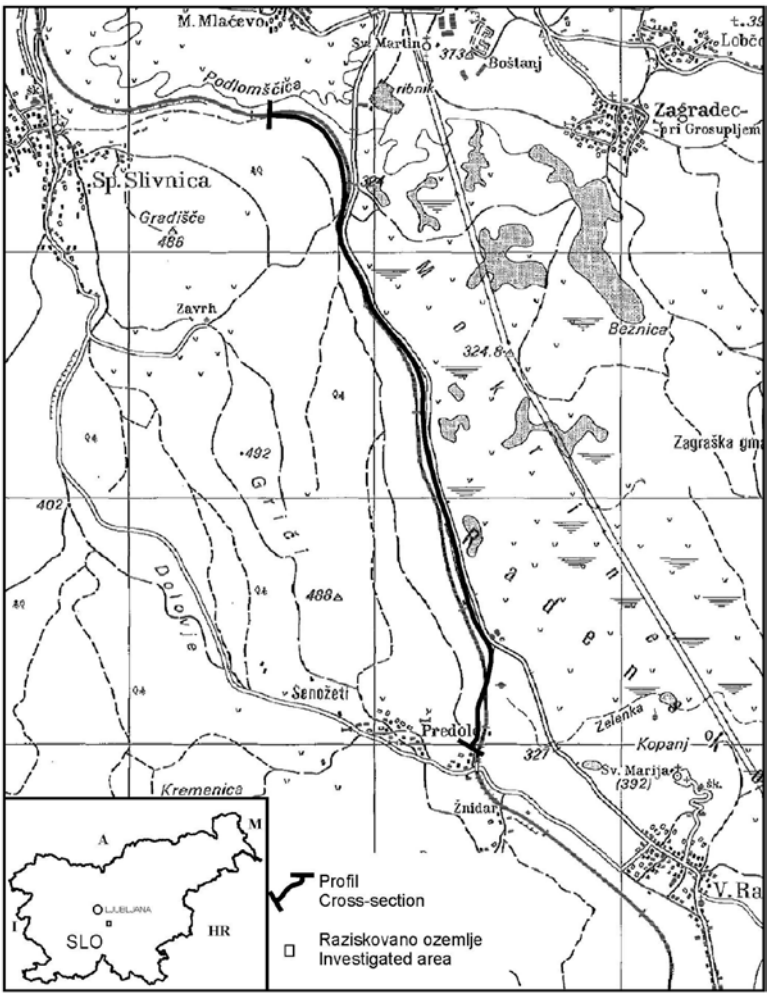

Figure 1. Location map of the investigated area

ritory. Next to the Lower Jurassic carbonate sequence we intend to research more in detail also rocks and their fossil contents at the lower and upper boundary of the discussed stratigraphic sequence.

Geological setting. The mapping area (Figure 1) lies on the Map Sheet Grosuplje on the scale of 1:25 000 (N°136) southeast of Ljubljana respectively on the western border of Radensko polje extending on the distance of 3.5 kilometers in the area between Spodnja Slivnica, Mlačevo and Predole at Račna. The Lower Jurassic carbonate rocks build smaller hills Gradišče (486 m) and Griči (492 m and 488 m) extending continually in NW-SE direction.

In structural respect the investigated area represents one of smaller tectonic units of External Dinarides defined by northwestern-southeastern (NW-SE) faults (BUSER, 1974; PLACER, 1998) belonging to the northern margin of Dinaric Carbonate Platform (BUSER, 1989).

Previous investigations. The oldest registered data on geologic structure of the considered area could be found in works of M. V. LIPOLD (1858), who in the Dolenjska and Notranjska regions attributed a greater part of Jurassic beds to Triassic. KERČMAR (1961) researched Jurassic beds in the area between Krka, Videm and Ilova gora. In the Explanatory text of the Map Sheet Ribnica BUSER (1969, 1974) described principal geological mapping lithostratigraphic units of this area. Tectonically he ranged the investigated area to the Dolenjska-Notranjska Mesozoic Blocks, paleogeographically however, to the Dinaric Carbonate Platform (BUSER, 1989). ŠRIBAR and coworkers (1966) investigated Jurassic sediments between Zagradec and Randol in the Krka valley. Within the framework of geologic investigation for his doctor's degree STROHMENGER (1988) carried out under the guidance of his comentor DOZET sedimentological and geochemical investigations in the cross-sections Kompolje (Mala gora) and Krka-Mali Korinj in Suha krajina (STROHMENGER & DOZET, 1991; STROHMENGER et al., 1987 a, b). DOZET (1993) recorded the complete Lofer cyclothems in lower part of the Lower Jurassic beds in the Krka area that compose the slovenian part of External Dinarides. BUSER and DEBELJAK (1994/95) determined rich findings of lithiotid bivalves. DEBELJAK & BUSER (1998) added the lithiotid horizon to Pliensbachian respectively Domerian. DOZET & ŠRIBAR (1981, 1997) and DOZET (1990 a) recognized and proved almost all litho- and biostratigraphic units applied for sub-

division of the Jurassic stratigraphic sequence in Dinarides. Dozet (1999 a, b) explored and described Lower Jurassic shallow-water carbonate succession with coal on the Dinaric Carbonate Platform in Southern Slovenia. The coal occurs in the form of lenses and thin seams among the limestone and dolomite beds of middle part of the Lower Jurassic age. Miler and Pavšič (2008) described the development of the Triassic and Jurassic beds in the Krim Mountain area. The Jurassic stratigraphic sequence involves Lower and Middle Jurassic shallow marine carbonate rocks.

Materials and methods

This work is based on data, obtained during the systematic regional geologic mapping in the field on the Map Sheet Grosuplje for elaboration of Geologic Map of Slovenia on the scale of 1 : 50 000, performed by Geological Survey of Slovenia. During geologic mapping of Central Slovenia we were focused on stratimetric researches in the field and systematic labor examinations. For planning of geologic mapping on the Map Sheet Grosuplje the Basic Geologic Map of SFRJ – Map Sheet Ribnica on the scale of 1:100 000 and its Explanatory text has been applied. For formation analaysis the cross-section Spodnja Slivnica-Predole has been chosen (Strohmenger & Dozet, 1991). Around 150 samples of carbonate rocks have been collected along the road on the southeastern border of Radensko polje and another 65 rock samples in the cross-section Ilova gora-Čušperk for micropaleontological analyses carried out by Rajka Radoičić and S. Dozet.

Carbonate rocks are classified according to Folk's (1959) practical petrographic classification of limestones and Dunham's (1962) classification of carbonate rocks according to depositional texture.

Results of the research work

Lower Jurassic

In the area between Spodnja Slivnica and Račna (Figure 2) five litostratigraphic units of the Lower Jurassic age is separated. Superpositionally from bottom to top they follow one other like that: 1 – bedded micritic and oolitic-oncolitic limestones, 2 – bedded *Orbitopsella* Limestones, 3 – bedded *Lithiotis* Limestones, 4 – bedded to massive oolitic and reef limestones, 5 – platy Spotty Limestones.

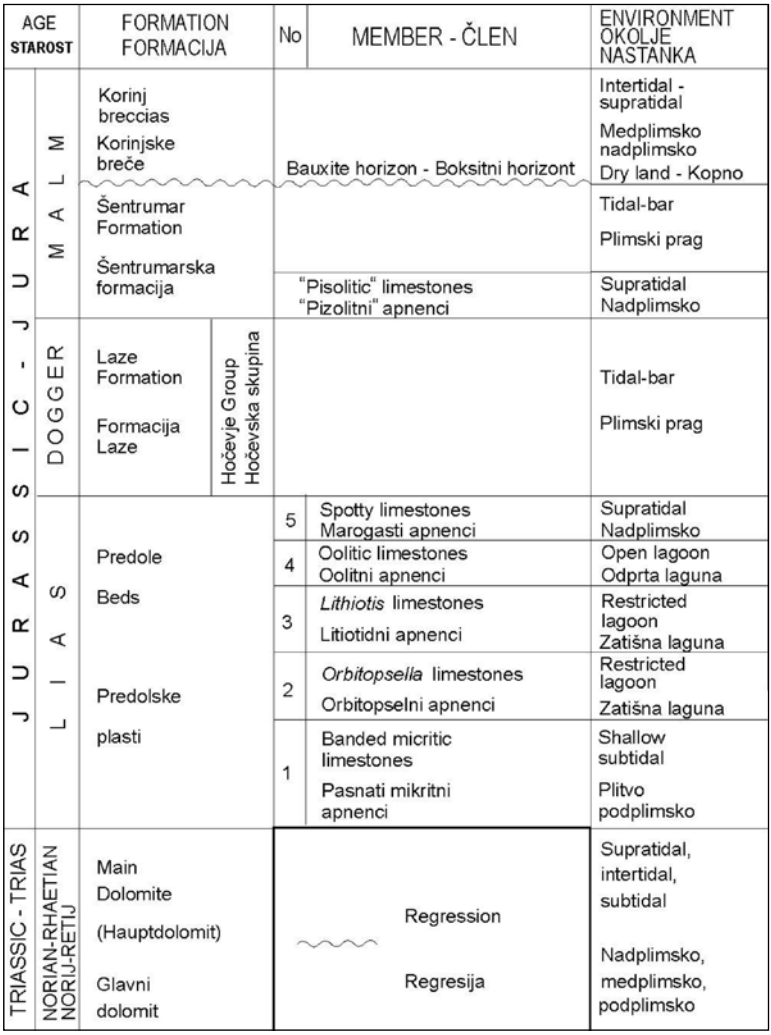

Figure 2. Stratigraphic position and environment of the Predole Beds and "pisolitic" horizon

Distribution: The Lower Jurassic limestones can be followed along the Dolenjska railway in the Spodnja Slivnica-Račna section, but Jurassic beds are, however, exposed also along the roads Mlačevo-Račna and Ilova gora-Čušperk; further on, they build the smaller hills Gradišče (486 m) and Griči (495 m and 488 m) that pass in the NW-SE direction as far as Račna. Similar limestone development is exposed also in the Krka area (DOZET & STROHMENGER, 2000), where these carbonate rocks compose Podbukovje For-

mation respectively Krka Limestones. Also isolated small hill Kopanj (392 m) and solid bedrock of the southern part of Radensko polje are built of Lower Jurassic carbonate rocks.

Stratigraphic position. We already mentioned, that about 325 m thick succession of limestones and to much minor extent of dolomites that compose Lower Jurassic carbonate succession lies conformably between the underlying Main Dolomite and overlying Laze Formation (Figure 2). Conformably upon the Main Dolomite repose bedded micritic and biomicritic limestones with algae *Palaeodasycladus*, that together with other fossils prove the Lower Jurassic age of the limestones. Platy and thin-bedded Lower Jurassic Spotty Limestones pass gradually upward into dark grey to grayish black oolitic limestones with Middle Jurassic diagnostic foraminifer *Gutnicella (Dictyoconus) cayeuxi* Lucas and *Spiraloconulus giganteus* Cherchi & Schroeder as well as alga *Holosporella siamensis* Pia. Dark oolitic limestones overlying the Lower Jurassic sequence correspond accordingly to the Laze Formation from Hočevje Group (Dozet, 2000 b). Also the upper boundary of the Lower Jurassic sequence is conformable, since the Lower Jurassic Spotty Limestones pass gradually into the dark oolitic limestones of Middle Jurassic age. Quite other case is with the Lower Jurassic carbonate sequence of Podbukovje Formation (Dozet & Strohmenger, 2000) where erosional discordance between the Lower Jurassic and Middle Jurassic sequences have been recorded and the relatively small thickness (only 15 m) of the Lower Jurassic dark platy limestones is explained, that greater part of Spotty Limestones was eroded.

Description of lithostratigraphic units

1st Unit – Bedded micritic (mudstone) limestones, Hettangian and Sinemurian

The oldest unit of Lower Jurassic limestones is represented by a carbonate succession (Figures 3, 5) in which prevail variously grey, bedded and occasionally banded (Figures 6, 7) micritic limestones containing in spots fragments of benthic foraminifers and molluscs (wackestone). Bedded micritic limestones contain sporadic interbeds of oosparitic (ooid grainstones), intraoosparitic, bioosparitic, biosparitic, biomiciritic and oncomicritic limestones, that alternate rhythmically. In the thick-bedded oosparitic limestones (ooid grainstones: Pl. 1, Fig. 6) are to be found intraclasts (intraclastic grainstones) and bioclasts (bioclastic grainstones). Intraclasts are subangular to poorly rounded and up to one centimeter in size. They belong to micritic, biosparitic, intrasparitic and laminated limestones. Bioclasts are represented by more or less rounded and micritized

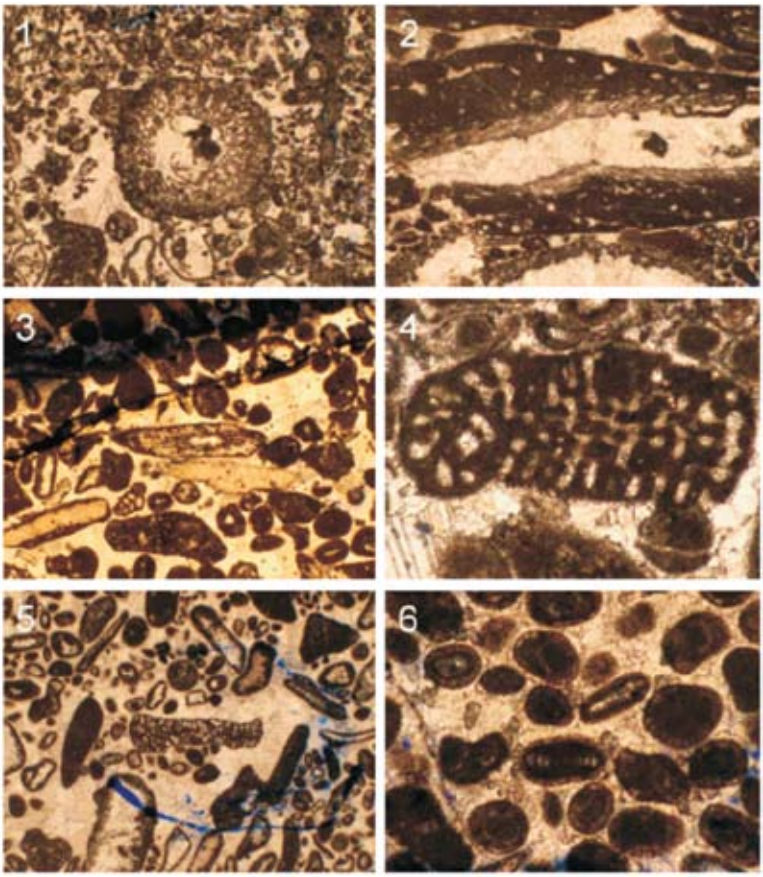

Plate 1. Fig. 1. Bioclastic packstone with algae *Palaeodasycladus mediterraneus* (Pia) and strongly changed (micritized) *Thaumatoporella parvovesiculifera* (Raineri) as well as foraminifers Textulariidae and Trochaminidae, Lower Lower Jurassic, Predole at Račna; **Fig. 2.** Strongly recrystallized mollusc fragment and alga *Palaeodasycladus elongatulus* Praturlon coated with algal or cyanobacterial crust as well as foraminifers Textulariidae, Lower Lower Jurassic, Predole at Račna; **Fig. 3.** Bioclastic-ooid grainstone with alga *Palaeodasycladus elongatulus* Praturlon and foraminifers *Orbitopsella praecursor* (Gumbel), Verneuilinidae, Textulariidae, Trochaminidae and echinoderms, Middle Lower Jurassic, Predole at Račna; **Fig. 4.** Foraminifer *Lituosepta recoarensis* Cati, Middle Lower Jurassic, Predole at Račna; Fig. 5. Foraminifers *Orbitopsella* sp. and *Trocholina* sp. in the bioclastic-intraclastic grainstone Lower/Middle Lower Jurassicsic, Predole at Račna; **Fig. 6.** Ooid-grainstone with foraminifer *Agerina* sp., Middle Lower Jurassic, Predole at Račna.

fragments of algae, molluscs and foraminifers (Pl. 1, Fig. 5). Some beds of the lower part of the Lower Jurassic carbonate succession were subjected to selective late diagenesis. Dolomitization affected especially coarse-grained sparitic limestones (grainstones), so that the limestones pass in spots into coarse-grained respectively coarse-crystalline dolomite. There are also pretty much strongly dolomitized limestones. The intergranular pores in the limestones of the grainstone type are filled with fibrous calcite cement A and/or mosaic sparry cement B.

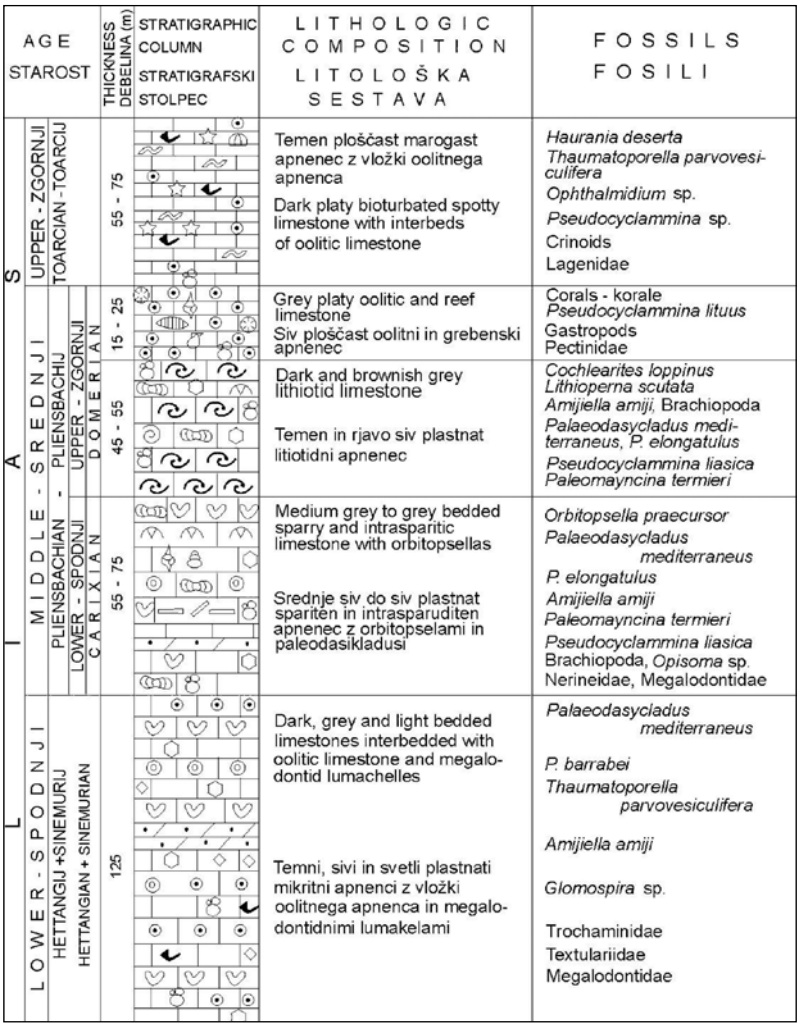

Figure 3. Stratigraphic column of the Lower Jurassicsic Beds in Predole at Račna area (Dolenjska)

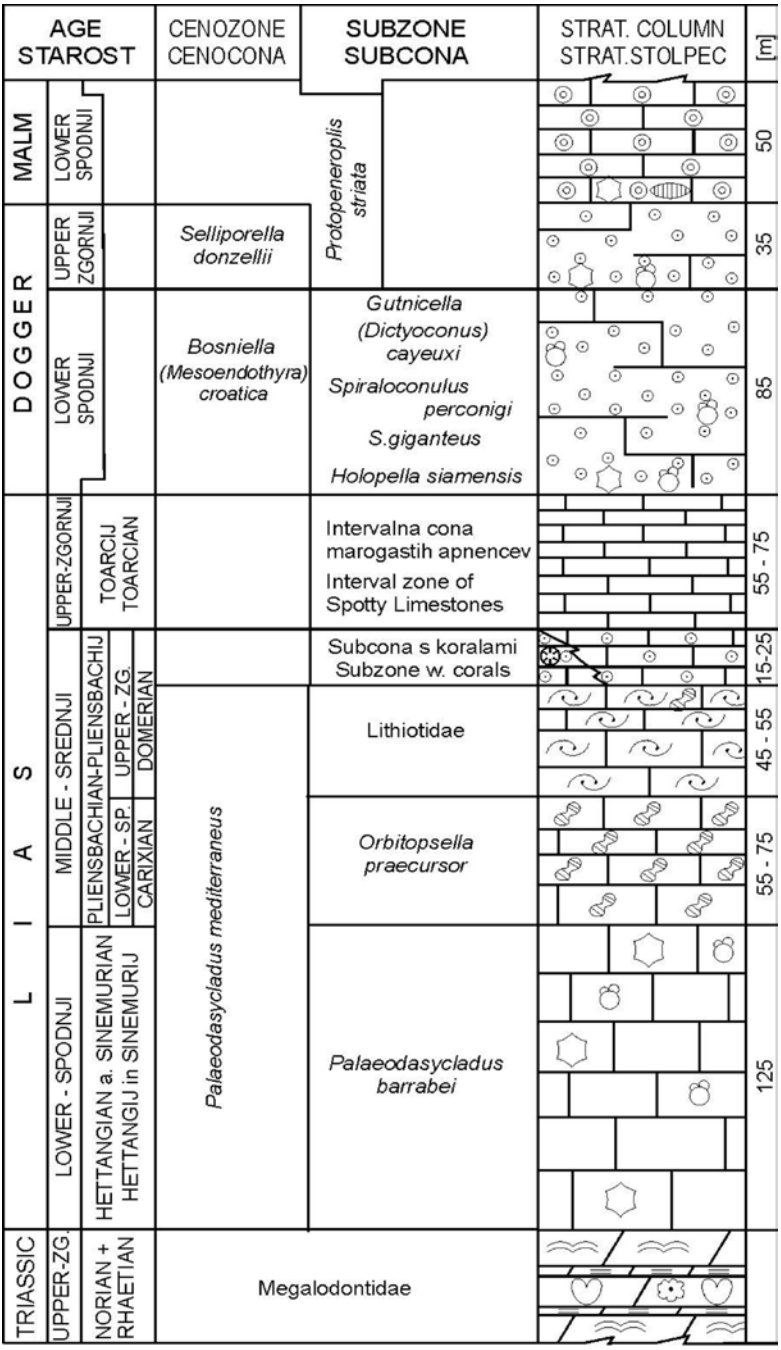

Figure 4. Biostratigraphic subdivision of Jurassic beds on the northern margin of Dinaric Carbonate Platform

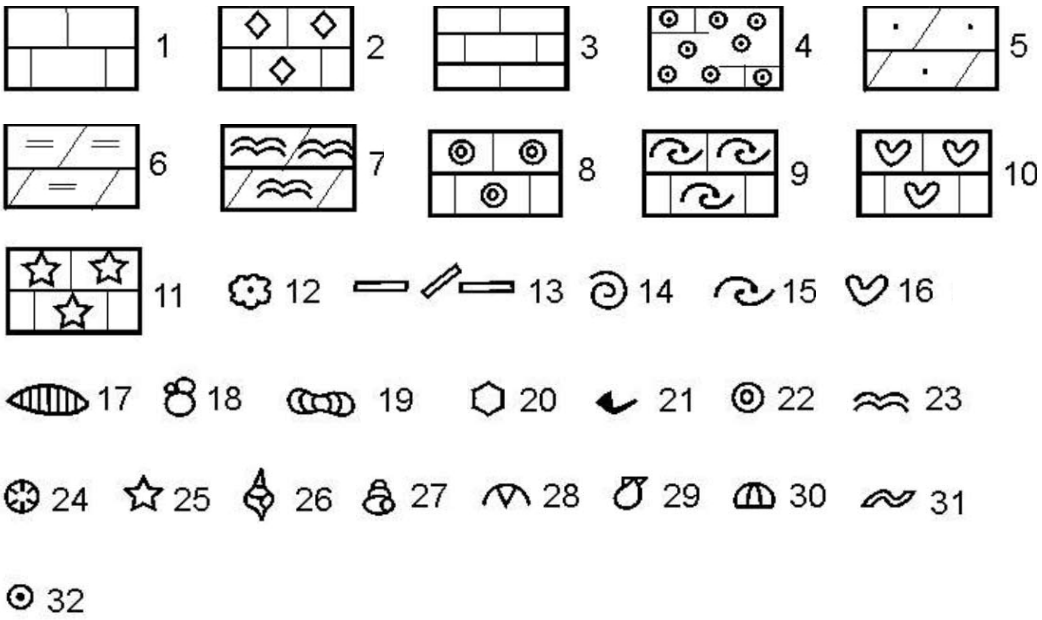

EXPLANATION

1 - Bedded micritic limestone, 2 - bedded sparry limestone, 3 - platy limestone, 4 - bedded and massive oolitic limestone, 5 - bedded dolosparite, 6 - laminated dolomite, 7 - stromatolitic dolomite, 8 - pisolitic limestone, 9 - lithiotid limestone, 10 - megalodontid limestone, 11 - crinoid limestone, 12 - oncoids of *Sphaerocodium* type, 13 - intertidal breccia, 14 - macrofauna, 15 - lithiotids, 16 - megalodontids, 17 - stromatoporoids, 18 - foraminifers, 19 - orbitopsellas, 20 - microflora, 21 - mollusc fragments, 22 - pisolites, 23 - stromatolites, 24 - corals, 25 - crinoids, 26 - gastropods (generally), 27 - nerineids, 28 - brachiopods, 29 - pectinids, 30 - echinoderms, 31 - bioturbation, 32 - ooids

Figure 5. Explanation

Figure 6. Grey bedded Lower Lower Jurassic micritic limestone

Figure 7. Bedded and banded Lower Lower Jurassic micritic limestone

Oolitic limestone interbeds are composed of ooids with radial microstructure and micritic ooids. They are bound with fibrous and mosaic calcite cement. The oolitic limestones with radial ooids originated in shoals with moderately agitated water (TIŠLJAR & VELIĆ, 1991). Micritic ooids are the result of diagenetic changes, chiefly due to micritization by *Cyanophiceae* and cryptocrystalline recrystallization.

Limestones of wackestone and mudstone type were deposited in a shallow subtidal environment in a restricted part of lagoon, while coarse-grained sparitic limestones originated in an intertidal belt, what is proved by erosional surfaces, stromatolitic belts, fenestral structures and textures, intraclasts, shrinkage pores and intertidal breccias.

The lower unit of Lower Jurassic carbonate sequence is relatively poor in fossils, what point at unfavourable life conditions for the then fauna and flora. Important characteristics of the oldest unit is especially an absence of echinoderms and rarity of foraminifers and molluscs (Figure 8). Limestones of the lowermost unit of Lower Jurassic succession contain the following fossils:

Figure 8. Black bedded limestone with megalodontid lumachelles, Lower Lower Jurassic, Radensko polje

Palaedasycladus mediterraneus (Pia) (Pl. 1, Fig. 1), *P. elongatulus* (Pratur-

Figure 9. Medium light grey massive limestone with interbeds of fine-grained intraformational breccia, Middle Lower Jurassic

Figure 10. Medium grey *"Megalodon"* Limestone, Middle Lower Jurassic

lon) (Pl. 1; Fig. 2, 3), *Palaeodasycladus* sp., *Sestrosphaera Lower Jurassicina* Pia, *Thaumatoporella parvovesiculifera* (Raineri), Codiaceae, *Cayeuxia*, *Amijiella amiji* (Henson), *Lituosepta recoarensis* Cati (Pl. 1, Fig. 4), *Haurania* sp., *Glomospira* sp., *Everticyclammina* sp., *Trocholina* sp., Textulariidae, Verneuilinidae, Trochaminidae, *Paleomayncina termieri* (Hottinger), Nerineidae and *Favreina salevensis* Parèjas. With reference to above listed fossil contents the lowermost limestones are ranged in the Hettangian and Sinemurian stages of the Lower Jurassic series.

The thickness of the first unit of the Lower Jurassic carbonate succession is estimated on around 125 m.

2nd Unit-Orbitopsella sparitic Limestones, Lower Pliensbachian (Carixian)

In the second lithostratigraphic unit predominate thick-bedded, medium grey, grey, dark grey and very dark grey prevalently sparitic limestones containing benthic foraminifer *Orbitopsella*; and that is why we designated them as ***Orbitopsella*** **Limestones** (Figures 3, 5). In considered limestones occur sporadic interbeds of breccia (Figure 9), oncoid (Figure 11), gastropod and megalodontid limestones (Figure 10). In this unit can also be seen a certain rhythmism of sedimentation, since there is present an alternation of micritic sediments (mudstone/wackstone) with sediments of packstone/floatstone and grainstone/rudstone type that contain oncoids, intraclasts, small megalodontids, gastropods (Figure 13) and horizons of oolitic limestones, benthic foraminifers and green algae, above all dasyclads. The rhythmic sedimentation is a consequence of sea-level oscillation.

Figure 11. Medium light grey oncolitic limestone, Middle Lower Jurassic

Figure 12. Medium light grey biomicritic limestone with small brachiopods, Middle Lower Jurassic

Figure 13. Medium grey biooncomicritic limestone with small gastropods, Middle Lower Jurassic

In the *Orbitopsella* Limestones the following fauna and flora have been determined: *Orbitopsella praecursor* (Gümbel) (Pl. 2, Fig. 1), *Lituosepta recoarensis* Cati, *Planisepta compressa* (Hottinger), *Involutina farinacciae* Bronnimann & Zaninetti (Pl. 2; Fig. 2, 3), *Thaumatoporella parvovesiculifera* (Raineri), *Paleomayncina termieri* (Hottinger), *Haurania deserta* Henson, *Agerina martana* (Farinacci), *Glomospira* sp., *Pseudocyclammina liassica* Hottinger, *Palaeodasycladus mediterraneus* (Pia), *Aeolisaccus dunningtoni* Elliott, *Linoporella (Tersella ?) lucasi* Cross & Lemoine (Pl. 2, Fig. 4), Codiaceae, *Cayeuxia* sp.and *Favreina salevensis* Parèjas, *Lenticulina* sp., gastropods *Opisoma* sp. and Nerineidae, as well as pelecypods Megalodontidae and Pectinidae. Above-enumerated fossil fauna and flora as well as the stratigraphic position range this unit of considered sediments in the Lower Pliensbachian stage (VELIĆ, 1977).

Orbitopsella Limestones were formed in a restricted shallow-marine environment with periodically agitated water, lagoon and shallow-subtidal environments respectively.

The thickness of the second unit of the Lower Jurassic carbonate succession (prevalently limestones with dolomite interbeds) ranges from 55 m to 75 m.

3rd Unit – Lithiotis Limestones, Upper Pliensbachian (Domerian)

Limestones with rock-building shells of Lithiotidae bivalves represent one of most characteristic and important facies in the Jurassic carbonate succession on the Dinaric Carbonate Platform (Figures 3, 5). The main particularity of this facies are bivalves of the family Lithiotidae, which are accumulated in carbonate sediments in the form of more or less thick lumachelles. The horizontal respectively parallel orientation of lithiotid shells in lumachelles indicates a transport of broken lithiotids from adjacent patch-reefs and shoals. Next to lithiotids, that are most important constituent part of these limestones, contribute to their composition also brachiopods (Figure 12), that appear in the lowermost and topmost part of the third unit. In the lower part of this unit there is also several lumachelles with megalodontids (Figure 14). The *Lithiotis* Limestones are grey, dark grey, dark brownish grey to grayish black, thick-bedded micrites (mudstones), biomicrites (wackstones) or biosparites (packstones, grainstones). Intermediate beds between lumachelles belong to biosparitic, biomicritic and biointrasparitic limestones. Some lithiotid and intermediate coarse-grained beds are more or less late diagenetically dolomitized. The considered limestones are medium to thick-bedded. Various textural types of limestones alternate rapidly having in spots interbeds of coarse-grained dolomite. Very rarely they are fine-laminated or even poorly stromatolitic.

Figure 14. Around 0,75 m thick "*Lithiotis*" lumachelle within the Middle Lower Jurassic grey bedded dolomitic limestone

Figure 15. Lumachelle from lithiotid genera *Cohlearites* and *Lithioperna* in the grey bedded Middle Lower Jurassic limestone

Lithiotis Limestones contain the following fauna and flora: *Cochlearites loppianus* (Tausch) and *Lithioperna scutata* (Dubar) (Figure 15), Brachiopoda, Megalodontidae (see Buser & Debeljak, 1994/95 and Debeljak &

BUSER, 1997), *Palaeodasycladus mediterraneus* (Pia), *Amijiella amiji* (Henson) and *Pseudocyclammina liassica* Hottinger. Concerning the collected fossils and with regard to stratigraphic position the *Lithiotis* Limestones belong to the Upper Pliensbachian, Domerian respectively.

During the early and middle Lower Jurassic the depositional environments were marked by continuous deposition of sheltered subtidal and intertidal zones, where periodically occurred suitable conditions for an extensive growth of calcareous algae, foraminifera, lamellibranches (especially lithiotids and megalodontids), gastropods and brachiopods.

The thickness of the third unit of Lower Jurassic lithologic column ranges from 45–55 meters.

4th Unit – Oolitic Limestones, Uppermost Pliensbachian

Above the beds with lithiotid bivalves known under the name *Lithiotis* Limestones lies a packet of thick-bedded and rarely platy or massive oosparitic (ooid grainstone), bioosparitic, intraoosparitic and intrabiosparitic, medium to dark grey, medium-grained limestones, we denoted as Oolitic Limestone unit (Figures 3, 5). Concordantly over the Oolitic Limestone unit repose the Spotty Limestones.

The Oolitic Limestone unit consists of pretty pure oosparitic limestones (ooid grainstones). Fragments of fossils occur in these limestones as a rule in ooid cores. Ooids reach the size no more than 1 milimeter. There are ooids with radial and concentric structure. Some ooids are tectonically deformed and more or less micritized, so that the inner structure is in greater or minor extent rubbed out. There are also ooids that were broken off and anew overgrown; on the other hand, some ooids are recrystallized so much, that only outer envelope is still preserved. Pretty frequent are also so-called composed ooids. Ooids and intraclasts are bound in medium-grained sediment with fibrous and mosaic calcite cement and they are more or less late diagenetically dolomitized. The oolitic limestones exibit occasionally a well-developed cross-stratification and contain thin horizons of superficial oolites. They look like pellets and are built of micritic mud enclosed by microsparitic envelope.

In the oolitic limestones rare larger fragments of algae and molluscs can be obtained as well. Recognized are also well-preserved prints of pectinids. In the Oolitic Limestone unit a late diagenesis is often present so that these limestones can pass in places into more or less dolomitized oolitic limestones, and somewhere even into coarse-grained respectively coarse-crystallized dolomite.

The described oolitic limestones were formed in an evironment with high-water energy, in shoals and bars respectively.

In the limestones of the Oolitic Limestone unit sections of alga *Palaeodasycladus mediterraneus* (Pia), rare foraminifers *Pseudocyclammina liassica* Hottinger and *Haurania deserta* Henson, pointing at upper part of middle Lower Jurassic (Domerian) as well as rare fragments of crinoids, molluscs, corals, stromatoporoids and pelecypod *Pecten* sp. were found.

The Oolitic Limestone unit is found in several places of central and southern Slovenia. In the oolitic-bioclastic limestones, that lie above the *Lithiotis* Limestone and are accordingly an equivalent of the Oolitic Limestone unit of the Lower Jurassic stratigraphic sequence, a corral patch reef with rich associations of corals and stromatoporoids were detected on Krim (Turnšek & Košir, 2000) and Trnovski gozd (Turnšek et al., 2003). Turnšek and Košir (2000) described systematically seven coral species, from which three species are new: *Thecactinastraea krimensis* Turnšek, *Siderosmilia perithecata* Turnšek and *Cuifastraea lopatensis* Turnšek. Turnšek et al. (2003) found in Trnovski gozd in the Lower Jurassic patch reef, lying upon the *Lithiotis* Limestone, a finding of Lower Jurassic corals. Systematically were determined and described 12 coral species belonging to eight genera. Four species were new: *Protoheterastraea trnovensis* Turnšek, *Apocladophyllia gozdensis* Turnšek, *Phacelophyllia bacari* Turnšek and *Heterostraea angelae* Turnšek. Corals built at least 70 meters long and 4 meters large patch reef, that grew on the northern border of the Dinaric Carbonate Platform. The corals range the Lower Jurassic reef limestone of the Trnovski gozd in Upper Pliensbachian, Domerian respectively.

The Domerian Oolitic Limestone originated in shallow and open parts of the Dinaric Carbonate Platform.

The thickness of Uppermost Pliensbachian oolitic limestones ammounts from 15 to 25 meters.

5th Unit – Spotty Limestones, Toarcian

The youngest unit of considered carbonate sequence (Figure 16) is composed of medium dark grey, dark grey and grayish black, platy (predominate) and bedded prevalently micritic (mudstone) and pelmicritic bioturbated limestones, which are due to activity of numerous organisms, that ate mud, became spotty. For the Spotty Limestones (Figures 3, 5) is also pretty characteristic that they are poor in fossils. They contain only rare remains of algae, benthic foraminifers and echinoderms. According to texture they are mostly mi-

critic, oomicritic and biomicritic limestones. In the limestones of the fifth unit locally a gently lamination can be observed. The stratigraphic sequence of Spotty Limestones include sporadic thinner interbeds of oolitic and bioclastic limestones (crinoid limestones: Pl. 2, Fig. 5).

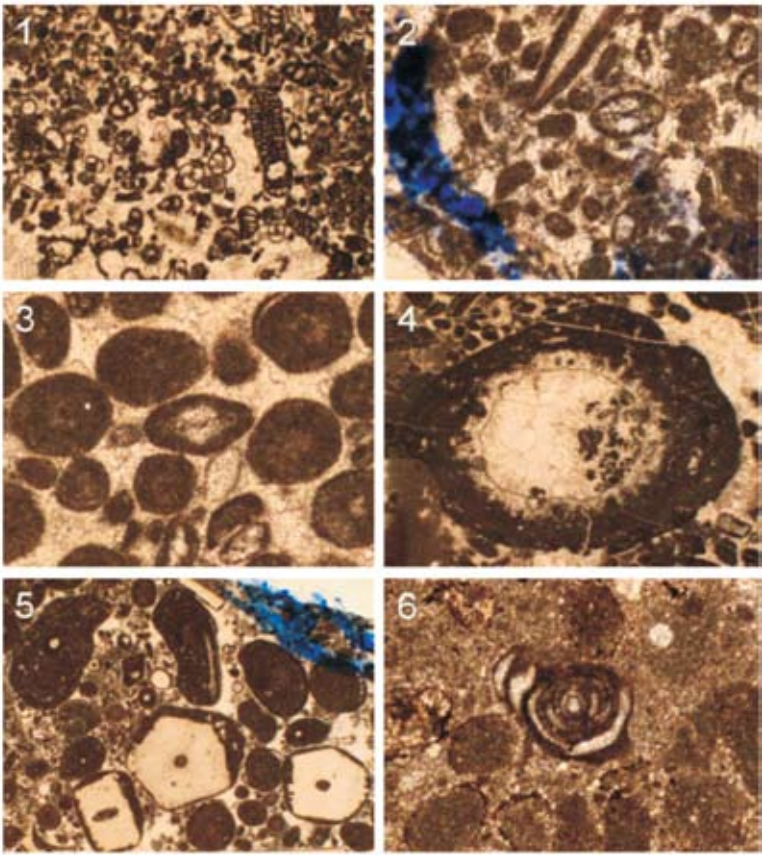

Plate 2. Fig. 1. Bioclastic-peloid packstone to grainstone with foraminifers *Orbitopsella praecursor* (Gümbel) Trochaminidae and Textulariidae, Middle Lower Jurassic, Predole at Račna; **Fig. 2.** Foraminifer *Involutina farinacciae* Bronnimann & Zaninetti in an intrasparitic packstone, Middle Lower Jurassic, Predole at Račna; **Fig. 3.** Ooid grainstone with foraminifer *Involutina farinacciae* Bronnimann & Zaninetti, Middle Lower Jurassic, Predole at Račna; **Fig. 4.** Alga *Linoporella (Tersella ?) lucasi* Cross & Lemoine coated with algal (cyanobacterial) envelope, Middle Lower Jurassic, Predole; **Fig. 5.** Crinoid limestone: bioclastic-intraclastic packstone, Upper Lower Jurassic, Predole at Račna; **Fig. 6.** Recrystallized ooid mudstone with foraminifer *Ophthalmidium* sp., Upper Lower Jurassic/ Dogger, Predole at Račna.

Figure 16. The contact between the underlying medium grey massive Middle Lower Jurassic oolitic limestone and the verlying dark platy Upper Lower Jurassic Spotty Limestone

Upper part of the Lower Jurassic limestones contain rare foraminifers *Haurania deserta* Henson, *Ophthalmidium* sp. (Pl. 2, Fig. 6), *Pseudocyclammina* sp., crinoids, small gastropods as well as algae *Aeolisaccus dunningtoni* Elliot and *Thaumatoporella parvovesiculifera* (Raineri).

The age of considered carbonate rocks is defined also by their stratigraphic position, since they lie between the Lower Jurassic biostromal (coral) beds and dark oolitic limestones with diagnostic Middle Jurassic fossils, so that they are surely of Toarcian age.

According to dark colour, abundant bituminous organic matter, structures and texture and regarding the fauna (ostracods, molluscs with thin shells) and flora can be concluded that the Spotty Limestones were deposited in restricted parts of shelf, where there were no favorable conditions for greater diversity of organisms.

The thickness of upper part of the Lower Jurassic limestones varies from 55 m to 75 m.

Midle Jurassic

Hanging wall of the considered carbonate succession is represented by a stratigraphic sequence (Figure 4, 5) of dark brownish grey to grayish black oolitic limestones (ooid grainstones) that are an equivalent of the Middle Jurassic Laze Formation (Dozet, 2000 a). They are overlain by around 50 meters thick horizon of "pisolitic" limestones (pisolite grainstones).

Around 85 meters thick Middle Jurassic lithologic column is composed of thin- and thick-bedded, well-sorted, prevalently medium-grained ***oolitic limestones*** (Figure 17). In the considered carbonate sediments predominate from 0,5 mm to 0,75 mm large ooids, but there are also more or less rounded intraclasts, bioclasts, pellets and pelletoids. In the field can be followed oosparitic (ooid grainstones), oointrasparitic, intrasparitic (intraclast grainstones), biosparitic (bioclast grainstones) as well as smaller patches of oomicritic and pure micritic limestones. In the composition of oolitic limestones strongly prevail medium-

Figure 17. Medium grey massive Dogger oolitic limestone

Figure 18. Grey to medium grey platy or bedded Lowermost Malm "pisolitic" limestone

grained well-sorted radial ooids bound with mosaic calcite cement, here and there with isopach granular cement A as well.

Among organogenic remains prevail foraminifers (Textulariidae, Trochaminidae and Verneuilinidae), that represent mostly cores of ooids. Paleontologically and biostratigraphically significant (RADOIČIĆ, 1987) for these carbonate rocks are Aalenian alga *Holosporella siamensis* Pia (Pl. 3; Fig. 1, 2, 3, 4) as well as foraminifers *Spiraloconulus giganteus* Cherchi & Schroeder (Pl. 3; Fig. 5, Fig. 6) and *Gutnicella (Dictyoconus) cayeuxi* Lucas. Oolitic limestones contain also greater or minor fragments of molluscs, echinoderms, pretty rare sections of stromatoporoids, alga *Thaumatoporella parvovesiculifera* (Raineri) and corals, that represent free clasts in sparitic cement.

Interbeds of micritic and sparitic limestones in the considered oolitic complex speak for subtidal to intertidal sedimentary environment in close vicinity of tidal channels. The isopach granular cement A indicates an episodic meteoric influence.

Upward follows 50 m thick lithologic interval (Figure 4, 5) represented by platy and bedded medium dark grey ***"pisolitic" limestones*** (Figure 18) composed of 1 cm to 2,5 cm large concentric pisolites, bound with coarse-crystallized (sandy) greatly dolomitized sparitic cement. Late diagenesis usually did not embrace pisolites. It took only sparitic cement, and in spots it changes the rock in a pure dolosparite. Similar "pisolitic" horizon is also found along the road between Vrhnika and Logatec, on Hrušica, at Vodice and to the east of Col (BUSER, 1978), This horizon within the Middle and Upper Jurassic oolitic limestones has been up to then ranged to Middle Jurassic, but BUSER

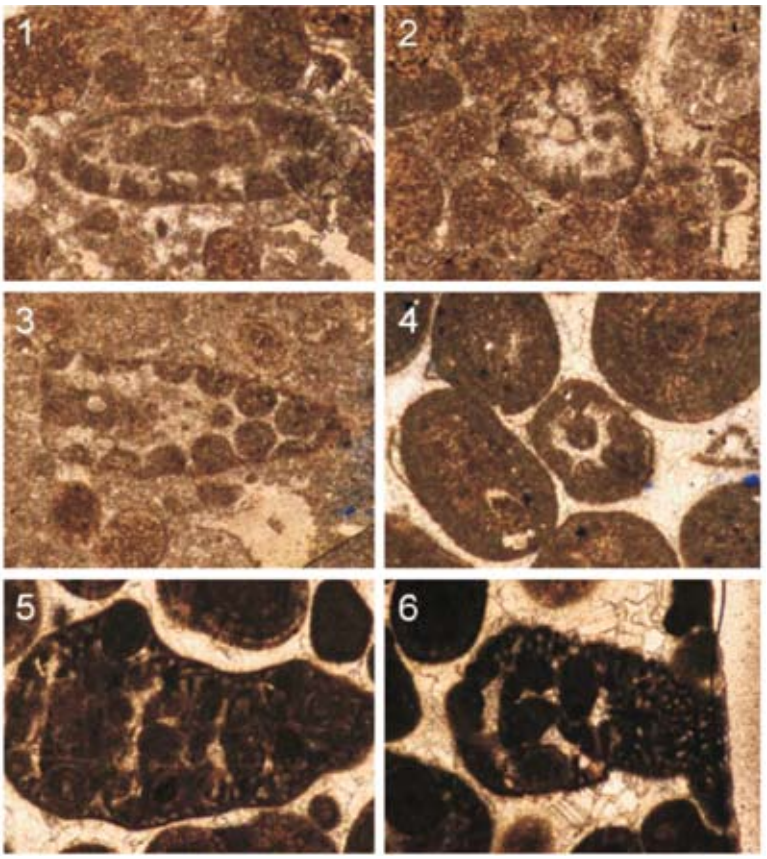

Plate 3. Fig. 1. Ooid wackstone-packstone with alga *Holosporella siamensis* Pia, Lower Dogger (Aalenian), Predole at Račna; **Fig. 2.** Ooid packstone with a section of alga *Holosporella siamensis* Pia, Lower Dogger (Aalenian), Predole at Račna; **Fig. 3.** More ore less recrystallized ooid-wackestone with section of alga *Holosporella siamensis* Pia, Lower Dogger (Aalenian), Predole at Račna; **Fig. 4.** Ooid grainstone with alga *Holosporella siamensis* Pia, Lower Dogger (Aalenian), Predole at Račna; **Fig. 5.** Foraminifer *Spiraloconulus giganteus* Cherchi & Schroeder in a coarse-grained ooid grainstone, Dogger, Predole at Račna; **Fig. 6.** Foraminifer *Spiraloconulus giganteus* Cherchi & Schroeder in a coarse-grained ooid grainstone, Dogger, Predole at Račna.

(1978) found bellow that horizon corals and hydrozoans, that proved the "pisolitic" horizon belongs already to the lowermost (basal) part of Upper Jurassic.

The "pisolitic" limestone at Predole contains the following fauna and flora: *Trocholina alpina* (Leupold), *Clado-*

coropsis mirabilis Felix, *Aeolisaccus dunningtoni* Elliott and *Cayeuxia* sp.

In the succession of oolitic limestones, that lie above the Lower Jurassic beds, we found and determined the following fossils: *Trocholina elongata* (Leupold), *Salpingoporella annulata* Carozzi and *Kurnubia palastiniensis* Henson.

On the basis of determined fauna and flora as well as considering correlation of the "pisolitic" limestones at Predole and "pisolitic" horizons on Hrušica, at Vodice, between Vrhnika and Logatec as well as east of Col (BUSER, 1978) the 50 meters thick succession of "pisolitic" limestones at Predole is attributed to Upper Jurassic, to the lowermost part of Upper Jurassic more precisely, that is overlain by the Upper Jurassic oolitic complex corresponding to the Šentrumar Formation (DOZET, 2000 b) or to the upper part of the Verd Oolitic Complex (DOZET, 2000 a).

PALEOGEOGRAPHIC EVOLUTION AND CORRELATION OF UPPER TRIASSIC TO MIDDLE JURASSIC SEDIMENTATION

This chapter deals with sedimentation and paleogeography in the Predole area on the northern margin of the Dinaric Carbonate Platform.

In the Norian and Rhaetian periods originated in the Predole area and the whole southern Slovenia on the stable Dinaric Carbonate Platform the well-known 900 to 1300 meters thick formation of Main Dolomite. It was formed in pretty shallow restricted environment, where supratidal, intertidal and subtidal conditions alternated. The most typical for the Main Dolomite is so-called Lofer facies (SANDER 1936, FISCHER, 1964) respectively cyclic alternation of red or green residual sediments (supratidal unit A), fenestral and stromatolitic dolomites, breccias (intertidal unit B) and micritic dolomites with megalodons – subtidal unit C (OGORELEC, 1988; DOZET, 1990 b, 1991; OGORELEC & ROTHE, 1992). The Rhaetian-Lower Jurassic development in the Krim Mountain area is interpreted (MILER & PAVŠIČ, 2008; MILER et al., 2007) as a consequence of short-termed marine regression that was also evidenced in the Northern Calcareous Alps (MC ROBERTS et al, 1997; KRYSTYN et al., 2005).

The sea-level changes in the Northern Calcareous Alps are explained as a consequence of a short-termed tectonic uplift, possibly a regional thermal uplift connected to the activity in the Central North Atlantic Magmatic Province, and slow rebound within a locally or regionally limited area (KRYSTYN et al., 2005). In the Lower Jurassic the sea was deepened and a sedimentation of variously grey, bedded micritic limestones interbedded with rare oolitic ones in preva-

lently quiet-water of restricted and episodically open lagoon followed. The deepening of the environment is interpreted as a consequence of global sea-level rise (Hallam, 1997; Mc Roberts et al, 1997; Miler & Pavšič, 2008).

In the Predole area the variously grey bedded micritic (mudstone), sparitic, oncolitic, laminated and stromatolitic dolomites of the Main Dolomite Formation pass upwards directly into the bedded prevalently micritic (mudstone) Lower Jurassic limestones so that the geological relations at the Triassic/Jurassic boundary were normal. Namely, in the Predole area the Rhaetian-Lowermost Jurassic breccia unit occurring in central Dolenjska (Buser, 1974; Dozet 2003 and Miler et al.) is not developed, what testifies that in the Uppermost Rhaetian and Lowermost Jurassic there were no larger tectonic movements in this area.

Sedimentologic particularities, fauna and flora show that the Lower Jurassic Krka Limestones in central Dolenjska (Dozet & Strohmenger, 1993) originated in similar sedimentary conditions as Dachstein Limestone and Main Dolomite in Northern and Southern Calcareous Alps. All three formations are namely characterized by typical Lofer rhythmic sedimentation.

The Lower Jurassic epoch is marked by lithiotid limestones. Lithiotid bivalves formed in southern Slovenia in prevalently quiet water environment of the restricted shelf sea-bottom mats or biostromes. Their shells can be only rarely found in their growth position (Buser & Debeljak, 1994/1995). The up to 75 m thick horizon with lithiotid bivalves is attributed to Pliensbachian. At high tides and storms the fresh water overflowed the adjacent barring "oolitic sand". Consequently, inside the former lagoon with lithiotid biostromes, dark oolitic limestones can be found as well.

Uppermost part of the middle Lower Jurassic is represented by a horizon of oolitic limestones originated in high energy open shallow-water environment (Dozet & Šribar, 1997; Dozet & Strohmenger, 2000).

The upper part of the Lower Jurassic intensively bioturbated Spotty Limestones with high organic contents were formed in a low-energy restricted lagoon environment. The Spotty Limestones contain rare interbeds of oolitic limestone that indicates an alternation with episodic high energy open shallow-water environment (Orehek & Ogorelec, 1981; Dozet & Šribar, 1997) The high organic contents in the Spotty Limestones is explained as a consequence of Toarcian Ocean anoxic event (Hallam, 1986; Jenkyns, 1998;

MILER & PAVŠIČ, 2008).
During the Lower Jurassic epoch in the region of Tethys vivaceous tectonic movements occurred. In northern Slovenia area a short land phase took place, and afterwards it rapidly subsided and disintegrated (BUSER, 1989). These events reached also the Dinaric Carbonate Platform. In the Stična, Šentvid, Radohova vas, Trebnje, Veliki Gaber and Valična vas areas the Upper Jurassic beds transgressively overlie the middle Lower Jurassic ones. In central Dolenjska numerous coal occurrences are known (BUSER, 1974; DOZET, 1999 a, b). All this may be understood as an evidence of an uplift of the area after the deposition of the Lower Jurassic sediments with bivalves. The same tectonic activity was reported also from the neighbouring Italy. On the Trento Carbonate Platform the shallow marine beds with bivalves are overlain by deep marine limestone of the ammonitico rosso type (BOSELLINI & BROGLIO LORIGA, 1971).

During the Middle Jurassic the paleoeogeography of southern Slovenia was marked by high-energy environments especially on the northern margin of the Dinaric Carbonate Platform.

Jurassic rocks and fossils from the cross-section Krka-Mali Korinj in Suha krajina (STROHMENGER & DOZET, 1991) clearly indicate a smaller stratigraphic gap during the Middle Jurassic epoch. The identified index fossils indicate an age older than Callovian or older than Upper Callovian respectively. Perhaps the break in sedimentation coincides with the assumed fall of sea-level during the Callovian or at the end of the Bathonian (HALLAM, 1987, 1997; BOSELLINI et al., 1981).

CONCLUSIONS

- The considered territory is situated in the southeastern border of Radensko polje (southeasterly of Ljubljana) comprising smaller hills Gradišče (486 m) and Griči (492 m and 488 m). From the palaeogeographic point of view the area in question belongs to the Dinaric Carbonate Platform (BUSER, 1989), geotectonically however, to the macrotectonic unit of External Dinarides (PLACER, 1998).
- According to the mineral composition monotonous, and with reference to texture pretty diverse carbonate succession, consisting prevalently of various limestones with some dolomite interbeds and lying conformably upon the Main Dolomite and conformably (gradual transition) under the dark oolitic limestones of Laze Formation (DOZET, 2000 b), is considered as an equivalent of the Podbukovje Formation (DOZET & STROHMENGER, 2000) .

- The discussed stratigraphic sequence between Predole and Mlačevo is composed of five lithostratigraphic units:
- 1 – Micritic and oolitic-oncolitic limestones, 2 – *Orbitopsella* Limestones, 3 – *Lithiotis* Limestones, 4 – Oolitic and reef limestones and 5 – Spotty Limestones.
- The first Jurassic lithostratigraphic unit is composed of bedded micritic (mudstone) limestones interbedded with oolitic (ooid grainstones) and oncolitic ones. The considered limestones are of Lower Jurassic (Hetangian a. Sinemurian) age (*Palaeodasycladus mediterraneus* Pia, *Sestrosphaera liasina* Pia). The limestones of mudstone type were deposited in a shallow subtidal environment in a restricted part of lagoon. The thickness of the first unit is about 125 m.
- In the second Lower Jurassic lithostratigraphic unit predominate thick-bedded variously grey prevalently sparitic limestones containing benthic foraminifers *Orbitopsella.* They are known under the name *Orbitopsella Limestones* and are ranged according to microfauna and microflora in the Lower Pliensbachian. The *Orbitopsella* Limestones were formed in a restricted shallow-marine environment with periodically agitated water, lagoon and shallow-subtidal environments. The thickness of the second unit ranges from 55 m to 75 m.
- Limestones with rock-bulding shells of Lithiotidae represent the third unit of the lower Lower Jurassic sequence. The main characteristic of this facies are bivalves of the family Lithiotidae that form lumachelles. According to the fossils *Cochlearites loppianus* (Tausch), *Lithioperna scutata* (Dubar) and *Palaeodasycladus mediterraneus* (Pia) they belong to the Upper Pliensbachian, Domerian respectively. During Middle and Lower Jurassic the depositional environments were marked by continuous deposition of sheltered subtidal and intertidal zones with suitable conditions for an extensive growth of calcareous alga, foraminifers, lamellibranchs, gastropods and brachiopods. The thickness of the third unit ranges from 45 m to 55 m.
- The fourth lithostratigraphic unit, lying concordantly between the *Lithiotis* Limestones and Spotty Limestones and consisting of grey massive, bedded and platy oolitic limestones is denoted as Oolitic Limestones. The Oolitic Limestones pass horizontally into reef limestones containing corals that range both facies into the Upper Pliensbachian, Domerian respectively. The Oolitic Limestones originated in an environment with high energy, in tidal channels respectively. The thickness of Uppermost

Pliensbachian Oolitic Limestones unit varies from 15 m to 25 m.

- The fifth Lower Jurassic unit is composed of prevalently dark, micritic (mudstones), bioturbated, so-called Spotty Limestones, with rare interbeds of oolitic and crinoid limestones that are all added to Toarcian. Spotty Limestones were deposited in restricted parts of shelf. The thickness of this unit varies from 55 m to 75 m.
- The Predole area and wider environs lie in southern Slovenia territory belonging paleogeographycally to the northern margin of Dinaric Carbonate Platform (BUSER, 1974), geotectonically however, to External Dinarides (BUSER, 1989; PLACER, 1998). It is built of Upper Triassic and Jurassic carbonate rocks. Upper Triassic sedimentation is represented by the Main Dolomite Formation composed of cyclic Lofer facies (SANDER, 1936; FISCHER, 1964) and originated in a shallow lagoonal subtidal, intertidal and supratidal environments. In the Predole area sediments of the Main Dolomite Formation pass upwards continually without any interruption in sedimentation directly into bedded, micritic Lower Jurassic limestones. The geological relations at the Triassic/Jurassic boundary were normal. Consequently, there were no larger tectonic movements in that time.
- The Lower Jurassic sedimentation is exclusively lagoonal and carbonate by character. In the lower part variously grey bedded prevalently micritic (mudstones) limestones with interbeds of oolites and dolomites occur. The middle part of the Lower Jurassic stratigraphic sequence consists of *Orbitopsella* and *Lithiotis* Limestones as well as Oolitic and Reef Limestones at the top. The above-enumerated carbonate sediments were formed in alternating restricted and open lagoonal environments. They coreespond to the outer part of the inner platform environments, proximal to the northern margin of Dinaric Carbonate Platform (BUSER, 1989; BUSER & DEBELJAK, 1996; TURNŠEK & KOŠIR, 2000; MILER & PAVŠIČ, 2008). Uppermost Lower Jurassic bioturbated Spotty Limestones have high organic contents. They were formed in high energy open shallow-water envioronment (DOZET & ŠRIBAR, 1997; DOZET & STROHMENGER, 2000). Oolitic limestones interbeds in the Spotty Limestones indicates an alternation with episodic high energy open shallow-water environment (OREHEK & OGORELEC, 1981; DOZET & ŠRIBAR, 1997). The high organic contents in the Spotty Limestones is explained as a consequence of Toarcian Ocean anoxic event (HALLAM, 1986; JENKYNS, 1998; MILLER & PAVŠIČ, 2008).

- The described stratigraphic sequence is of Lower Jurassic age. Bedded, prevalently banded micritic limestones with oolitic-oncolitic interbeds (1) belong to Hettangian and Sinemurian, the *Orbitopsella* Limestones (2) to the Lower Pliensbachian (Carixian), *Lithiotis* Limestones (3) to the Upper Pliensbachian (Domerian), oolitic and coral reef limestones (4) to the Uppermost Pliensbachian, and the Spotty Limestones to Toarcian.
- Biostratigraphically, in the Lower Jurassic carbonate sequence are recognized: the cenocona *Palaeodasycladus mediterraneus* (Pia), subzones *Palaeodasycladus barrabei* (Lebouche & Lemoine), *Orbitopsella praecursor* (Gümbel) and Lithiotidae, subzone with corals, as well as the interval zone of Spotty Limestones (Figure 7).
- The Middle Jurassic stratigraphic sequence in the Predole area is composed of various dark oolitic limestones of grainstone type that contain the Middle Jurassic diagnostic foraminifers: *Spiraloconulus giganteus* Cherchi & Schroeder and *Gutnicella (Dictyoconus) cayeuxi* Lucas as well as alga *Holosporella siamensis* Pia.
- The beds with above-mentioned fossils in the Predole area correspond to the beds of Laze Formation representing the lower part of Hočevje Group (Dozet, 2000 b) and are quite comparable with Muča ooid-bioclastic unit in Croatia (Velić & Tišljer, 1988). Muča ooid-bioclastic Limestones are in fact positioned within the Lim unit. The shallow-water limestones of the Muča unit are typical tidal-bar winnowed carbonate sands i.e sediments of the sixth Wilson'S (1975) standard facies belt. They originated by the transport of ooid sand and fossil detritus by tidal streams and waves and the deposition on tidal sand bars.
- With regard to determined fossil fauna and flora and on the basis of correlation of "pisolitic" horizon at Predole with "pisolitic" horizons elsewhere in Slovenia (Buser, 1978), the 50 meters thick sequence of "pisolitic" limestones at Predole is ranged into the lowermost part of Upper Jurassic.

Acknowledgements

This research was performed in the framework of the Programme Group Regional Geology of Geological Survey Slovenia. It was financially enabled by Slovenian Research Agency and Geological Survey of Slovenia. For ambitious and efficient determination of the relatively scarce Jurassic micro fauna and flora the author owes a great debt of thanks to Ph. D. Rajka Radoičić.

REFERENCES

BOSELLINI, A. & BROGLIO LORIGA, C. (1971): I "Calcari grigi di Rotzo (Giurassico Inferiore, Altopiano d' Asiago). Ann. Univ. Ferrara, n. s., 9, *Sc. Geol. Paleont.*; 5/1, pp. 1–61, Ferrara.

BOSELLINI, A., MASETTI, D. & SARI, M. (1981): A Jurassic "Tongue of the Ocean" infilled with oolitic sands. The Belluno Trough, Venetian Alps, Italy. *Marine Geol.*; 44, pp. 59–95, Amsterdam.

BUSER, S. (1969): Osnovna geološka karta SFRJ 1:100 000, list Ribnica. *Zv. geol. Zavod*; Beograd.

BUSER, S. (1974): Tolmač lista Ribnica. Osnovna geološka karta SFRJ 1:100 000. *Zv. geol. Zavod*; 60 p., Beograd.

BUSER, S. (1978): Razvoj jurskih plasti Trnovskega gozda, Hrušice in Logaške planote. *Rud. met. Zbornik*; 4, pp. 385–406, Ljubljana.

BUSER, S. (1989): Development of the Dinaric and Julian Carbonate Platforms and of the intermediate Slovenian Basin (NW Yugoslavia). *Mem. Soc. Geol. It.*; 40, pp. 313–320 (1987), Roma.

BUSER, S. & DEBELJAK, I. (1994/95): Lower Jurassic beds with bivalves in south Slovenia. *Geologija*; 37/38, pp. 23–62, Ljubljana.

DEBELJAK, I. & BUSER, S. (1997): Lithiotid bivalves in Slovenia and their model of life. *Geologija*; 40, p.p. 11–64, Ljubljana.

DOZET, S. (1990 a): Biostratigrafska razčlenitev jurskih plasti Kočevske in Gorskega Kotarja. *Rud. met. Zbornik*; 37/1, pp. 3–18, Ljubljana.

DOZET, S. (1990 b): Loferske cikloteme v glavnem dolomitu Kočevske. *Rud. met. Zbornik*; 37/4, pp. 507–528, Ljubljana.

DOZET, S. (1991): Norijski onkoidi v glavnem dolomitu Kočevske. *Rud. met. Zbornik*; 38/1, pp. 79–95, Ljubljana.

DOZET, S. (1993): Lofer cyclothems from the Lower Lower Jurassic Krka Limestones. *Riv. It. Paleont. Strat.*; 99/1, pp. 81–100, Milano.

DOZET, S. (1999 a): Lower Jurrassic dolomite-limestone succession with coal in the Kočevski Rog and correlation with neighbouring areas (Southeastern Slovenia). *Geologija*; 41, pp. 71–101, Ljubljana.

DOZET, S. (1999 b): Lower Jurassicni premog na območju južne Slovenije in Gorskega Kotarja. *Rud. –met. Zbornik*; 50/2, pp. 525–541, Ljubljana.

DOZET, S. (2000 a): Stratigraphy of the Verd olitic limestone complex. *Rud. met. Zbornik*; 47/3–4, pp. 245–254, Ljubljana.

DOZET, S. (2000 b): Hočevje oolitic group, Central Slovenia. *Acta Carsologica*; 29/1, 14, pp. 185–199, Ljubljana

DOZET, S. & Strohmenger (2000): Podbukovška formacija, osrednja Slovenija. *Geologija*; 43/2, pp. 197–212 (2000), Ljubljana.

DOZET, S. (2003): Middle Liassic-Lower Malm stratigraphic gap in Suha krajina. *RMZ – Mater. Geoenvir.*; 50/2, pp. 524–541, Ljubljana.

DOZET, S. & ŠRIBAR, LJ. (1981): Biostratigrafija jurskih plasti južno od Prezida v Gorskem Kotaru. *Geologija*; 24/1, pp. 109–126, Ljubljana.

DOZET, S. & ŠRIBAR, LJ. (1997): Biostratig-

raphy of shallow-marine Jurassic beds in South – eastern Slovenia. *Geologija*; 40, pp. 187–221, Ljubljana.

Dunham, R. J. (1962): Classification of carbonate rocks according to depositional texture. In: Ham, W. E. (ed.) : Classification of carbonate rocks. *AAPG, Mem.*; 1, pp. 108–121, Tulsa.

Fischer, A. G. (1964): The Lofer cyclothems of the Alpine Triassic. In: D. F. Meeriam (ed.), Symposium on cyclic sedimentation. *Kansas Geol. Soc. Bull.*; 169/1, pp. 107–150, Lawrence.

Folk, R. (1959): Practical petrographic classification of limestones. *Bull. Am. Ass. Petrol. Geol.*; 43/1, pp. 2–38, Tulsa.

Hallam, A. (1986): The Pliensbachian and Tithonian extinction events. *Nature*; 319, pp. 765–768, London.

Hallam, A. (1997): Estimates of the ammount and rate of sea-level change across the Rhaetian-Hetangian and Pliensbachian-Toarcian boundaries (latest Triassic to early Jurassic). *Jour. Geol. Soc.*; 154, pp. 733–779, London.

Jenkyns, H. C. (1988): The early Toarcian (Jurassic anoxic event: Stratigraphic, sedimentary and geochemical evidence. *Amer. Jour. Sci.*; 288, pp. 101–151,

Kerčmar, D. (1961): Poročilo o geološkem kartiranju ozemlja md Grosupljem, Velikimi Laščami, Dobrepoljem in Višnjo goro. Geološki zavod Slovenije, 40 p., Ljubljana.

Krystyn, L., Böhm, F., Kürschner, W. & Delecat, S. (2005): The Triassic-Jurassic boundary in the Northern Calcareous Alps. Abstracts and Field guide. 5th Field Workshop of IGCP 458 Project, 5–10 Sept. 2005 (Tata and Hallein, pp. 1.14.

Lipold, M. V. (1858): Bericht über die geologische Aufnahmen in Unterkrain im Jahre 1857. Jb. d. geol. R.-A., Bd. 9, pp. 257–276, Wien.

Mc. Roberts, C. A., Furrer, H. & Jones, D. S. (1997). Palaeoenvironmentental interpretation of the Triassic /Jurassic boundary section from Western Austria based on palaeoecological and geochemical data. P*alaeogeography, Palaeoclimatology, Palaeoecology, Elsevier*; 136, pp. 79–95, Amsterdam.

Miler, M. & Pavšič, J. (2008): Triassic and Jurasic beds in Krim Mountain area (Slovenia). *Geologija*; 51/1, pp. 87–99, Ljubljana.

Miller, M., Pavšič, J. & Dolenec, M. (2007): Določitev meje T/J z analizo stabilnih izotopov $\delta^{13}C$ in $\delta^{18}O$ (Krim, Slovenija. *RMZ – Mater. a. Geoenviron.*; 54/1, pp. 189–202, Ljubljana.

Ogorelec, B. (1988): Mikrofazies, Geochemic und Diageneze des Dachsteinkalkes und Hauptdolomits in Süd-West-Slowenien, Jugoslawien. Dissertation. *Univ. Heidelberg*; 173 p., Heidelberg.

Ogorelec, B. & Rothe, P. (1992): Mikrofazies, Diagenese und geochemie des Dachsteinkalkes und Hauptdolomits in Süd-West-Slowinien. *Geologija*; 35, pp. 81–181, Ljubljana.

Orehek, S. & Ogorelec, B. (1981): Korelacija mikrofacijalnih i geohemijskih osobina jurskih i krednih stena južne karbonatne platforme Slovenije. *Glas. Rep. Zav. Zašt. Prir.- Prir. Muzeja*; 14, pp. 161–181, Titograd.

PLACER, L. (1998): Contribution to the macrotectonic subdivision of the border region between Southern Alps and External Dinarides. *Geologija*; 41, pp. 223–255, Ljubljana.

RADOIČIĆ, R. (1987): *Spiraloconulus perconigi* Allemann & Schroeder (foraminifera) u nekim jurskim serijama Jugoslavije, Grčke i Iraka. Zav. Geol. istraž. SR Crne Gore. *Geol. Glasnik*; 12, pp. 117–125, Titograd.

SANDER, B. (1936): Beiträge zur Kenntniss der Anlangerungsgefüge (Rhytmische Kalke Dolomite aus Tirol). *Tschermarks Mineral. Petrogr. Mitt*; 46, pp. 27–209, Wien.

STROHMENGER, CH. (1988): Mikrofazielle und diagenetische Entwicklung jurassicher Karbonate (Unter-Lower Jurassic bis Ober-Malm) von Slowenien (NW Jugoslawien). Heidelberger Geowiss. Abh. 24, pp. 1–293, Heidelberg.

STROHMENGER, CH. & DOZET, S. (1991): Stratigraphy and geochemistry of Jurassic carbonate rocks from Suha krajina and Mala gora Mountain (Southern Slovenia). *Geologija*; 33, pp. 315–351 (1990), Ljubljana.

STROHMENGER, CH. & DOZET , S. & KOCH, R. (1987 a): Oolith-Sequenzen im Jura Südwest-Sloweniens (Mala Gora – Gegierge, Ober-Lower Jurassic bis Ober-Malm). In: Koch, R., Müller, G. & Schmitz, W. (eds.): *Heidelberger-Geoowiss. Abh.*; 8, pp. 245–248, Heidelberg.

STROHMENGER, CH. DOZET, S. & KOCH, R. (1987 b): Diagenesemuster-Stratigraphie: Oolith-Horizonte im Jura von SW-Slowenien. *Facies*; 167, pp. 253–266, Erlangen.

ŠRIBAR, LJ. (1966): Jurski sedimenti med Zagradcem in Randolom v dolini Krke. *Geologija*; 9, pp. 379–383, Ljubljana.

TIŠLJAR, J. & VELIĆ, I. (1991): Carboante facies and depositional environments of the Jurassic and Lower Cretaceous of the coastal Dinarides (Croatia). *Geol. Vjesnik*; 44, pp. 215–234, Zagreb.

TURNŠEK, D. & KOŠIR, A. (2000): Early Jurassic corals from Krim Mountain, Slovenia. Razprave 4. razr. SAZU, XL-1; pp. 81–113, Ljubljana.

TURNŠEK, D., BUSER, S. & DEBELJAK, I. (2003): Lower Jurassicsic coral patch reef above the Lithiotid Limestone on Trnovski Gozd Plateau, West Slovenia. Razprave 4. razr. SAZU, XLIV-1, pp. 285–331, Ljubljana.

VELIĆ, I. (1977): Jurassic and Lower Cretaceous assemblage zones in Mt. Velika Kapela, Central Croatia. *Acta geologica IX/2;* Prir. istraž. 42, pp. 15–37, Zagreb.

VELIĆ, I. & TIŠLJAR (1988): Litostratigrafske jedinice u doggeru i malmu zapadne Istre (zapadna Hrvatska, Jugoslavija). *Geol. Vjesn.*; 41, pp. 25–49, Zagreb.

WILSON, J. L. (1975): Carbonate facies in geologic history. 471 p. Springer Verlag, Berlin-Heidelberg – New York.

Device for thermal conductivity measurement of exothermal material

Naprava za merjenje toplotne prevodnosti eksotermnega materiala

Grega Klančnik[1,*], Urška Klančnik[2], Jožef Medved[1], Primož Mrvar[1]

[1]University of Ljubljana, Faculty of Natural Science and Engineering, Department of Materials and Metallurgy, Aškerčeva 12, SI-1000 Ljubljana, Slovenia
[2]University of Ljubljana, Faculty of Mathematics and Physics, Department of Techniques of Measurement in Physics, Jadranska 19, SI-1111 Ljubljana, Slovenia.

*Corresponding author. E-mail: grega.klancnik@ntf.uni-lj.si

Received: February 11, 2009 **Accepted:** March 11, 2009

Abstract: Thermal conductivity is an important parameter, which helps us to design vital components in industry, where the right geometry (thickness) and material is needed.

The main role of measuring thermal conductivity is in improving the existing data bases with data for new materials. Usually unmeasured materials are those with intense reaction areas. Some are called exothermal or insulation materials. They are made from different exothermal materials which means, that the heat is liberated during an exothermal reaction. For exact determination of thermal conductivity more samples are usually required, especially if exothermal-insulation material is investigated. The samples are thermally very unstable. In this paper the solution is presented by using two methods in a single experiment with one sample.

It is also discussed which method is better for determining the thermal conductivity in the intense reaction area. It is interesting that one of the methods is used for absolutely steady state conditions, and the other one is a typical transient method. The measurements were obtained for the temperature interval from 100 °C to 900 °C.

Izvleček: Toplotna prevodnost je pomembna lastnost, ki nam omogoča lažje konstruiranje vitalnih delov v industriji, kjer sta potrebna pravilna geometrija (debelina) ter material.

Original scientific paper

Glavna vloga meritev toplotne prevodnosti je dopolnitev baz podatkov s podatki novih materialov. Navadno v bazah manjkajo podatki za materiale z intenzivnimi predeli reakcij. Taki primeri so eksotermni ali izolacijski materiali. Ti so sestavljeni iz različnih eksotermnih materialov, kar pomeni, da se toplota pri eksotermni reakciji sprošča. Za natančnejše določanje toplotne prevodnosti je treba opraviti večje število meritev, posebno pri preiskavah eksotermnih izloacijskih materialov. Vzorci so navadno toplotno nestabilni. V tem delu je predstavljena rešitev, ki zajema dve metodi z enim preizkusom ter z enim vzorcem.

V delu je prav tako nakazano, katera metoda je primernejša pri določanju toplotne prevodnosti v predelu intenzivnih reakcij. Zanimivo je, da ena metoda zajema popolnoma enakomerne pogoje, medtem ko druga metoda spremenljive. Meritve so bile izvedene v temperaturnem intervalu med 100 °C in 900 °C.

Key words: thermal conductivity, exothermal materials, differential thermal analysis

Ključne besede: toplotna prevodnost, eksotermni materiali, diferenčna termična analiza

INTRODUCTION

Thermal conductivity is a physical property with a well known definition: thermal conductivity is the property of a material that indicates its ability to conduct heat[1]. The Fourier thermal conduction equation states that the density of heat flux Φ/A is proportional to the temperature gradient[2]. Fourier law:

$$q = \frac{\Phi}{A} = -k \cdot gradT \qquad (1)$$

q – density of heat flux
Φ – heat flux
A – area
k – heat conductivity

Equation 1 can be written in a finite form as[1]:

$$\Phi = k \cdot A \frac{\Delta T}{\Delta L} \qquad (2)$$

where Φ represents the heat flux trough a thickness ΔL on a surface A. Equation 2 is used for measuring a single thermal property at a time under steady state conditions. The calculated value of k is usually an average thermal conductivity in a specific temperature range. Using equation 2 can perform a significant error when thermocouples are used, because the location of thermocouples is not included. Instead the insertion of thermocouples can be made inside the upper cover of the

sample and inside the heater plate to attain repeatedly. Without the cover the upper thermocouple could measure the temperature of the atmosphere instead of the sample, if the preparation of the measurement is not sufficient.

In the year 1974 Beck and Al-Araji[3] introduced a transient solution for the simple calculation of thermal conductivity. One of the advantages of this method is that the location of thermocouples is included in the calculation. Another advantage is a shorter time of measuring, but that also depends on the thickness of a sample and the quantity of heat added into the sample. In our calculations we used equation 3 for a flat plate:

$$k = \frac{LQ\left[(\frac{x_1}{L}-1)^2-(\frac{x_2}{L}-1)^2\right]}{2\int_0^{\infty}\left[T(x_1,t)-T(x_2,t)dT\right]} \qquad (3)$$

where x_1 and x_2 represent the location of the thermocouples, L is the thickness of the plate and Q the heat passing through the plate. Figure 1 shows a schematical drawing of a sample with a plate geometry and a solid cylinder.

From Figure 1 it is seen that with the same geometry of a sample, different approaches for heating can be made. If

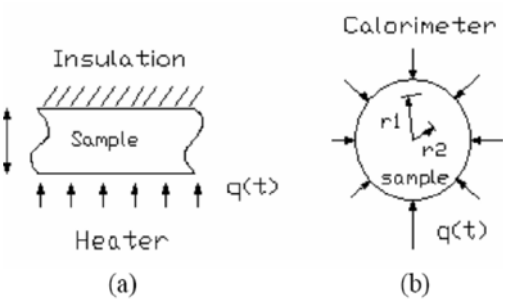

Figure 1. Various geometries with one surface heated and the other insulated for: (a) Plate geometry and (b) without insulation for a solid cylinder[2]

the calorimeter is used as a heater device and solid cylinder for the sample, no insulation is needed, because in a while the temperatures of the first (initial) and second (final) thermocouple will both approach the same value (Figure 2). In our experiment we also used a cylinder, but we did not use a calorimeter as a heater, but instead a separate heating device. In this case the calorimeter was used just for preserving the same working temperature (isothermal cell).

The measurements were made on metals and insulation materials with both methods. If both methods were not used, several samples would have been necessary for determining the thermal conductivity constants. The right constant would be calculated by using an average of the recorded values[4].

EXPERIMENTAL WORK

In the present research a device for thermal conductivity measurement was designed. The temperature range for measuring is between 100 °C and 900 °C. The furnace had to be preheated, so when the heater was turned on, the heat flow was directed entirely into the sample. Otherwise the heater would heat the entire device, not only the sample, thus the heat losses created would not have been negligible. We used two type K thermocouples in our measurement, because of a good sensitivity. The thermocouples were connected to the measuring card from the National Instruments and the card to the personal computer. Signal Express 2.1 software was used for determining and converting the signal from the thermocouples. The measurement was started, when the temperatures from both thermocouples approached the same value. Measurements started when the initial and final temperature were in proximity to each other. The corresponding factor of thermal conductivity is at an average temperature $(T_{\text{Initial}} + T_{\text{Final}})/2$. Initial and final temperature rises till initial temperature closes to the final one. The whole measurement was terminated, when the temperature of the initial and final thermocouple stabilized[2].

Device for measuring thermal conductivity of exothermal materials

For measuring thermal conductivity at various temperatures, the furnace with capability of heating the sample up to 1000 °C was needed. The lower tunnel furnace with a sufficient and stable heating cone was used. This is needed to achieve a homogeneous temperature all over the sample, before starting the measurement. The heat flux was made with another heater, located under the sample. The heater was connected to the VDC PS3020 Lab laboratory power supply (0–30 V). The schematic presentation of the designed device is shown in Figure 2.

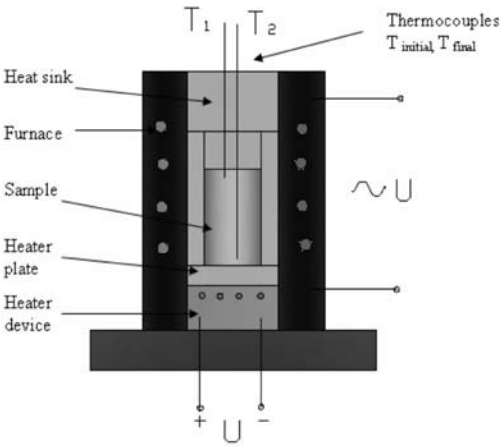

Figure 2. Device for thermal conductivity measurement – a schematic presentation

The construction of the device for thermal conductivity measurement is similar to the one described by J. FILLA[5, 6] specified for measuring thermal conductivity of ceramics.

The Heater

Kanthal wire was used in constructing the heater. The diameter of the wire was 0.5 mm, with a measured electrical resistance of 5.3 Ω/m. The wire was protected with corundum tubes. The wire was inserted on the top of the concrete grounding with good thermal and electrical resistance. The good thermal resistance was needed to maintain a one-dimensional heat flow. One of the options is discussed in papers by Beck and Al-Araji[2], where for the substrate two metal (copper) disks are used. The wire is placed in the middle of the two disks. Two samples are needed for this solution.

Heat sink

In this case the heat sink exists just for a small period of time in comparison to the whole measurement. During this period a linear temperature dependency appears, which is ideal for calculating the first average value of thermal conductivity according to Fourier. When the cooling system is switched of, the heat sink began to behave as an insulator. The time period must be long to minimize the effect of the first measurement. That is why the low current and voltage were used to get the temperature loop as long as possible.

The Measurement

The measurement of each sample started, when the initial and final temperatures were stable and in proximity. In this case the equilibrium of the device was reached. When the heater was turned on with an accurate electric power, the measurements began. The added heat into the sample was always between 7 W and 8 W, which is very low. With that, overheating of the sample was prevented and the linear rise of both temperatures was easier to achieve. Because of the low current and voltage used, a longer time was needed for the experiment, which was an advantage for determination of thermal conductivity using Fourier's law. For calculating constants using Fourier's equation was always done in the temperature region where the linear temperature dependence exists. The whole measurement was taken under air. The highest error appeared in metals, especially in aluminum, which was expected, because the temperature differences were less than 1 °C. An error can quickly appear if samples used are too short. Also, the value of added heat into the sample is also of importance.

Results and discussion

The complexity of the measurement will appear when exothermal material is examined. The starting (working) temperature must be determined in a way, that the whole exothermal reaction is measured and calculated according to both equations. The results for magnesium, calculated with Equations 2 and

Table 1. Thermal conductivities for magnesium

Temperature, T/°C	k/(W m^{-1} K^{-1}) Fourier	k/(W m^{-1} K^{-1}) Beck-Araji	k/(W m^{-1} K^{-1}) Average value	k/(W m^{-1} K^{-1}) Literature[7]	Error, E/%
94	137.359	137.359	137.359	154.34	11
140.18	137.552	137.079	137.315	153.24	10.3
234.58	135.084	135.435	135.259	150.98	10.4
284.16	133.630	134.122	133.876	149.78	10.6
299.38	132.906	133.028	132.967	149.41	11

3, are presented in Table 1. It is seen that a small variation appears between the Fourier and Beck-Araji method. The meausered thermal conductivities are done without any calibration. The calculated values were than used for calibration.

After calibration, a diagram for thermal conductivity for magnesium was made. A good compromise was made with the calculation of average values of thermal conductivity for both methods.

It is seen from Figure 4 that both methods are comparable in the temperature range from 100 °C to 400 °C. The difference between both methods under 100 °C and over 400 °C appears because a temperature difference formed between the starting temperatures. The temperature difference did not appear because of a non equilibrium state, but because the temperature homogeneity was not reached. One of the ways how to eliminate the starting temperature difference without building a new

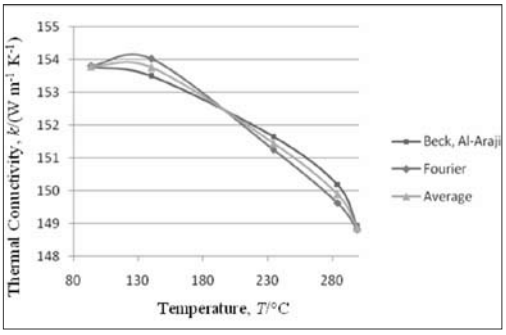

Figure 3. Thermal conductivity of magnesium calculated according to FOURIER[1] and BECK, AL-ARAJI[2]

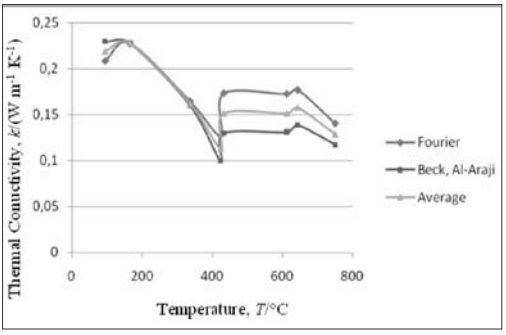

Figure 4. Thermal conductivity of insulation material

furnace is to make the samples smaller. With that solution the temperature homogeneity is easier to achieve. From Figure 4 it is seen that errors appear at higher temperatures, but nonetheless a clear tendency for both calculations is visible. Also noticeable in Figure 4 is the temperature drop at about 400 °C. This happens due to the internal heat source that arises as a result of the exothermal reaction occurring inside the sample itself.

With differential thermal analysis (*DTA*) the characteristic temperatures were obtained for the exothermal reaction. With that information, the starting temperature for measuring the thermal conductivity constant was determined. Differential thermal analysis was made on a DTA 701 Bähr device. The maximum temperature of heating was 1500 °C. The heating and cooling rate was 10 K/min under air. Alumina was used as a reference. From Figure 5a it is visible that between the temperature region between 313 °C and 439 °C the main exothermal peak appears. This is interesting for determination of thermal conductivity using both methods to see, if a comparison of both methods can be made. The starting temperature for the thermal conductivity measurement must always be chosen in such a way, that the reaction will appear in the steady state measurement first.

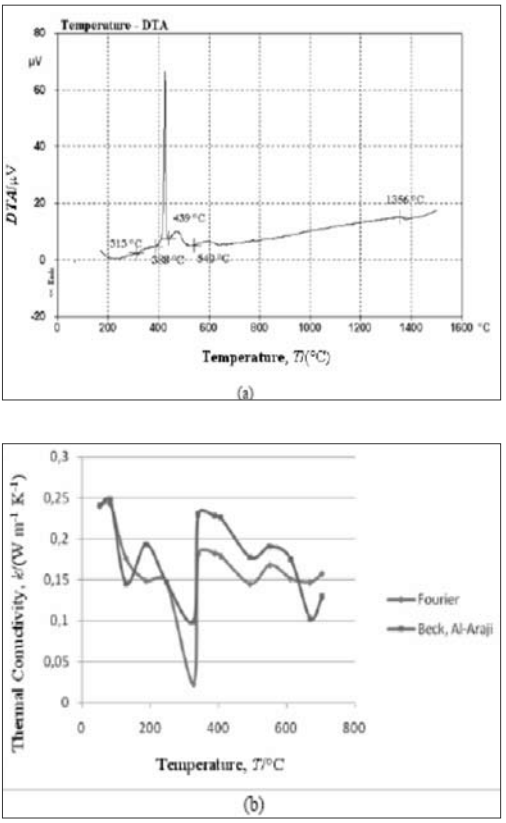

Figure 5. *DTA* heating curve (a) and thermal conductivity curve (b) for insulation material

The correspondent thermal conductivity diagram is presented in Figure 5b. It is seen that the determination of thermal conductivity according to both methods in the area of the exothermal reactions are similar, but not quite the same. Both methods showed a decrease in thermal conductivity when the exothermal reaction appeared, which indicates there was an internal heat source in the sample.

CONCLUSION

The basic idea of our work was to compare two different methods in a way that fewer samples are needed. In our calculations the Fourier and Beck, Al-Araji equations were used. The results showed that the combination of both methods can be used in the temperature range where no intense reactions are present. In the intense reaction range both methods showed similar tendency to lower constants. The equation according to Beck and Al-Araji has been shown as a good method for fast determination and estimation of thermal conductivity even for the intense reaction area. The best results were obtained under steady state conditions.

REFERENCES

[1] MARCUS, S. M., BLAINE, R. L. (1993): Thermal Conductivity of Polymers, Glasses and Ceramics by modulated DSC. *Thermochimica Acta*, Vol. 243, pp. 231–239.

[2] TZENG, J., JIM, W., WEBER, W., TOM, KRASSOWSKI, W., DAN. (2000): *Technical Review on thermal conductivity measurement techniques for thin thermal interfaces*. Sixteenth IEEE SEMI-THERM Symposium, pp 174–181.

[3] BECK, J. V., AL-ARAJI, S. (1974): Investigation of New Simple Transient Method of Thermal Property Measurement. ASME J. Heat Transfer, Vol. 96, pp. 59–64.

[4] OWATE, I., ABUMERE, O. E., AVWIRI, G. O. (2007): A device for thermal conductivity measurement in a developing economy, Vol. 2 (4), pp. 122–126.

[5] FILLA, B. J. (1997): A steady-state high temperature apparatus for measuring thermal conductivity of ceramics. *Sci. Instrument*, Vol. 68, pp. 592–605.

[6] SLIFKA, A. J., FILLA, B. J., PHELPS, J. M. (1998): Thermal Conductivity of magnesium Oxide From Absolute, Steady-State Meauserement. *Journal of Research of the national institute of standards and technology*, Vol.103, pp. 357–363.

[7] TOLOUKIAN, Y. S., HO, C. Y. (1970): Thermal conductivity, Metallic elements and alloys. *Thermophysical properties of matter*, Vol. 1; New York – Washington 1970.

Underground natural stone excavation technics in Slovenia

Tehnike podzemnega pridobivanja naravnega kamna v Sloveniji

Jože Kortnik[1, *]

[1]University of Ljubljana, Faculty of Natural Sciences and Engineering, Department of Geotechnology and Mining, Aškerčeva 12, SI-1000 Ljubljana, Slovenia

*Corresponding author. E-mail: joze.kortnik@ntf.uni-lj.si

Received: January 13, 2009 **Accepted:** February 10, 2009

Abstract: In recent years in addition to the economic reasons environmental concerns are the ones, which lead to the consideration of production of natural stone blocks by underground methods. Such development is on the way in most developed European Union countries, particularly in Italy as leading natural stone producing country.

Underground excavation of natural stone in Slovenia started in 1993, when company Marmor Hotavlje was affronted with a higher and higher overburden of this coloured and mechanically very favourable natural stone in Hotavlje I. quarry, which treatened to stop the production, because of increasing costs of excavation. In the year 2001 a test project of new natural stone production technology started also in Lipica II. quarry in company Marmor Sežana.

The paper describes situation of the natural stone quarries, shows basic technical data about underground excavations of natural stone and gives a brief description possibilities of revitalization for a number of abandonned surface natural stone quarries.

Povzetek: V zadnjih nekaj letih se predvsem zaradi ekonomsko-ekoloških razlogov vedno pogosteje razmišlja o uvajanju podzemnega načina pridobivanja blokov naravnega kamna. Tak razvoj je mogoče opaziti v večini razvitih držav Evropske unije, še posebej pa v Italiji kot vodilni državi na področju pridobivanja in predelave naravnega kamna.

Podzemno pridobivanje naravnega kamna se je v Sloveniji pričelo poskusno uvajati leta 1993 v podjetju Marmor Hotavlje, kjer so zaradi naraščajočih stroškov pri odstranjevanju vedno večjih količin odkrivke nad barvno pisanim in mehansko zelo iskanim naravnim kamnom v kamnolomu Hotavlje I. celo razmišljali o prenehanju pridobivanja. Leta 2001 so s poskusnim projektom pričeli uvajati novo tehnologijo pridobivanja tudi v kamnolomu Lipica II. podjetja Marmor Sežana.

V članku je pregledno predstavljeno predhodno stanje v obeh kamnolomih naravnega kamna, osnovni tehnični podatki podzemnega pridobivanja naravnega kamna in kratek opis možnosti oživljanja številnih, danes zapuščenih površinskih kamnolomov naravnega kamna.

Key Words: dimension stone, Hotavlje I. quarry, Lipica II. quarry, natural stone, room and pillar mining method, underground mining

Ključne besede: rezani kamen, kamnolom Hotavlje I., kamnolom Lipica II., naravni kamen, komorno-stebrna odkopna metoda, podzemno pridobivanje

INTRODUCTION

Natural stone is a common name for all rock masses of natural origin that are suitable for cutting, grinding and polishing as well as for construction in regard to composition, properties and appearance. The term "natural" denotes that this is exclusively a natural material which is used in this natural form. Its working merely emphasises its structure, but does not change it – the basic properties, the distribution of minerals and grains as well as the appearance remain unchanged in this process. Terms such as decorative or ornamental (dimensional) stone, natural decorative stone, architectural

and construction stone, paving stone, building stone, sculptural stone etc. are also used. When naming stone, the adjective usually describes the mode of stone's use[11]. For natural stone to be suitable for mining and working, it must have sufficiently good physical and mechanical properties, such as strength, compactness, wear resistance, water absorption, freezing resistance etc. Along with appropriate physical and mechanical properties of the rock, it is its colour that most commonly affects the choice of the stone and often has a decisive influence on its use. The source of the rock mass (igneous, metamorphic or sediment rock), its chemical composition (carbonate or silicate) and other geological conditions at the rock mining site (tectonics) are the decisive factors that affect the selection of the mining method.

Underground mining of natural stone is not an idea conceived by the modern information society – it originates from the times of the ancient Romans. There is evidence that Romans were probably the first to undertake underground mining of stone, for example in the now already abandoned quarry in the Eastern British town of Beer in the province of Devon, which has been changed to a museum[7].

In Europe, underground mining of natural stone is nowadays performed in various quarries in Italy (Carrara, Apuan Alps, Bolzano, etc.), Great Britain (Avon, Somerset, Dorset[7], etc.), Greece (Dionysos – Athens[8]), Portugal (Solubema-Lisbon) and elsewhere.

In Slovenia, underground mining of natural stone began to be introduced in 1993 at the Hotavlje I. coloured limestone quarry, and since 2001 also at the Lipica II. limestone quarry.

Marmor Hotavlje, one of Slovenia's leading stonecutting companies, began with organised mining of natural stone

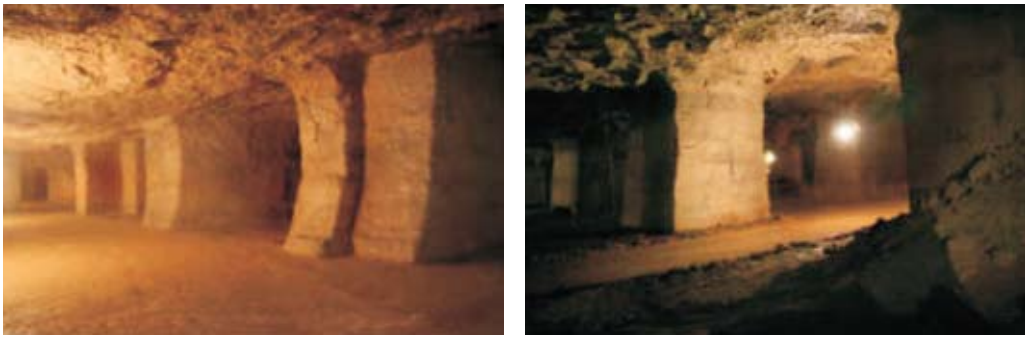

Figure 1. Underground mining of natural stone at the Beer quarry[7]

at the Hotavlje I. quarry in the year 1948[9]. The beginnings of mechanical breaking of natural stone at the quarry's current site date back to the seventeenth century. At the Hotavlje I. quarry, the so-called Hotavlje natural stone is mined, a limestone which comes in various colours (red, grey, pink, and sometimes almost black, with white calcite veins, coral remnants and limestone algae). The management of Marmor Hotavlje decided to implement underground mining due to the geological structure of the site and the quarry's condition resulting from an increasing demand for this raw material.

Figure 2. Lipica II. quarry[10]

Marmor Sežana, which has been the main company performing the stonecutting activities in the Karst region for over five decades, began mining natural stone at the Lipica II. quarry in 1986. Karst stonecutters named the natural stone mined at the Lipica II. quarry Lipica-Unito and Lipica-Fiorito[6]. In terms of size, the Lipica II. quarry belongs among the largest Slovene natural stone quarries. For similar reasons as for the Hotavlje I. quarry, the management of Marmor Sežana also decided in 2001 to begin with trial underground mining of natural stone blocks in Lipica II. quarry.

Before the beginning of underground mining, numerical modeling and stability calculation of underground spaces foreseen were performed by finite difference method (FLAC^{2D}), for the evaluation of global stability of the openings foreseen and to derive a sensitivity analysis of input parameters, such as shape and dimensions of galleries, primary stress field and mechanics characteristic of the rock mass. Another block analysis (Unwedge) was also made, which was concentrated on block stability underground structures. Monitoring of stability was followed indirectly by monitoring relative deformations of the discontinuities. Results given by calculations were finally the basis for the design of underground spaces for a long term underground extraction of natural stone blocks[1].

Work at both quarries used to be partially seasonal. During the winter, interruptions of the mining process lasted between one and three months in case

of poor weather conditions (snow or rain).

The following factors have a crucial role in the selection of the mining method:

- Geological factors: overburden thickness, site compactness - wall masses, waste rock, shape of the rock body,
- Ecological factors: lesser surface damage to the environment, smaller rock waste deposits and significantly lower noise burden on the surroundings (because works are performed underground),
- Technical and technological factors: development of the technology and the mining methods enables efficient, simple and safe mining,
- Economic factors: expensive overburden works are unnecessary; mining can be done throughout the year and even in poor weather conditions (winter, rain); the costs of mining are initially higher due to quarry opening works and additional research costs, but they decrease rapidly with the development of open underground spaces called galleries,
- Regulatory factors: in the majority of countries, there are no stipulations in the legislation on this mining method, therefore regulations on the performance of underground work are reasonably applied.

Excavation technics for mining of natural stone

Natural stone quarries are much smaller than technical stone quarries. Their annual production rarely exceeds 1500 m^3 of natural stone blocks. A low utilitization value of natural stone blocks, which ranges between 8 % and 25 %, results in the fact that natural stone quarries always have sufficient waste, which can be used for final quarry site rehabilitation.

Excavation technics for mining natural stone are as follows[4]:

- performatic drilling,
- drilling and cutting with helicoid wire and flintstone sand,
- drilling and cutting with a diamond wire saw,
- cutting with a chain cutting machine (belt saw),
- combined cutting method.

The performatic drilling method consists of drilling into the rock with the use of pneumatic drilling hammers or drilling machines. Drilling is done in the horizontal and vertical directions, at several places. The bore diameter (usually ϕ 34 mm) and the distance between the bores (usually 100 mm) depends primarily on the splitting capacity of the rock mass[2]. Separation of a block from the rock mass is done using rock splitting wedges, which are ham-

mered into the bores in alternation until a block is separated off the rock, or by using black blasting powder for mining or detonation string. This mining method is being gradually abandoned due to the formation of microcracks within the rock at the mining site (rock damage), large energy consumption, difficult and heavy work, and excessive noise burden on the surrounding areas.

Figure 3. Diamond wire

The drilling and cutting method involving the use of helicoid wire and flintstone sand is based on cutting of the rock using flintstone sand, which is harder than rock, as the abrasive. Helicoid wire (with diameters up to 5.8 mm) is a woven steel wire rope made from three strands, which serves as a means of transporting flintstone sand into the cut. In this method, flintstone sand represents the cutting tool, and the added water acts as a coolant. The cutting speed amounts to between 0.3 m^2/h and 0.9 m^2/h and depends primarily on hardness of the rock mass. At cutting sites, ϕ 240 mm vertical and horizontal bores are first drilled; stands with wire guiding wheels are then installed and a helicoid wire is fed over them. The helicoid wire is joined at the ends to form an endless wire with a length of up to 1500 m. The wire is then led into the cut, over the driving wheel and the guiding wheels. A mixture of flintstone sand and water is added at the point of contact between the helicoid wire and the rock. This method was very widely used in the past for the mining of compact limestones and marbles, but nowadays is has been completely replaced by the method of diamond wire cutting.

The stone cutting method with the use of diamond wire saw is based on cutting of the rock with a diamond wire. A diamond wire with a diameter of 5 mm is a woven wire rope with diamond rings (the diamonds are sintered or inserted/bonded galvanically), springs and spacer rings arranged along it in alternation.

Figure 4. Drilling of vertical bores using a drilling machine

The mining of stone blocks according to this method is performed in several phases:

- Drilling of a vertical bore with a diameter of 240 mm and two horizontal bores with a diameter of 90 mm in such manner that all the three of them converge at the same point;
- Sawing of both vertical cuts; the diamond wire is drawn through the vertical and horizontal bores, and then its ends are connected together to form an endless wire rope using special joints. The wire is placed on the driving wheel ring of an electric aggregate and the wheel is placed on guides with a cogged rail that enables uniform movement of the diamond wire during sawing;
- Sawing of horizontal cuts; the diamond wire is drawn through the horizontal bores; its ends are then joined together to form an endless wire rope and mounted on the driving wheel of the electric aggregate.

The cutting speed using a diamond wire saw amounts to 5 m^2/h to 10 m^2/h and is by far the highest compared to other cutting methods.

The cutting method involving the use of a chain cutting machine is based on cutting of rock using "widia" or diamond plates that are mounted on the cutting machine's chain blade. Chain cutting machines can cut rock in a horizontal or vertical direction. The cutting machine's blade moves along the cogged rail and guiding rails. For work in underground spaces, cutting machines with hydraulic guides for blade movement in the horizontal and vertical directions are used, with hydraulic pillars that enable machine stabilization during operation. This method is simple and safe. The chain cutting machine is placed directly in front of the stope face and attached rigidly. Horizontal cuts are first made from below upwards and finally on the side. Technical water is used for cooling the saw chain and washing the stone slurry out of the cut. The cutting speed is between 2 m^2/h and 4 m^2/h, the cut thickness is 4 cm and the cut depth 2.40 m or more. The speed of blade movement is up to 7 cm/min and the chain speed up to 0.7 m/s.

Figure 5. Cutting of the lower horizontal cut using a chain cutting machine

The combined cutting method unites the methods of chain cutting machine and diamond wire saw cutting. It is primarily suitable for opening and prepa-

ration of upper underground mining levels (galleries, cross-cuts, niches), which later enable increasing of the depth by creating chambers with the use of the more cost-efficient diamond wire saw cutting method.

UNDERGROUND MINING OF NATURAL STONE BLOCKS

Underground method of mining natural stone blocks has many advantages over surface mining. In the Hotavlje I. and Lipica II. quarries, it is suitable primarily due to terrain configuration, shape of the quarry and the large amount of the overburden. In addition to a considerable reduction in the amount of overburden, which certainly improves the cost-efficiency of natural stone mining, the underground mining method also enables selective exploitation of the high-quality portions of the site, much more so than surface mining. This increases the utilization value of natural stone blocks, which can result in lower costs of mining per unit product and ultimately in a higher cost-efficiency of mining, which is certainly the greatest advantage of underground mining of natural stone. However, when planning the technological equipment to be used in underground mining, it is necessary to observe the applicable regulations for mines with underground exploitation of mineral raw materials, and this could make mining slightly more expensive.

In addition to the research that is necessary for planning the galleries, underground mining of blocks also requires extensive systematic geological and geotechnical observation and measurements during the performance of works. Only in this way is it possible to prove that the planned mining system ensures safe work and that it will increase utilization value of high-quality stone blocks. To a certain extent, the underground mining method also enables selective mining which results in the achievement of a higher average quality of mined natural stone that can be sold on the market at a higher price.

In both quarries, Hotavlje I. and Lipica II., the room and pillar mining method with irregular distribution of pillars will be used in future, along with the combined cutting method. The combined method of natural stone cutting is primarily suitable for opening and preparing underground open spaces (galleries, cross-cuts, niches and chambers). This method has so far been proved to be the most successful for underground mining of natural stone. The horizontal and then vertical cuts are first made using the chain cutting machine. If necessary, depending on the required block size and load-carrying capacity of the transport machine equipment, several

intermediate horizontal and vertical cuts are then made. In order to cut the rear surface of the natural stone blocks, a channel is first made with a width of between 0.5 m and 0.8 m. Blocks in the channel are obtained using hydraulic bags. The rear surface of other blocks is cut using a diamond wire saw. The depth of one stage depends on the blade length of the chain cutting machine and amounts to between 2.40 m and 2.80 m or even more. The minimum stope face width is 5.80 m. The heights of individual mining levels depend on the technological and geological conditions and range between 4 m and 6 m (usually 4.50 m). Water is used for cooling the cutting tool, washing of slurry from the cut and reducing dust formation.

Figure 6. Stope face with underground mining of natural stone

In the future, surface and underground mining of natural stone blocks will be done concurrently using the diamond wire saw cutting method or the combined cutting method, and the lower lying mining levels will be opened from up downwards.

Conclusions

The development of new technologies and mining methods for underground mining of natural stone enables more cost-efficient mining, better raw material and labour utilisation, smaller damage to the environment and safer work, but it also requires a significantly higher level of professional training from employees. The introduction of underground mining of natural stone means an immediate possibility of renewed operation for many already abandoned natural stone quarries, while for active ones it should be considered as a significant alternative from the viewpoints of ecology, cost-efficiency, selective mining and possibilities for further development and mine expansion, better raw material and labour utilisation, reduced influence of weather and seasonal changes, as well as from other viewpoints.

In the future, experience acquired in the two Slovene natural stone quarries will serve for the introduction of underground mining also in other Slovene and foreign natural stone quarries which are suitable for this mining method.

REFERENCES

[1] BAJŽELJ, U., KORTNIK, J., PETKOVŠEK, B., FIFER, K., BEGUŠ, T. (1999): Okolju prijazno podzemno pridobivanje naravnega kamna. *RMZ*; Vol. 46, No. 2, pp. 203–214.

[2] BIZJAK, J., FRLIC, M. (1998): Metode pridobivanja naravnega kamna. *2. strokovno izobrazevalni seminar "Lastnina, vrednotenje varstvo pri delu*; Hotavlje, pp. 19–26.

[3] KORTNIK, J., BAJŽELJ, U. (2005): Underground mining of natural stone in Slovenia. *20th World Mining Congress*; Tehran, Iran, pp. 277–286.

[4] KORTNIK, J., BAJŽELJ, U. (1998): Prednosti podzemnega pridobivanja naravnega kamna. *2. strokovno izobrazevalni seminar*: Lastnina, vrednotenje varstvo pri delu; Hotavlje, pp. 89–92.

[5] KORTNIK, J. (2003): Podzemno pridobivanje naravnega kamna v Sloveniji. *Posvetovanje ob 38 skoku čez kožo*; pp. 97–103.

[6] RENČELJ, S., (2002): Kras kamen in življenje. Založba Libris, pp. 10–23.

[7] Beer quarry. Accessible on Internet: http://www.beerquarrycaves.fsnet.co.uk.

[8] Dionisos quarry. Accessible on Internet: http://www.dionyssomarble.gr.

[9] Company Marmor Hotavlje. Accessible on Internet: http://www.marmor-hotavlje.si.

[10] Company Marmor Sežana. Accessible on Internet: http://www.marmorsezana.com.

[11] Underground stone mines. Accessible on Internet: http://www.serve.com/scmc.

Raziskava možnosti za nadaljnjo eksploatacijo zalog rjavega premoga v Sloveniji – RTH, Rudnik Trbovlje-Hrastnik

Evaluation of possibilities for further exploitation of brown coal reserves in Slovenia – RTH, Rudnik Trbovlje-Hrastnik

Evgen Dervarič[1,*], Bojan Klenovšek[2], Željko Vukelič[1]

[1]Univerza v Ljubljani, Naravoslovnotehniška fakulteta, Oddelek za geotehnologijo in rudarstvo, Aškerčeva cesta 12, SI-1000 Ljubljana, Sloveni,a
[2]RTH, Rudnik Trbovlje-Hrastnik, d. o. o., Trg revolucije 12, SI-1420 Trbovlje, Slovenija

*Korespondenčni avtor. E-mail: evgen.dervaric@ntf.uni-lj.si

Received: January 13, 2009 **Accepted:** February 17, 2009

Izvleček: Evropsko premogovništvo izraža enakovredno podporo doseganju vseh treh ciljev trajnostnega razvoja, in sicer vzpostavljanju ravnotežja med človekom in okoljem, ohranjanju naravnih virov in biološke raznovrstnosti ter etiki odnosa do okolja in narave. V zvezi s tem je zanesljivost oskrbe z energijo sestavni del ekonomskega in socialnega razvoja. Vendar pa je osnovni pogoj za ekonomski in socialni razvoj zanesljiva, poceni in okolju prijazna oskrba z energijo, kjer pa premog prispeva glavni delež.

RTH, Rudnik Trbovlje-Hrastnik bo do vključno leta 2009 dobavljal premog Termoelektrarni Trbovlje (TET) v predvideni količini 0,6 mio. ton na leto. Glede na stanje energetike v Evropi in svetu smo priča stalnemu porastu cen energentov, tudi premoga. V danih razmerah bomo v Sloveniji prisiljeni izkoristiti vse razpoložljive zaloge premoga, zato je smiselno ponovno preučiti preostale zaloge v odkopnih poljih RTH in na osnovi konkurenčnih izhodišč predstaviti možnosti za njihovo izkoriščanje v povezavi s TET. V tem prispevku so predstavljeni rezultati študije »Upravičenost odkopavanja preostalih zalog premoga v jamah Ojstro in Trbovlje po letu 2009«. Študijo je izdelala Naravoslovnotehniška fakulteta v Ljubljani v sodelovanju z Ekonomskim inštitutom pri Pravni fakulteti v Ljubljani, Inštitutom za rudarstvo, geotehnologijo in okolje v Ljubljani in s sodelavci naročnika RTH.

Abstract: The European coal mining industry expresses equal support to the pursuit of all three objectives of sustainable development, i.e. the establishment of balance between man and environment, preservation of natural sources and biodiversity, and the ethics of the attitude towards the environment and nature. Regarding all this, the reliability of energy supply is an integral part of the economic and social development. However, the main condition for the economic and social development is reliable, affordable and environmentally friendly energy supply, where the main portion is covered by coal.
Trbovlje-Hrastnik Coal Mine (Rudnik Trbovlje-Hrastnik - RTH) will provide, until 2009 inclusive, Trbovlje Thermal Power Station (Termoelektratna Trbovlje - TET) with coal in the planned amount of 0.6 million ton per year. Regarding the situation of the energy industry in Europe and in the world, we are witnessing a constant rise of prices of fuels, including coal. In the given circumstances, Slovenia will be forced to exploit all available coal reserves. It is therefore reasonable to review the remaining reserves in the extraction areas of RTH and, based on competitive points of view, to present a possibility for their exploitation in relation to TET. This article presents the results of the study »Justifiability for Extraction of the Remaining Coal Reserves in the Mines Ojstro and Trbovlje After the Year 2009«. The study was done by the Faculty of Natural Sciences and Engineering in Ljubljana, in co-operation with the Economic Institute of the Faculty of Law in Ljubljana, Institute for Mining, Geotechnology and the Environment in Ljubljana and co-workers of the institution that requested the study, RTH.

Ključne besede: premog, premogovne tehnologije, električna energija, energijski viri, konkurenčnost, varnost, zanesljivost
Key words: coal, coal technologies, electricity, energy sources, competitiveness, security, reliability

Uvod

Delež premoga v energetski bilanci EU-25 je danes približno 20 %. Sedaj je EU že 50-odstotno energijsko odvisna, do leta 2030 pa se bo uvozna odvisnost povzpela na 70 %. (Vir: Word Energy Outlook 2008 – WEO 2008).

Proizvodnja premoga v RS pada. Od rekordnih 6,8 milijonov ton v začetku 80-ih let je proizvodnja padla na 4,5 milijone ton v letu 2007. Podobne, vendar še izrazitejše težnje se dogajajo tudi v EU (Vir: Euracoal 2008). Kljub vsem ekonomskim in ekološkim slabostim premoga v EU se ne bo bistveno

zmanjševala sedanja poraba domačega in uvoženega premoga.

Zamenjava premoga z drugimi fosilnimi gorivi (predvidoma s plinom) bo v RS neizogibno poslabšala samozadostnost in povečala uvozno odvisnost tudi pri proizvodnji električne energije.

RS se je z Zakonom o postopnem zapiranju Rudnika Trbovlje-Hrastnik in razvojnem prestrukturiranju regije (Uradni list RS, št. 61/2000) odločila, da zapre premogovnike rjavega premoga v Zasavju. Do leta 2009 naj bi potekala proizvodnja za potrebe Termoelektrarne Trbovlje, s sočasnim zapiranjem po tem letu pa naj bi se izvajala samo zapiralna dela.

Rudnik Trbovlje-Hrastnik, ki je nastal leta 1995 z razdružitvijo dotedanjega podjetja RRPS, je vse do leta 1999 gradil svojo perspektivo na gradnji novega termoenergetskega objekta, do realizacije pa iz znanih razlogov ni prišlo. Glede na to, da je bila proizvodnja iz jam RTH vezana izključno na porabo premoga v energetiki ter da po referendumski odločitvi dolgoročno ni bilo več možno zagotavljati porabe premoga v omenjenih objektih, je bilo nujno poiskati alternativno rešitev.

Izdelana je bila študija »Ocena stroškov zapiranja RTH pri proizvodnji premoga do konca leta 2005«, ki je bila tudi recenzirana (Montan Consulting GmBH in Erico). Ta dokument je postal podlaga za sprejem »Zakona o postopnem zapiranju RTH«, ki pa je s politično proceduro dobil še t. i. »tretji del«, ki se nanaša na spodbude pri regionalnem razvoju, samo obdobje tako proizvodnje ob sočasnem zapiranju kot tudi zapiranje pa je bilo brez trdnih argumentov skrajšano iz leta 2015 na 2007 oziroma iz 2019 na 2012.

Torej, julija leta 2000 je bil sprejet »Zakon o postopnem zapiranju RTH in razvojnem prestrukturiranju regije«, ki je poleg energetskega zakona osnova za delovanje RTH tako na proizvodnem kot tudi zapiralnem delu.

Vlada Republike Slovenije je julija leta 2004 sprejela dopolnitev zakona o zapiranju RTH, ki je proizvodnjo premoga podaljšal do leta 2009 in zapiralna dela do leta 2015.

Rast cen energetskih surovin na svetovnem trgu pa ponovno postavlja vprašanje smiselnosti še nadaljnjega izkoriščanja potencialnih odkopnih zalog, ki naj bi bile po letu 2009 še približno 24 milijonov ton premoga. To pomeni, da bi RTH lahko še podaljšal odkopavanje premoga po letu 2010 pri letni proizvodnji od 200 000 t do 300 000 t in povprečni kurilnosti premoga 11 GJ/t.

Poraba premoga je zagotovljena do leta 2009 v TET na osnovi prednostnega di-

spečiranja, za katerega ima TET z ELESOM sklenjeno dolgoročno pogodbo.

Zapiranje in proizvodnja sta medsebojno povezani predvsem pri izvajanju zapiralnih del v jamah, tako s kadrovskega kot tudi tehnološkega vidika. V Programu zapiranja RTH I. faza (2000–2004) so zato opredelili področja, kjer bodo nadaljevali proizvodnjo in katere jame in polja bodo prioritetno zapirali. Odločitev je temeljila predvsem na stopnji zahtevnosti in s tem povezanimi stroški v posameznih jamah oziroma odkopnih poljih. Kot proizvodni del so ohranili jamo Ojstro in III. polje jame Trbovlje. To sta področji, kjer geološke in rudarskotehnične razmere omogočajo uporabo ustrezne opreme tako pri logističnih rešitvah, izdelavi jamskih prog kot pri odkopavanju.

V RTH-ju so v zadnjih letih veliko pozornosti namenili iskanju tehničnih rešitev, s katerimi so zagotovili primeren nivo storilnosti ter stopnjo humanizacije in varnosti pri delu.

Poleg tega namenjajo največ pozornosti obvladovanju stroškov proizvodnje. Zato so izdelali »Program racionalizacije stroškov poslovanja«, v katerem so predvideli določene ukrepe, tako organizacijske kot tehnične narave, s katerimi bodo dosegli zastavljeni cilj, tj. realizacijo načrtovane proizvodne cene. Le-ta je bila določena ob sprejetju zakona o postopnem zapiranju RTH 3,42 €/GJ. Ta nivo cene je RTH dosegel že v letu 2002, stroškovna cena leta 2007 pa je nekoliko nižja in je 3,36 €/GJ.

Po Elaboratu o zalogah s stanjem na dan 31. 12. 2002 ima RTH evidentiranih še 53 893 000 t zalog, od tega 24 564 100 t odkopnih.

Osnova za izvajanje zapiralnih del je Zakon o postopnem zapiranju RTH in razvojnem prestrukturiranju regije (Ur. l. 61/2000) z dopolnitvami (Ur. l. 55/2003).

Prva ocena obsega vseh potrebnih zapiralnih del in potrebnih sredstev za pokritje stroškov le-teh je bila izdelana v letu 1999 z naslovom »Ocena stroškov zapiranja RTH pri proizvodnji premoga do leta 2015«. Predvideni stroški bodo tudi po oceni recenzentov tega dokumenta okvirno 300 milijonov EUR (5,5 mrd. SIT). RTH skladno z zakonom pripravlja programe za petletna obdobja, v katerih se predvidijo obseg potrebnih del in njihovi stroški. Dejansko pa je operativni dokument, po katerem se dela tudi izvajajo, Program zapiranja za tekoče leto. V grobem delijo proces zapiranja na:

- zapiranje jam
- prostorsko in ekološko sanacijo površin
- kadrovsko-socialni program

Prvi del zajema opustitev, zaprtje ali sanacijo jam in podzemnih objektov, ki jih ne bodo več potrebovali. Ta dela v celoti izvaja RTH v lastni režiji. Tehnologija, ki se pri tem uporablja, pa je izbrana na podlagi učinkov, ki jih v končni fazi želijo doseči. Na eni strani gre za objekte, ki imajo povezavo s površino ali so locirani plitko pod njo – te zapolnjujejo s t. i. črpanim zasipom, pri čemer se kot polnilni material uporablja elektrofiltrski pepel, voda pa kot transportni medij. Tako dosegajo več kot 90-odstotno zapolnitev in s tem preprečujejo nekontrolirano rušenje oziroma kasnejše vplive na površino.

Objekte, po katerih predvidevajo odvajanje in dreniranje vode, se zapolnjujejo z gramozom z uporabo pnevmatskega zasipa.

Za aktivnosti na področju prostorske in ekološke sanacije površin porabi RTH okvirno 20 % letno razpoložljivih sredstev, saj pridobivalni prostor RTH-ja obsega slabih 1 500 ha površin, od katerih precejšen del pride na urbano okolje (predvsem na področju Hrastnika). Zato je poleg same sanacije in rekultivacije degradirane površine pomemben segment in posledično tudi strošek obnova ali novogradnja cestne in druge infrastrukture. Na neki način pa je najtežji del zapiranja kadrovsko-socialni program, ki ga izvajajo na osnovi Programa kadrovskega prestrukturiranja. Zaradi postopnega zapiranja in zmanjševanja obsega poslovanja nastajajo tehnološki presežki v podjetju, ki jih v osnovi skušajo razreševati s t. i. »aktivnimi« oblikami, ki vodijo v končni fazi k prezaposlitvi oz. samozaposlitvi, in s »pasivnimi« oblikami, ki imajo končno posledico upokojitev.

Vsebina

Cilj študije je bil preučitev ocene izvedljivosti in upravičenosti nadaljevanja odkopavanja po letu 2009, ko z veljavnim zakonom prenehajo državne subvencije v prednostno dispečiranje električne energije TET in odkopavanje premoga po Zakonu o postopnem zapiranju RTH.

Vsebina študije se nanaša na:

- ovrednotenje potrjenega elaborata zalog premoga;
- ocenitev eksploatacijskih zalog v premogovem sloju Ojstro in Trbovlje;
- določitev potrebnega obsega dopolnilnih raziskav zalog premoga;
- določitev obsega pripravljalnih del s tehnološkega, terminskega in finančnega vidika;
- določitev terminskega načrta odkopavanja glede na količinsko in energijsko vrednost premoga.

Tabela 1: Zaloge premoga v jami Ojstro

Zaloge kategorija	Bilančne	Skupaj zaloge	Odkopne izgube	Odkopne zaloge
	(t)	(t)	(%)	(t)
A – dokazane				
B – raziskane	2 212 000	2 212 000	25	1 659 000
C_1 – premalo raziskane	3 215 000	3 215 000	25	2 661 250
Skupaj A+B+C_1	**5 427 000**	**5 427 000**	**25**	**4 320 250**

ZALOGE PREMOGA, OBSEG PRIPRAVLJALNIH DEL IN RAZISKAV

Ocena eksploatacijskih zalog premoga v jamah Ojstro in Trbovlje

Izhodiščni podatki

Izhodišče za določitev velikosti eksploatacijskih zalog premoga v premogovnem sloju Trbovlje – Ojstro je »Elaborat o klasifikaciji in kategorizaciji izračunanih zalog in virov premoga na pridobivalnem prostoru RTH s stanjem 31. 12. 2007«, RTH Rudnik Trbovlje-Hrastnik, d. o. o., marec 2008. Avtorica elaborata je Branka Bravec, inž. geol. Datum stanja elaborata zalog je v nadaljevanju datum preseka stanja kot izhodiščni datum nadaljnjih obravnav.

V elaboratu zalog so sistematično podani rezultati predhodnega potrjenega elaborata zalog s stanjem na dan 31. 12. 2002, kot tudi izvedene raziskave in preiskave v obdobju do datuma preseka stanja.

Jama Ojstro

Kvaliteta premoga

Tabela 2: Kvaliteta premoga v jami Ojstro

Vlaga	20,25 %
Pepel	25,95 %
S-cel	3,34 %
Kurilnost	13,39 MJ/kg
*Hobvp	26,71 MJ/kg

*kurilnost brez vlage in pepela

V jami Ojstro se zaloge premoga nahajajo v območju med profiloma $Y = 2350$ in $Y = 3100$. Večina teh zalog se je pod zadnjo odkopano etažo na k. 46 in koto 0. Višje se nahajajo zaloge premoga na skrajnem vzhodnem delu jame, kjer ga niso odkopavali zaradi dokaj majhne širine sloja in zaradi vplivov na površino.

Te zaloge premoga v jami Ojstro so dokaj zanesljive, poleg tega v sloju premoga ni večjih jalovinskih con. Pri eventualnem odkopavanju zalog premoga v jami Ojstro bo težava velika globina jamskih objektov, dolge transportne poti in dolomitni vodonosnik, ki je v zahodnem delu ležišča blizu sloja premoga. Zato bi bilo treba v primeru eksploatacije teh zalog znižati nivo vode v dolomitnem vodonosniku. Takšno znižanje nivoja vode pa bi precej podražilo proizvodnjo. Brez tega zniževanja je možno odkopati pribl. 420 000 ton kvalitetnega premoga.

Zaloge premoga na odkopnih etažiah k. 30 in k. 15

V jami Ojstro je smiselno odkopavanje zalog na še dveh etažah: k. 30 in k.15, v odkopnih poljih Lopata, Javor in Zahodno polje. Na teh dveh etažah je še 915 000 ton kvalitetnega premoga s toplotno vrednostjo 13,39 MJ/kg, mogoče celo več. Ker smo pri sedanji odkopni mehanizaciji omejeni na odkopno širino, nadkopno pridobivanje in ker je na vzhodnem delu jame treba puščati varnostni steber zaradi vplivov na površino, se lahko iz teh polj pridobi naslednjo količino premoga:

• Etaža k. 30	430 000 t
• Etaža k. 15	300 000 t
• Skupaj	730 000 t

Potrebna izdelava odpiralnih objektov in priprav

Odpiranje jame Ojstro do k. 15

Odpiranje jame Ojstro se bo izvedlo z izdelavo transportnega in dostavnega vpadnika na k. 15 z izdelavo prekopov na etažah in pomožnega črpališča. Tako bi bilo treba za odprtje obeh etaž izdelati pribl. 650 m objektov. Ocenjena vrednost izdelave teh odpiralnih objektov skupaj s pomožnim črpališčem je 2,0 mio. EUR.

Izdelava priprav na k. 30 in k. 15

Etaža k. 30

Na etaži k. 30 bi bilo treba izdelati še pribl. 750 m smernih odkopnih prog in drugih objektov. Skupna vrednost objektov priprav bi bila okoli 1 870 000 EUR. Po odkopanju etaže bo vrednost demontiranega ločnega podporja znašala še pribl. 270 000 EUR, tako bo dejanski strošek priprav 1 600 000 EUR.

Etaža k. 15

Smerna dolžina etaže na k. 15 bo znašala pribl. 270 m, tako bo treba skupno izdelati pribl. 620 m smernih odkopnih prog in drugih objektov na etaži. Skupna vrednost teh objektov bo okoli 1 550 000 EUR. Po odkopanju etaže bo vrednost demontiranega ločnega podporja še pribl. 200 000 EUR.

Potrebne raziskave

Namen raziskav v jami Ojstro je:

- ugotavljanje lege in kvalitete zalog premoga;
- ugotavljanje lege eventualnega vodonosnika pod slojem premoga in ob njem;
- ugotavljanje eventualnih tekočih mas v starih delih nad odkopom.

Raziskave pri izdelavi odpiralnih objektov

Pri izdelavi odpiralnih objektov se bo izvajalo raziskovalno vrtanje predvsem za odkrivanje morebitnih nevarnosti. Pri tem se bo izvajalo vrtanje jamskih vrtin z vzorčevanjem brez jedrovanja. Predvidoma se bo izdelovalo raziskovalne vrtine s 6 stojišč. Pri tem se iz vsakega stojišča zavrta po pribl. 4 vrtine, in sicer:

- 1 vrtino v smeri napredovanja;
- 2 poševno navzdol v smeri napredovanja;
- 1 v smeri proti starim delom.

Po potrebi se bo naredilo še dodatne vrtine. Predvidoma se z enega stojišča izdela okoli 150 m vrtin.

Raziskave pri izdelavi priprav

Pri izdelavi priprav se bo izvajalo vrtanje jamskih vrtin za odkrivanje nevarnosti in ugotavljanje lege sloja premoga. Vrtanje se bo izvajalo s stojišč na vsakih 50 m.

Etaža k. 30

Na etaži k. 30 se bo izdelovalo raziskovalne vrtine z 10 stojišč. Pri tem se z vsakega stojišča zavrta po 6 vrtin, in sicer:

- 1 vrtino v smeri napredovanja;
- 1 poševno navzdol v smeri napredovanja;
- 1 horizontalno v smeri sever ali jug za raziskavo sloja;
- 2 poševno navzdol za raziskave etaže k. 15;
- 1 vertikalno navzgor za ugotavljanje eventualnih tekočih mas v starih delih.

Po potrebi se bo naredilo še dodatne vrtine. Predvidoma se z enega stojišča izdela okoli 230 m vrtin.

Etaža k. 15

Na etaži k. 15 se bo izdelovalo raziskovalne vrtine z 8 stojišč. Pri tem se z vsakega stojišča zavrta po 4 vrtine, in sicer:

- 1 vrtino v smeri napredovanja;
- 1 poševno navzdol v smeri napredovanja;
- 1 horizontalno v smeri sever ali jug za raziskavo sloja;
- 1 vertikalno navzgor za ugotavljanje eventualnih tekočih mas v starih delih.

Po potrebi se bo naredilo še dodatne vrtine. Predvidoma se z enega stojišča

izdela okoli 150 m vrtin.

Z obeh etaž se tako zavrta 3 500 m vrtin.

Jama Trbovlje - III. polje

Zaloge premoga

Tabela 3: Zaloge premoga v jami Trbovlje – III. polje

Zaloge, kategorija	Bilančne	Odkopne izgube	Odkopne zaloge
	(t)	(%)	(t)
Rjavi premog			
A – dokazane	677 000	20	542 000
B – raziskane	405 000	20	324 000
C_1 – premalo raziskane	238 000	20	190 000
Skupaj A+B+C_1	**1 320 000**	**20**	**1 056 000**
Rjavi kotlovni premog			
A – dokazane	2 273 000	20	1 818 000
B – raziskane	2 475 000	20	1 980 000
C_1 – premalo raziskane	1 327 000	20	1 062 000
Skupaj A+B+C_1	**6 075 000**	**20**	**4 860 000**

Tabela 4: Zaloge premoga na posameznih etažah v III. polju

Etaža, kota	Zaloge premoga na etaži (m^3)
k. 300	350 000
k. 290	305 000
k. 280	267 000
k. 265	297 000
k. 250	88 000
k. 230	340 000

V III. polju so zaloge premoga med površino in zveznim obzorjem na približni k. 230. Te zaloge so že odprte in so tudi dokaj lahko dostopne. Zato jih v RTH-ju tudi nameravajo odkopati. Glavnina zalog v III. polju je med profiloma VII. in XXIII. Neodkopan del sloja premoga je debel do 30 m. Mislimo, da je iz III. polja možno pridobiti še pribl. 1,1 mio. ton premoga brez gradnje dodatnih odpiralnih objektov. V III. polju težavo pri odkopavanju povzročajo jalovinski vložki v sloju premoga.

Te zaloge so po stanju 31. 12. 2007. Od takrat je bil večji del zalog na etaži k. 300 že odkopan, tako da je sedaj s te etaže možno pridobiti še okoli 180 000 t premoga. Ob upoštevanju odkopnih izgub in jalovinskih con v sloju premoga mislimo, da lahko iz tega polja pridobimo še okoli 1,1 mio. ton premoga.

Potrebna izdelava odpiralnih objektov in priprav

Odpiranje III. polja jame Trbovlje

III. polje je že v celoti odprto, zato v njem ne bo treba več izdelovati odpiralnih objektov. Izdelati bo treba le še etažne objekte.

Obseg priprav

Predvidevamo, da bo treba izdelati še 4600 m etažnih objektov v III. polju jame Trbovlje. Z izdelavo teh objektov bodo izdelali priprave za okoli 920 000 t proizvodnje premoga, kar je 5 m etažnih objektov na 1000 t proizvodnje. Objekti na etaži k. 300 so že izdelani.

Potrebne raziskave

Namen raziskav v III. polju jame Trbovlje je:

- ugotavljanje lege in kvalitete zalog premoga na etaži, na kateri se že izdelujejo odpiralni objekti;
- raziskave za ugotavljanje lege in kvalitete premoga na eni etaži nižje;
- raziskave starih del in hribin nad odkopom.

Raziskave pri izdelavi priprav

Pri izdelavi priprav se bo izvajalo vrtanje jamskih vrtin s posameznih stojišč v smernih odkopnih progah. Predvidoma bodo stojišča v smernih progah na vsakih 50 m. Po potrebi se na mestih večjih montanogeoloških sprememb poveča gostota raziskav. V III. polju bo predvidoma še okoli 70 stojišč. Z vsakega stojišča se bo zavrtalo predvidoma po 6 vrtin, in sicer:

- 2 vrtini v smeri napredovanja;
- 1 horizontalno proti drugi smerni odkopni progi;
- 2 poševno navzdol za raziskavo ene etaže nižje;
- 1 vrtina navzgor za raziskavo nadkopnega dela sloja premoga in za raziskavo starih del.

Po potrebi se bo naredilo še dodatne vrtine. Predvidoma se z enega stojišča izdela 200 m vrtin, kar pomeni, da bo treba v III. polju izdelati še okoli 14 000 m vrtin. Vse te vrtine se izvrta na izpih brez jedrovanja. Vzorce iz vrtin bo treba analizirati za ugotavljanje kurilnosti in vsebnosti pepela in žvepla.

Kot je razvidno, bo treba v III. polju jame Trbovlje izdelati še veliko etažnih objektov in tudi veliko raziskovalnih vrtin, ker se geološke razmere hitro spreminjajo. Obseg teh del je možno zmanjšati, če bi nekoliko povečali višino etaž in opustili odkopavanje na manj produktivnih odkopih. S tem bi pocenili proizvodnjo in nekoliko zmanjšali pridobljene količine premoga.

Fiksni stroški proizvodnje iz jame Trbovlje bodo veliko manjši v primerjavi z jamo Ojstro, ker ni treba črpati veli-

kih količin vode, intenzivnost jamskih pritiskov je nižja, krajše so tudi transportne poti.

Jama Trbovlje – polje Plesko

Zaloge premoga

Tabela 5: Zaloge premoga v jami Trbovlje – Plesko polje

Zaloge, kategorija	Bilančne			Odkopne izgube	Odkopne zaloge
	Plesko	Podaljšek Plesko	Skupaj		
	(t)	(t)	(t)	(%)	(t)
Rjavi premog					
A – dokazane					
B – raziskane	313 000	875 000	1 188 000	20	950 000
C_1 – premalo raziskane		3 208 000	3 208 000	20	2 567 000
Skupaj A+B+C_1	**313 000**	**4 083 000**	**4 396 000**	**20**	**3 517 000**
Rjavi premog					
A – dokazane	123 000		123 000	20	98 000
B – raziskane	1 644 000		1 644 000	20	1 315 000
C_1 – premalo raziskane		563 000	563 000	20	451 000
Skupaj A+B+C_1	**1 767 000**	**563 000**	**2 330 000**	**20**	**1 864 000**

Po elaboratu o zalogah premoga so največje zaloge premoga v III. polju in v polju Plesko. Tam je podobna količina zalog kot v III. polju, vendar skoraj ni zalog A-kategorije. V polju Plesko se nahaja rjavi in rjavi kotlovni premog. Zaloge premoga so med profiloma VII. in XVI. Raziskanost tega polja je slabša, zato je tudi veliko teh zalog uvrščenih v C_1-kategorijo. Večina zalog premoga je nad nivojem savskega oziroma zveznega obzorja, to je nad k. 230. Če bi se odločili za odkopavanje teh zalog premoga, bi bilo treba izvesti raziskave in izdelati nekaj odpiralnih objektov.

Potrebna izdelava odpiralnih objektov in priprav

Odpiranje polja Plesko jame Trbovlje

Polje Plesko bi odprli z navezavo odpiralnih objektov na sedanje, po katerih je šel transport premoga z gumitransporterji iz jame Ojstro, in z navezavo na objekte Polaj in AB-polja. Ker ni potrebe, da bi odkopali celotne zaloge premoga v polju Plesko, se bo izdelalo odpiralne objekte samo do najlažje do-

stopnih delov ležišča, in sicer med kotama 210 in 260. Tako bi lahko odprli in odkopali okoli 1,0 mio. ton premoga. Predvidevamo, da bi bilo treba za odpiranje tega dela polja Plesko izdelati okoli 900 m odpiralnih objektov. Ocenjena vrednost izdelave le-teh objektov skupaj s pomožnim črpališčem je 2,0 mio. EUR.

Obseg priprav

Predvidevamo, da bo treba izdelati 4,0 m objektov priprav na 1000 t proizvodnje. Glede na to bo treba za odkopavanje 1,0 mio. ton premoga v III. polju izdelati še 4 000 m objektov.

Potrebne raziskave

Namen raziskav v III. polju jame Trbovlje je:

- ugotavljanje lege in kvalitete zalog premoga na etaži, na kateri se že izdelujejo odpiralni objekti;
- raziskave za ugotavljanje lege in kvalitete premoga na eni etaži nižje;
- raziskave starih del in hribin nad odkopom.

Raziskave pri izdelavi odpiralnih objektov

Pred odpiranjem tega polja je treba narediti raziskave, ki se izvedejo z raziskovalnimi vrtinami, ki se izdelajo iz obstoječih objektov v dolomitu v AB-polju. Raziskave se izvede s pahljačami vrtin, usmerjenimi proti jugu v dolžini po 50. Vrtine se izdela na vsakih 50 m smerne dolžine. Obseg raziskav za odpiralna dela:

- 12 stojišč, z vsakega stojišča se zavrta po 4 vrtine dolžine 50 m. Z vsakega stojišča se zavrta eno horizontalno vrtino, eno vrtino poševno navzdol in dve vrtini poševno navzgor. Skupno se z 12 stojišč izdela pribl. 2 400 m vrtin.

Raziskave pri izdelavi priprav

Pri izdelavi priprav se bo izvajalo vrtanje jamskih vrtin s posameznih stojišč v smernih odkopnih progah. Predvidoma bodo stojišča v smernih progah na vsakih 25 m. Po potrebi se na mestih večjih geotehničnih sprememb poveča gostota raziskav.

Za proizvodnjo 1,0 mio. ton bo treba iz objektov priprav zavrtati okoli 9 000 m vrtin s pribl. 45 stojišč. Z vsakega stojišča se zavrta po 4 vrtine, in sicer:

- 1 vrtino v smeri napredovanja;
- 1 horizontalno proti drugi smerni odkopni progi;
- 2 poševni navzdol za raziskavo ene etaže nižje;
- 1 vrtino navzgor za raziskavo nadkopnega dela sloja premoga in za raziskavo starih del.

Po potrebi se bo naredilo še dodatne vrtine. Predvidoma se z enega stojišča izdela 200 m vrtin. Vse te vrtine se zavrta na izpih brez jedrovanja. Vzorce iz vrtin bo treba analizirati za ugotavljanje kurilnosti in vsebnosti pepela in žvepla.

Potrebna pripravljalna dela, strošek del in raziskav

V naslednji tabeli je prikazan obseg odpiralnih objektov in raziskav po posameznih odkopnih poljih:

li z upoštevanjem proizvodnih stroškov še lastno ceno proizvodnje premoga. Privzeli smo predvideno proizvodnjo vsakega odkopnega polja, stroške odpiranja in raziskav ter upoštevali de-

Tabela 6: Obseg in strošek priprave odpiralnih objektov

Polje	Zaloge po elaboratu	Predvidena proizvodnja	Količina odpiralnih objektov	Etažni objekti	Raziskovalno vrtanje
	(t)	(t)	(m)	(m)	(m)
Jama Ojstro	3 320 000	730 000	650	1 370	900 + 3500
III. polje	1 197 000 + 4 860 000	1 100 000	-	4 600	14 000
Polje Plesko	3 517 000 + 1 864 000	1 000 000	900	4 000	2 400 + 9 000
Stroški odpiranja in raziskav - jama Ojstro			**2 000 000,00 EUR**	**220 000,00 EUR***	
Stroški odpiranja in raziskav - jama Trbovlje – III. polje				**700 000,00 EUR***	
Stroški odpiranja in raziskav - jama Trbovlje - Polje Plesko			**2 000 000,00 EUR**	**572 000,00 EUR***	

Stroške odpiranja in raziskav smo ovrednotili po posameznih odkopnih poljih še s ceno v EUR/GJ, tako da smo dobi-

jansko kurilnost izkopanega premoga v višini 11 GJ/t.

* Strošek izdelave vrtine je ocenjen na 50 EUR/m

Tabela 7: Izračun stroškov odpiralnih in raziskovalnih del

Polje	Proizvodnja	Kurilnost	Strošek odpiranja in raziskav	Strošek odpiranja in raziskav
	(t)	(GJ/t)	(EUR)	(EUR/GJ)
Jama Ojstro	730 000	11	2 000 000,00	0,249
III. polje	1 100 000	11	700 000,00	0,0579
Polje Plesko	1 000 000	11	2 572 000,00	0,234

LASTNA CENA PREMOGA IZ POSAMEZNIH ODKOPNIH POLJ

Lastna cena premoga po poljih bo naslednja:

Tabela 8: Proizvodna cena premoga po odkopnih poljih

Jama oziroma odkopno polje	**Proizvodna cena**
III. polje – jama Trbovlje	3,14 + 0,06 = 3,2 EUR/GJ
Polje Plesko – jama Trbovlje	3,14 + 0,18 = 3,32 EUR/GJ
Jama Ojstro	3,14 + 0,19 = 3,33 EUR/GJ

Osnova za določitev proizvodne cene po posameznih odkopnih poljih je bila proizvodna cena iz III. polja jame Trbovlje (odkop št. 1 iz konca leta 2007 in iz 1. polovice 2008). Do te lastne cene smo prišli tako, da smo privzeli, da bodo podobni pogoji odkopavanja v polju Plesko in v III. polju jame Trbovlje. Obseg raziskav in izdelave odpiralnih objektov pa smo privzeli iz poglavij 4.1.1, 4.1.2 in 4.1.3 predmetne študije. Tako smo ugotovili, da bodo stroški odpiranja in odkopavanja v polju Plesko za 0,18 EUR/GJ višji kot v III. polju. Razlika je v glavnem le v tem, da je v polju Plesko treba še izdelati odpiralne objekte, medtem ko so v III. polju že izdelani. Pri izračunu lastne cene iz jame Ojstro pa smo upoštevali izračun cene, ki je bil izdelan v januarju 2008 in primerja stroške odkopavanja v jami Ojstro in v III. polju jame Trbovlje. Po tej primerjavi stroškov odkopavanja bi bili stroški proizvodnje iz jame Ojstro za 0,19 EUR/GJ višji od stroškov proizvodnje iz III. polja jame Trbovlje.

PRIHODKI Z IZKOPAVANJEM ODKOPNIH POLJ PO IZRAČUNU LASTNE CENE PREMOGA

Načrtovano proizvodnjo iz vseh treh odkopnih polj smo ovrednotili še z izračunom celotne količine nakopanega premoga in izračunom povprečne cene premoga po izkopu 2 830 000 t.

Tabela 9: Prihodki pri izkopavanju odkopnih polj

Polje	Proizvodnja	Cena	Cena	Prihodki
	(t)	(EUR/t)	(EUR/GJ)	EUR
III. polje – jama Trbovlje	1 100 000	35,20	3,2	38 720 000,00
Polje Plesko – jama Trbovlje	1 000 000	36,52	3,32	36 520 000,00
Jama Ojstro	730 000	36,63	3,33	26 739 900,00
SKUPAJ	2 830 000	36,04	3,28	101 979 900,00

Skupni prihodki z izkopavanjem premoga iz odkopnih polj III. polje, polje Plesko – jama Trbovlje in jama Ojstro po izračunu lastne cene premoga bodo 101 979 000,00 EUR, povprečni strošek izkopanega premoga bo 36,04 EUR/t in skupna povprečna cena eksploatacije premoga 3,28 EUR/GJ.

Terminski plan odkopavanja po poljih

Terminski plan odkopavanja smo izdelali za vsa tri odkopna polja v obdobju od leta 2009 do 2015.

Tabela 10: Terminski plan izkopavanja po odkopnih poljih

Aktivnost/leto	2009	2010	2011	2012	2013	2014	2015
III. polje							
- priprave + odkopavanje							
- priprave							
Jama Ojstro							
- odpiranje + priprave							
- priprave + odkopavanje							
Polje Plesko							
- raziskave							
- odpiranje							
- priprave							
- priprave + odkopavanje							
Proizvodnja iz III. polja	200 000		400 000	350 000			
Proizvodnja iz jame Ojstro	250 000	450 000					
Proizvodnja iz Polja Plesko					300 000	250 000	200 000
Skupaj	450 000	450 000	400 000	350 000	300 000	250 000	200 000

V letih 2009 in 2010 je načrtovana proizvodnja v višini 450 000 t, po tem obdobju pa bo postopno upadala do 200 000 t v letu 2015. To je načrtovano skladno s kadrovsko-socialnim programom zapiranja RTH in z drugimi razpoložljivimi viri, ki jih ima družba RTH.

Izračun lastne cene premoga po letih v obdobju od leta 2009 do vključno leta 2015

V spodnji tabeli je prikazana lastna cena premoga pri odkopavanju po posameznih letih glede na dinamiko izkopavanja odkopnih polj.

Predvidena proizvodnja premoga v letih od 2009 do vključno 2015 bi bila skupaj 2 400 000 t. Lastna cena letne proizvodnje premoga bo med 3,2 in 3,33 EUR/GJ oziroma med 35,2 in 36,6 EUR/t.

Povzetek

RTH, Rudnik Trbovlje-Hrastnik bo do vključno leta 2009 dobavljal premog Termoelektrarni Trbovlje (TET) v predvideni količini 0,6 mio. ton na leto. Glede na stanje energetike v Evropi in na svetu smo priče stalnemu porastu cen energentov, tudi premoga. Po podatkih International Coal Report (september 2008) se bodo cene enrgetskega premoga v letu 2009 po kvartalih gibale v razponu med 4,32 do 4,36 EUR/GJ (Steam Coal Marker). V takih razmerah bomo v Sloveniji, s ciljem uravnotežene oskrbe z električno energijo (1/3 termoenergija, 1/3 vodna energija in 1/3 nuklearna energija – kar je tudi usmeritev EU 27), prisiljeni izkoristiti vse razpoložljive zaloge premoga.

Zato je smiselno ponovno računati na preostale zaloge v odkopnih poljih RTH in na osnovi konkurenčnih izhodišč predstaviti možnosti za njihovo izkoriščanje v povezavi s TET.

Tabela 11: Izračun cene proizvodnje premoga po letih

Aktivnost/leto	2009	2010	2011	2012	2013	2014	2015
Proizvodnja (t)	450 000	450 000	400 000	350 000	300 000	250 000	200 000
Cena (EUR/GJ)	3,27	3,33	3,2	3,2	3,32	3,32	3,32
Cena (EUR/t)	35,99	36,63	35,2	35,2	36,52	36,52	36,52
Prihodek (mio. EUR)	16,197	16,483	14,080	12,320	10,956	9,130	7,304

Poprečna cena proizvodnje premoga iz RTH bi bila v obdobju od leta 2009 do 2015 3,28 EUR/GJ ob izkopu 2 400 000 t premoga. Lastna cena premogovnika je danes povsem konkurenčna.

Glede na dejstvo, da se RTH v skladu z Zakonom o postopnem zapiranju Rudnika Trbovlje-Hrastnik in razvojnem prestrukturiranju regije (Uradni list RS, št. 61/2000) zapira, bi bilo smiselno poiskati pravno rešitev glede na zakonodajo v EU 27, ki bi omogočila nadaljnje izkopavanje odkopnih polj v jami Trbovlje (III. polje, polje Plesko) in v jami Ojstro do leta 2015 ter možnosti za ponovno pridobivanje premoga v jami Hrastnik, kjer RTH razpolaga še s približno 20 milijoni odkopnih zalog. Preučevanje odkopavanja v jami Hrastnik je predmet nadaljevanja te študije v II. in III. fazi.

Predlagamo, da se v skladu z zakonodajo EU 27 preuči možnost podaljšanja odkopavanja do leta 2015 in kasneje do izkopa preostalih zalog premoga v jami Hrastnik.

V prvem delu je smiselno že v fazi zapiranja RTH, ki je predvidena do leta 2015, načrtovati sanacijsko odkopavanje v obdobju od leta 2009 do vključno 2011. Tako bi dodatno odkopali še 1 300 000 t premoga in bi se znatno izboljšali pogoji poslovanja RTH ter kadrovsko-socialni del prestrukturiranja družbe.

Po letu 2011 pa je smiselno ustanoviti novo družbo, ki bi skupaj s Termoelektrarno Trbovlje dolgoročno načrtovala proizvodnjo premoga in električne energije na energetski lokaciji v Trbovljah. Ta bo za Slovenijo nepogrešljivi člen v verigi proizvodnje električne energije.

Viri

Coal Industry Across Europe 2008, Bruselj 2008.

E. Dervarič s sodelavci (2008): Upravičenost odkopavanja preostalih zalog premoga v jamah Ojstro in Trbovlje po letu 2009 in zaprtega dela jame Hrastnik – I. faza, *Študija NTF*, Ljubljana.

Elaborat o klasifikaciji in kategorizaciji izračunanih zalog in virov rjavega premoga na pridobivalnem prostoru RTH s stanjem 31. 12. 2007.

International Coal Report, London, September 2008.

Nacionalni energetski program Republike Slovenije. DZ RS, 2004.

Odgovori na pripombe študije »Upravičenost odkopavanja preostalih zalog premoga v jamah Ojstro in Trbovlje po letu 2009 in zaprtega dela jame Hrastnik« - I. faza, Trbovlje, oktober 2008.

Poročilo o poslovanju RTH, Rudnik Trbovlje Hrastnik za leto 2007, Trbovlje, 2008.

Razvojni program RTH, Rudnik Trbovlje-Hrastnik, d. o. o., do leta 2016, Trbovlje, marec 2006.

World Energy Outlook 2008.

Zakon o postopnem zapiranju Rudnika Trbovlje-Hrastnik in razvojnem prestrukturiranju regije. Uradni list RS, št. 61/2000.

Vpliv zračenja visoko produktivnega odkopa na zračilno območje Premogovnika Velenje

Influence of air conditioning at high productive mining field in ventilation area of the Velenje Coal Mine

Boris Salobir[1, 2, *]

[1]Univerza v Ljubljani, Naravoslovnotehniška fakulteta, Oddelek za geotehnologijo in rudarstvo, Aškerčeva cesta 12, SI-1000 Ljubljana, Slovenija
[2]PROTOS Inženirski biro, d. o. o., Cesta III, št. 26, SI-3320 Velenje, Slovenija

*Korespondenčni avtor. E-mail: protos@siol.net

Received: January 13, 2009 **Accepted:** February 10, 2009

Izvleček: Pri vključevanju novih odkopnih polj v sistem prezračevanja jame Premogovnika Velenje moramo dobro poznati obstoječi sistem in osnovne zakonitosti jamskega zračenja, posebej če vključujemo odkope z izjemno veliko proizvodnjo. Visoko produktivni odkop, kakor tak odkop imenujemo, se v dolžini, večji od dvesto metrov, uporablja prvič. Zaradi povečane dolžine odkopnega čela je treba uvesti dodatne varnostne ukrepe in poostren nadzor klimatskih razmer v vseh fazah gradnje in obratovanja odkopa in jih preverjati tudi za nadaljnje odkope. Pri projektiranju visoko produktivnih odkopov se izboljšajo razmere pri delu in zračenje v smislu zmanjšanja hitrosti zraka, povečanja svetlega preseka prog, kontinuirnega opazovanja emisij nevarnih plinov in zmanjšanja nevarnosti za požare.

Abstract: When new faces are incorporated into the ventilation system of the Coal mine Velenje, good knowledge of the existing ventilation and legalization will be welcome. Highly production face has been used for the first time in such, over than two hundred meters, lenght. As faces become longer, extra safety measures must be introduced and better control of the climatic conditions in all places of the face finalization. Also, such faces have to be continnually checked for future operations.

Planning highly productive excavation, the working conditions, especially in the area of ventilation, has been improved. Working conditions have became better, that is, lover air velocity, profile conditions, continual observation of emissions of dangerous gases and less danger of fire.
The calculations show that it is possible to simultaneously incorporate two such highly productive excavations so that they would not affect the ventilation system of a coalmine.

Ključne besede: rudarstvo, zračenje, klimatizacija, programiranje zračenja
Key words: mining, ventilation, air conditioning, network simulation program

UVOD

Z jamskim zračenjem zagotavljamo rudarjem zdravo ozračje, varnost pred eksplozijo in pojavi škodljivega prahu ter primerne delovne razmere med napredovanjem jamskih del ob upoštevanju odkopnih metod in fizičnih naporov delavcev pri delu. Za ohranjanje konkurenčnosti in zviševanje produktivnosti v Premogovniku Velenje največ pozornosti namenjajo izboljšavam na področju tehnologije odkopavanja in vpeljavi visoko produktivnih odkopov (VPO). Zračenje visoko produktivnega odkopa bi lahko bila težava zaradi svoje dolžine in drugih zračilnih parametrov, ki na to vplivajo, zato je treba vse parametre temeljito preveriti in simulirati način zračenja in vpliv vključevanja v zračilni sistem jame.

PREZRAČEVANJE PRIPRAVSKIH DELOVIŠČ

Priprava visoko produktivnega odkopa se prične z izdelavo pripravljalnih jamskih prog ali pripravskih delovišč, ki se po svoji zasnovi ne odmikajo od ustaljenega sistema izdelave za druge odkope. Pri izračunu potrebne količine zraka, ki jo moramo dovajati k ventilatorju na pripravskih deloviščih, upoštevamo izgube, ki nastanejo pri prehodu zraka skozi zračilne cevi. V izračunu upoštevamo 5-odstotno izgubo zraka na dolžini 100 m zračilnih cevi. To pomeni, da končni vrednosti količine zraka na delovišču prištejemo tisto, ki je posledica izgub in je odvisna od dolžine zračilnih cevi. S tem dobimo začetno količino zraka, ki jo moramo dovajati k ventilatorju.

Potrebno depresijo zraka izračunamo po naslednji enačbi:

$$h_{sk} = \sum h_{l_i} + \sum h_{kri} = \sum \frac{R_{100} \cdot l_i \cdot Q_i^2}{100} + \sum n \cdot \xi \cdot \left(\frac{Q_i}{F_i} \right) \cdot \frac{\rho}{2} \quad (1)$$

kjer pomeni:

h_{sk}/Pa	skupna depresija
$\sum h_{l_i}$ /Pa	vsota kompresij uporov v 100-metrskih odsekih ravnih zračilnih cevi
$\sum h_{kri}$ /Pa	vsota kompresij uporov krivin v posameznih 100-metrskih odsekih zračilnih cevi
R_{100}/(N s^2/m^8)	upornost 100-metrskega odseka ravnih zračnih cevi
l_i/m	100-metrski odsek ravnih zračnih cevi
Q_i/(m^3/s)	potrebna količina zraka v posameznem 100-metrskem odseku zračilnih cevi
n	število krivin v posameznem 100-metrskem odseku zračilnih cevi
ζ	koeficient upornosti krivin
F_i/m^2	prerez zračilnih cevi

Za prezračevanje pripravskih delovišč visoko produktivnega odkopa uporabljamo dva tipa aksialnih ventilatorjev pri različnih naklonih lopatic in načinih vezave. Zračenje teh odsekov nima posebnosti, ki bi se razlikovale od dosedanjih izkušenj v Premogovniku Velenje. Za prezračevanje zadošča pretok zraka V = 280 m^3/min in depresija h_{sk} = 2988 Pa na ventilator.

Prezračevanje med odkopavanjem

Med visoko produktivnim odkopavanjem vzpostavimo pretočno zračenje. Pri gradnji visoko produktivnega odkopa, posebej pri njegovi veliki dolžini, ki je lahko tudi do 210 m (plošča G2/b), se zaradi povečanja odkopnih dolžin pojavijo težave s prezračevanjem, ki se kažejo v naraščanju količin škodljivih in nevarnih snovi, v slabšanju rudarsko-geoloških razmer za delo in v negativnih vplivih na trajnost in obstojnost pretočnih prerezov zračilnih poti. Težava lahko nastane, kadar bi se odkopne višine povečale nad višino horizontalne koncentracije.

Zato je treba preverjati ekshalacijo škodljivih plinov CH_4 in CO, ekshalacijo premogovega prahu, možnosti ogrevov in požarov, konvergence podpornih elementov, velikost profilov in zasedenost zračilnih poti ter hitrost zraka in upornost zračilnih poti. Potrebno količino zraka na odkopu izračunamo na podlagi:

- povprečnega koeficienta izdatnosti

plina $q_{pov}(CH_4)$ iz razrušenega premoga in
- povprečne količine dnevno razrušenega premoga P_{pov}.

Ti dve količini določimo na podlagi podatkov, dobljenih na najbližjem, v podobnih razmerah ležečem odkopu. Upoštevati moramo večje ekshalacije plinov zaradi napredka na večji dolžini odkopa. Za izračun povprečne potrebne količine zraka uporabimo obrazec:

$$Q_{pov} = \frac{P_{pov} \cdot q_{pov} \cdot 100}{A_k \cdot 1440} \qquad (2)$$

kjer pomenijo:

$Q_{pov}/(m^3/s)$	povprečna potrebna količina zraka na odkopu
$P_{pov}/(t/d)$	povprečna količina razrušenega premoga na dan ($P_{pov} = S \cdot b \cdot \gamma$)
S/m^2	prerez odkopa
b/m	dnevni napredek odkopa
$\gamma/(t/m^3)$	specifična masa premoga
$q_{pov}/(m^3/t)$	povprečni koeficient izdatnosti plina za CH_4
$A_k/\%$	dovoljena koncentracija plina iz nahajališča za CH_4
1440	faktor pretvorbe ur dneva v minute

Izračunana količina zraka, ki je Q_{pov} = 1498 m^3/min, je orientacijska, saj na izdatnost plinov lahko vplivajo tudi drugi faktorji, kot sta hitrost napredovanja delovišča in višina rušenja premoga. Zato dopuščamo možnost zračenja tudi z drugačno količino zraka od izračunane, vendar mora spremenjena količina zraka ustrezati dovoljeni koncentraciji CH_4 in CO_2, ki je največ 1,5 % na odkopu, ter dovoljeni hitrosti zraka preko odkopa, ki ne sme presegati v_{max} = 5 m/s, po zadnjih spremembah tudi 8 m/s.

KONTROLNI IZRAČUN ZRAČENJA

Izračun kontrolnih parametrov zračenja izdelamo za tri stanja:
- stanje pred vključitvijo visoko produktivnega odkopa (VPO);
- stanje po vključitvi VPO in pred razširitvijo na polno dolžino in kapaciteto proizvodnje;
- stanje po vključitvi na polno dolžino in pri polni kapaciteti proizvodnje.

Po vključitvi VPO se bodo spremenili vsi parametri zračenja v jami: ekvivalentna odprtina, izračunana upornost jame, skupna depresija zračilnega kroga, obratovalna točka ventilatorja, ker je vpliv samo na en ventilator, količina zraka ter njegova hitrost. Ekvivalentna odprtina jame se zmanjša, prav tako koeficient regulacije.

Ob razširitvi VPO na polno dolžino odkopa (210 m) se pokažejo prave razsežnosti, torej povečanje vseh parametrov v primerjavi s tistimi, izračunanimi takoj po vključitvi odkopa.

V primeru kontinuirne proizvodnje se lahko, ob potrebi po še večji proizvodnji, en odkop izključi iz ventilacijskega sistema, drugi pa vključi, kar pomeni, da je obremenitev glavnega ventilatorja praktično enaka, če upoštevamo sistemsko odkopavanje odkopnega polja.

Ekshalacije plinov CH_4 in CO_2

Ekshalacije plinov CH_4 in CO_2 upoštevamo primerjalno glede na najbližji podoben odkop in tudi v smislu podaljšanja odkopa kot tudi razrušenja premoga iz stropnega dela odkopa. Pričakujemo lahko občasne povečane ekshalacije jamskih plinov.

Ekshalacija premogovega prahu

Dviganje premogovega prahu je vezano na hitrost zračilnega toka preko delovišča in velikost največjih delcev, ki jih ta tok še lahko dvigne oziroma nosi s seboj. Ker je ob dvigu premogovega prahu izpostavljena velika dolžina odkopa, lahko prah povzroča precejšnje neprijetnosti in kopičenje na turbulentnih mestih, zato je treba hitrost zraka manjšati in naj ne preseže $v_{max} = 4{,}6$ m/s.

Možnost ogrevov in požarov

Pri izdelavi visoko produktivnega odkopa je potrebna previdnost zaradi možnosti nastanka eksogenih požarov. Pri delu je treba dosledno upoštevati delovnovarstveni načrt za preprečevanje požarov. Na območju odkopa ni velike verjetnosti za endogene požare, saj je količina zraka in hitrost na delovišču dovolj velika, da preprečuje nastanek le-teh.

Konvergenca podpornih elementov

Zaradi povečanih pritiskov in deformacij v zgornjem delu podpornih elementov, ki so posledica velike dolžine visoko produktivnega odkopnega čela, nastajajo premiki oziroma konvergence v podpornih elementih podzemnih objektov. Te lahko povzročijo veliko zasedenost profila, kar povzroči spremembo zračilnih parametrov.

Velikost profilov in zasedenost zračilnih poti

Velikost profilov podzemnih prostorov in zasedenost zračilnih poti – tokovodnikov vplivata na zadovoljivost prezračevanja pri zagotavljanju ustreznih delovnih razmer. Za reguliranje ustrezne klime in delovnih razmer sta ta dva parametra ključnega pomena. Pri gradnji visoko produktivnega odkopa uporabimo povečan profil s svetlim prerezom $S = 17{,}26$ m^2.

Pri predpostavljeni zasedenosti profila do 35 % pomeni, da je omogočen pretok zraka skozi zračilne veje s svetlim premerom: $S = 17{,}26 \cdot 0{,}65 = 11{,}2$ m^2.

V dosedanji praksi v premogovniku so se uporabljali profili jamskih prog, ki so ob predpostavljeni zasedenosti omogočali svetli profil pribl. 8 m^2.

Hitrost zraka in upornost

Hitrost zraka in upornost zračilne veje sta parametra, ki pokažeta ustreznost izračunane ali izmerjene vrednosti za določen zračilni sistem jamskih prostorov. Hitrost zraka je določena s pravilnikom in sme biti na odkopu do 5 m/s, izjemoma 8 m/s. Upornost zraka se pri pretoku povečuje zaradi ovir v tokovodniku in zasedenosti profila, kar povzročajo vgrajene naprave ter ljudje in zožitve jamskega prostora. Prevelika hitrost povzroča prekomerno dvigovanje premogovega prahu, prepih na delovišču in znižanje efektivne temperature na delovišču pod dovoljeno vrednost. Zaradi povečanja profila in zmanjšanja zasedenosti se pretok zraka na VPO zmanjša. Iz tega izhaja, da zmanjšanje pretoka izboljšuje zračenje na visoko produktivnem odkopu. Hitrost na VPO je v primerjavi s hitrostjo pri drugih odkopih višja za pribl. 0,3 m/s. Kadar se zmanjša pretok, se posledično zmanjša tudi hitrost zraka. Njeno zmanjšanje izboljšuje zračenje in delovne razmere na visoko produktivnem odkopu.

Upornost R na visoko produktivnem odkopu se je v primerjavi z upornostjo na drugih odkopih povečala za pribl. od od 0,41 N s^2/m^8 do 0,60 N s^2/m^8.

VKLJUČEVANJE V SISTEM ZRAČENJA

Pri vključevanju VPO v sistem zračenja v Premogovniku Velenje je treba zagotoviti zadostno količino in pretok zraka za vse zaposlene rudarje ter preprečiti nevarne pojave. Pri vključevanju novega odkopnega polja v kompleksen sistem prezračevanja jame se za izračun glavnih kazalcev jamske klime uporabi barometrska metoda, ki se simulira z računalniškim programom ZRAK. S programom ZRAK se ugotovi upornostni faktor (R, R_{100}) zračilnega tokovodnika in določi skupni padec tlaka zračilne veje. Program omogoča simulacijo različnih stanj in izračune zračilnih parametrov v skladu s I. in II. Kirchoffovim zakonom, z Atkinsonovo enačbo in s Hardy-Crossovo iteracijsko metodo.

Podatki o vozliščih in zračilnih vejah

Pri podatkih o zračilnih vejah ločimo obvezne in neobvezne podatke zračilnih vej. Obvezni podatki zračilnih vej so: oznaka zračilne veje, dolžina vozlišča od točke do točke, kota vozlišča, presek proge, hitrost zraka in pretok zraka.

VPLIV VISOKO PRODUKTIVNEGA ODKOPA NA CELOTNO OBMOČJE

Za vpliv visoko produktivnega odkopa na celotno zračilno območje so na karakterističnem grafu glavnega ventilatorja Šoštanj pomembna tri stanja:

Stanje pred vključitvijo visoko produktivnega odkopa

Odčitani podatki so: h = 3659,0967 Pa, Q = 253,1 m^3/s .
Odčitana obratovalna točka 1: naklon lopatic $\acute{\alpha}$ = 0^o

Odčitek je izveden tako, da se na abscisi odčita količina zraka [m^3/min], na ordinati pa depresija [Pa]. Kjer se liniji sekata, izberemo najbližjo krivuljo delovanja ventilatorja pod karakterističnim naklonom lopatic.

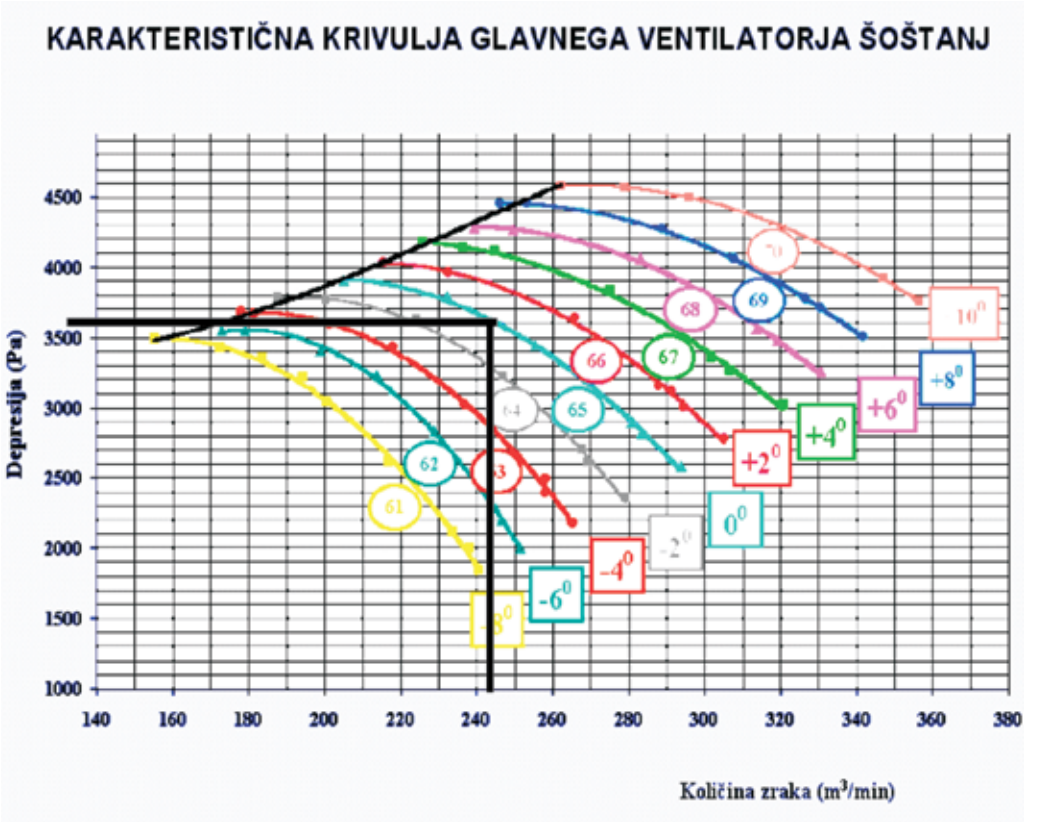

Slika 1: Karakteristična krivulja glavnega ventilatorja Šoštanj in njegova obratovalna točka v času pred vključitvijo visoko produktivnega odkopa

Stanje po vključitvi in pred doseganjem polne proizvodnje odkopa

Odčitani podatki so: h = 3171,43040 Pa, Q = 241,68 m^3/s
Odčitana obratovalna točka 2: naklon lopatic $\acute{\alpha}$ = –2°

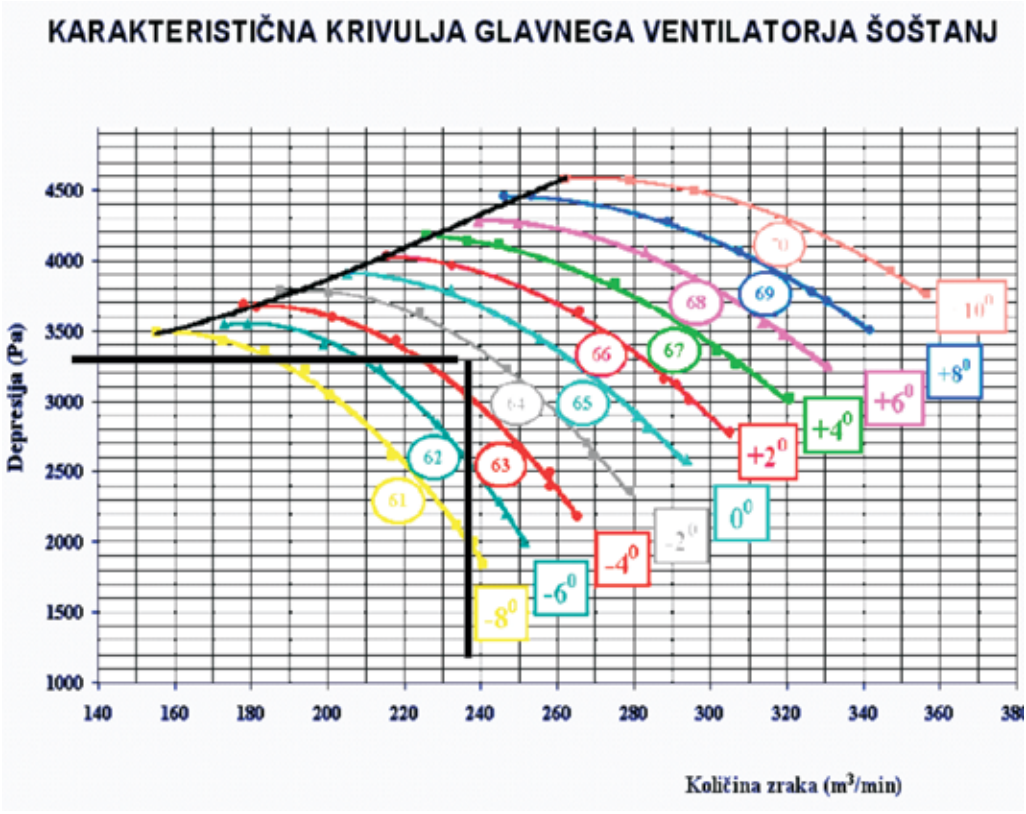

Slika 2: Karakteristična krivulja glavnega ventilatorja Šoštanj in njegova obratovalna točka v času po vključitvi odkopa in pred razširitvijo na celotno dolžino

Stanje ob doseganju polne proizvodnje odkopa

Odčitani podatki so: h = 3776,82133 Pa, Q = 247,08 m^3/s
Odčitana obratovalna točka 3: naklon lopatic $\acute{\alpha}$ = +2^o

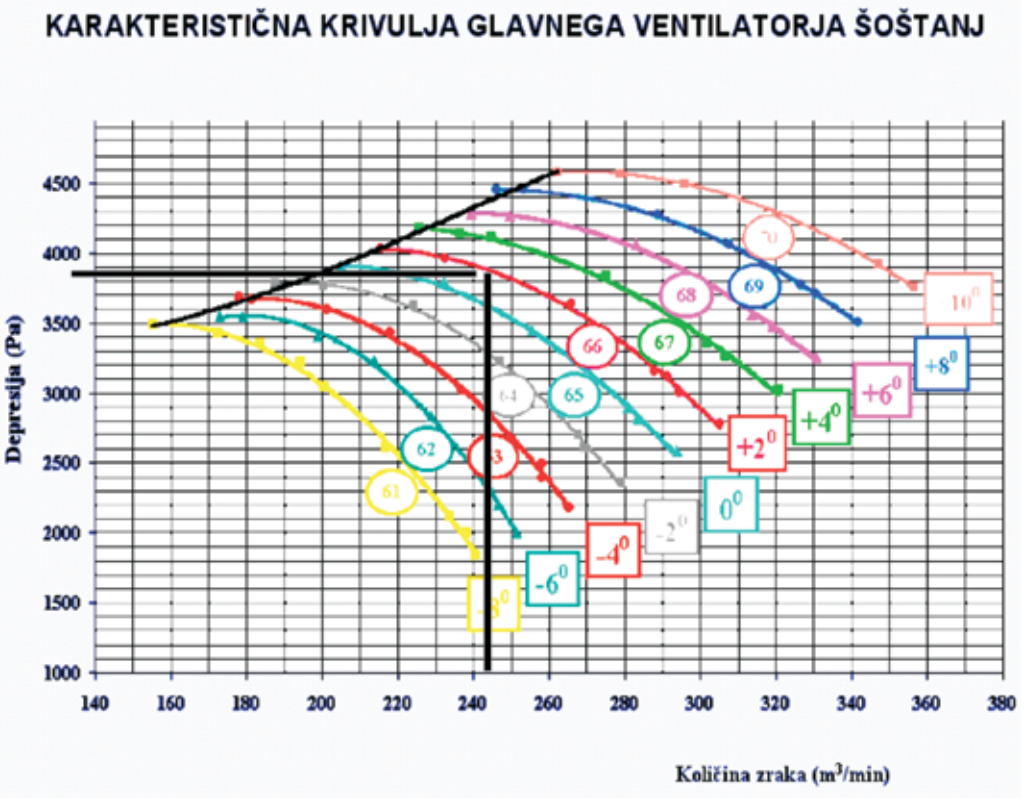

Slika 3: Karakteristična krivulja glavnega ventilatorja Šoštanj in obratovalna točka v času doseganja polne proizvodnje

Stanje se je v tem primeru spremenilo tako, da sta se povečala depresija in pretok zraka. Če se pri odkopavanju VPO ne poveča profil vstopne in izstopne proge ter profil odkopa, se pogoji prezračevanja odkopnega polja poslabšajo zaradi potrebne večje količine zraka glede na večje ekshalacije plinov, kar je treba upoštevati.

Glede na spremenjeno stanje pri razširitvi se je obratovalna točka spremenila na takšen način, da se je naklon lopatic spreminjal od $\acute{\alpha}$ = –2^o do +2^o. Pri tem so ostale še rezerve za spremembo naklona lopatic do $\acute{\alpha}$ = +8^o. To pomeni, da je na danem obsegu zračenja in zmogljivosti ventilatorja zadovoljivo velika rezerva, ki omogoča na danem

območju obratovanje še enega takšnega odkopa enakih razsežnosti.

POVZETEK

Pri projektiranju visoko produktivnih odkopov so se v smislu zračenja in zaradi upoštevanja predvidenih sprememb zračilnih parametrov teoretično izboljšali pogoji za delo.

Zmanjšala se je hitrost zraka, povečan je svetli presek tokovodnikov, izvaja se kontinuirno opazovanje emisij nevarnih plinov, v večji meri je preprečeno dvigovanje prahu in zmanjšale so se nevarnosti za požare. Zaradi povečanja varnosti in velike ekshalacije metana pa so izjemoma dovoljene večje hitrosti zraka, kar v praksi slabša pogoje za delo rudarjev.

Vpliv visoko produktivnega odkopa je zaenkrat vezan samo ne en ventilator, to je tisti v zračilni postaji v Šoštanju, zato moramo morebitno vključevanje več odkopov locirati tako, da bo vsak vplival na samo en ventilator, glede na sistem prezračevanja velenjske jame.

Visoko produktivne odkope je možno vključevati v velenjsko jamo ob upoštevanju v članku naštetih pogojev. Kljub prvotni hipotezi o poslabšanju zračilnih razmer zaradi dolžine odkopa in večje ekshalacije plinov ter možnosti ogrevov izračuni kažejo, da je mogoče vključiti hkrati dva takšna visoko produktivna odkopa, ne da bi bistveno vplivala na zračilni sistem premogovnika, lahko pa tudi več, odvisno od sistema razpeljave zraka.

VIRI

AHČAN, R. (1985): Racionalno vodenje zraka v pogojih eksploatacije v Rudniku lignita Velenje. *Rudarsko metalurški zbornik*; Vol. 32, No. 2–3, pp. 289–299.

ORLIČNIK, R. (2008): Zračenje visoko produktivnega odkopa. Diplomsko delo. Mentor doc. dr. Boris Salobir, Univerza v Ljubljani, Naravoslovnotehniška fakulteta, Oddelek za geotehnologijo in rudarstvo, Ljubljana.

SALOBIR, B. (2004): Optimiranje delovanja glavnega ventilatorja v odvisnosti od izmerjenih parametrov, program raziskovalne naloge. Premogovnik Velenje, d. d., in Protos inženirski biro, d. o. o., Velenje.

SALOBIR B., ŽIBERT, Z., ZALOŽNIK, Z., BIŠČIĆ, A. (2005): Optimiranje delovanja glavnega ventilatorja v odvisnosti od izmerjenih parametrov, raziskovalna študija, št. PRO-PV-RS-1/2004. Premogovnik Velenje, d. d., in Protos inženirski biro, d. o. o., Velenje.

TEPLY, E.(1971): Proračun regulacije rudničkih vjetrenih mreža. *Rudarsko metalurški zbornik*; Vol. 1971, No. 1, pp. 11–29.

ŽIBERT, Z.(2006): Določitev zračilnih parametrov po barometrski metodi, magistrsko delo. Mentor doc. dr. Boris Salobir, Univerza v Ljubljani, Naravoslovnotehniška fakulteta, Oddelek za geotehnologijo in rudarstvo, Ljubljana.

Svetovna konferenca podiplomskih študentov v Brnu na Češkem

PhD World Foundry Conference, Brno, Czech Republic

Stanislav Kores

[1]Univerza v Ljubljani, Naravoslovnotehniška fakulteta, Oddelek za materiale in metalurgijo, Aškerčeva cesta 12, SI-1000 Ljubljana, Slovenija

E-mail: stanislav.kores@ntf.uni-lj.si

Kot vsako leto smo se tudi letos odzvali vabilu na konferenco podiplomskih študentov v Brnu na Češkem, ki je potekala od 1. do 4. junija 2009. Letošnja konferenca je bila toliko bolj pomembna, saj je bila prva svetovna konferenca podiplomskih študentov, ki je potekala v okviru WTF (World Technical Forum). Na konferenci je bilo predstavljenih 7 znanstvenih prispevkov predavateljev iz Naravoslovnotehniške fakultete Univerze v Ljubljani, Oddelka za materiale in metalurgijo, in sicer, 2 na svetovnem tehniškem forumu in 5 prispevkov na svetovni konferenci podiplomskih študentov. S konference se vračamo zelo ponosni, saj smo na njej prejeli dve nagradi za najboljša prispevka. Prvo nagrado za najboljši prispevek na podiplomski konferenci je prejel as. Mitja Petrič z znanstvenim prispevkom »Ability of feeding for Al-alloys dependant on grain refinement and modification«, drugo nagrado pa as. Maja Vončina s prispevkom »Transition phases in Al-Cu alloy – temperatures and activation energies«. Takšna svetovna priznanja nam dajejo motivacijo in veselje za naše raziskovanje in nadaljnje delo.

Short paper

Slika 1. Slovenska delegacija s predsednikom WTF (iz leve proti desni): Grega Klančnik, Jožef Medved, Maja Vončina, Milan Horaček, Stanislav Kores, Mitja Petrič, Primož Mrvar in Sebastjan Kastelic

Slika 2. Prva nagrada za as. Mitja Petriča in druga nagrada za as. Majo Vončina

Author`s Index, Vol. 56, No. 2

Belashev B. Z.	belashev@krc.karelia.ru
Dervarič Evgen	evgen.dervaric@ntf.uni-lj.si
Dozet Stevo	stevo.dozet@geo-zs.si
Fajfar Peter	peter.fajfar@ntf.uni-lj.si
Falkus Jan	
Klančnik Grega	grega.klancnik@ntf.uni-lj.si
Klančnik Urška	
Klenovšek Bojan	bojan.klenovsek@rth.si
Knap Matjaž	matjaz.knap@ntf.uni-lj.si
Kores Stanislav	stanislav.kores@ntf.uni-lj.si
Kortnik Jože	joze.kortnik@ntf.uni-lj.si
Lamut Jakob	jakob.lamut@ntf.uni-lj.si
Malina Jadranka	malina@simet.hr
Medved Jožef	jozef.medved@ntf.uni-lj.si
Mrvar Primož	primoz.mrvar@ntf.uni-lj.si
Olugbenga A. Okunlola	o.okunlola@mail.ui.edu.ng
Rađenović Ankica	radenova@simet.hr
Richardson E. Okoroafor	
Rozman Alojz	
Salobir Boris	protos@siol.net
Skamnitskaya L. S.	
Štrkalj Anita	strkalj@simet.hr
Večko Pirtovšek Tatjana	
Vukelič Željko	zeljko.vukelic@ntf.uni-lj.si

INSTRUCTIONS TO AUTHORS

RMZ-MATERIALS & GEOENVIRONMENT (RMZ- Materiali in geookolje) is a periodical publication with four issues per year (established 1952 and renamed to RMZ-M&G in 1998). The main topics of contents are Mining and Geotechnology, Metallurgy and Materials, Geology and Geoenvironment.
RMZ-M&G publishes original Scientific articles, Review papers, Technical and Expert contributions (also as short papers or letters) **in English**. In addition, evaluations of other publications (books, monographs,...), short letters and comments are welcome. A short summary of the contents in Slovene will be included at the end of each paper. It can be included by the author(s) or will be provided by the referee or the Editorial Office.
**** Additional information and remarks for Slovenian authors:***
English version with extended "Povzetek", and additional roles (in Template for Slovenian authors) ***can*** *be written. Only exceptionally the articles in the Slovenian language with summary in English will be published. The contributions in English will be considered with priority over those in the Slovenian language in the review process.*

Authorship and originality of the contributions. Authors are responsible for originality of presented data, ideas and conclusions as well as for correct citation of data adopted from other sources. The publication in RMZ-M&G obligate authors that the article will not be published anywhere else in the same form.

Specification of Contributions

Optimal number of pages of full papers is 7 to 15, longer articles should be discussed with Editor, but 20 pages is limit.
Scientific papers represent unpublished results of original research.
Review papers summarize previously published scientific, research and/or expertise articles on the new scientific level and can contain also other cited sources, which are not mainly result of author(s).
Technical and Expert papers are the result of technological research achievements, application research results and information about achievements in practice and industry.
Short papers (Letters) are the contributions that contain mostly very new short reports of advanced investigation. They should be approximately 2 pages long but should not exceed 4 pages.
Evaluations or critics contain author's opinion on new published books, monographs, textbooks, exhibitions...(up to 2 pages, figure of cover page is expected).

In memoriam (up to 2 pages, a photo is expected).
Professional remarks (Comments) cannot exceed 1 page, and only professional disagreements can be discussed. Normally the source author(s) reply the remarks in the same issue.

Supervision and review of manuscripts. All manuscripts will be supervised. The referees evaluate manuscripts and can ask authors to change particular segments, and propose to the Editor the acceptability of submitted articles. Authors can suggest the referee but Editor has a right to choose another. **The name of the referee remains anonymous.** The technical corrections will be done too and authors can be asked to correct missing items. The final decision whether the manuscript will be published is made by the Editor in Chief.

The Form of the Manuscript

The manuscript should be submitted as a complete hard copy including figures and tables. The figures should also be enclosed separately, both charts and photos in the original version. In addition, all material should also be provided in electronic form on a diskette or a CD. The necessary information can conveniently also be delivered by E-mail.

Composition of manuscript is defined in the attached Template

The original file of Template is temporarily available on E-mail addresses:
peter.fajfar@ntf.uni-lj.si,
barbara.bohar@ntf.uni-lj.si

References - can be arranged in two ways:
- first possibility: alphabetic arrangement of first authors - in text: (Borgne, 1955),
or
- second possibility: [1] numerated in the same order as cited in the text: example[1]

Format of papers in journals:

Le Borgne, E. (1955): Susceptibilite magnetic anomale du sol superficiel. *Annales de Geophysique*, 11, pp. 399-419.

Format of books:

Roberts, J. L. (1989): Geological structures, *MacMillan*, *London*, 250 p.

Text on the hard print copy can be prepared with any text-processor. The electronic version on the diskette, CD or E-mail transfer should be in MS Word or ASCII format.
Captions of figures and tables should be enclosed separately. **Figures (graphs and photos)** and tables should be original and sent separately in addition to text. They can be prepared on paper or computer designed (MSExcel, Corel, Acad).
Format. Electronic figures are recommended to be in CDR, Al, EPS, TIF or JPG formats. Resolution of bitmap graphics (TIF, JPG) should be at least 300 dpi. Text in vector graphics (CDR, Al, EPS) must be in MSWord Times typography or converted in curves.
Color prints. Authors will be charged for color prints of figures and photos.
Labeling of the additionally provided material for the manuscript should be very clear and must contain at least the lead author's name, address, the beginning of the title and the date of delivery of the manuscript. In case of an E-mail transfer the exact message with above asked data must accompany the attachment with the file containing the manuscript.
Information about RMZ-M&G:
Editor in Chief prof. dr. Peter Fajfar (tel. ++386 1 4250-316) or
Secretary Barbara Bohar Bobnar, un. dipl. ing. geol. (++386 1 4704-630),
Aškerčeva 12, Ljubljana, Slovenia

or at E-mail addresses:
peter.fajfar@ntf.uni-lj.si,
barbara.bohar@ntf.uni-lj.si

Sending of manuscripts. Manuscripts can be sent by mail to the **Editorial Office** address:

- RMZ-Materials & Geoenvironment
  Aškerčeva 12,
  1001 Ljubljana, Slovenia

or delivered to:

- **Reception** of the Faculty of Natural Science and Engineering (for RMZ-M&G)
  Aškerčeva 12,
  1001 Ljubljana, Slovenia
- E-mail - addresses of Editor and Secretary
- You can also contact them on their phone numbers.

These instructions are valid from September 2003

TEMPLATE

The title of the manuscript should be written in bold letters (Times New Roman, 14, Center)

Naslov članka (Times New Roman, 14, Center)

NAME SURNAME[1], …. , & NAME SURNAME[X] (TIMES NEW ROMAN, 12, CENTER)

[x] University of ..., Faculty of ..., Address…, Country ... (Times New Roman, 11, Center)

*Corresponding author. E-mail: ... (Times New Roman, 11, Center)

THE LENGTH OF FULL PAPER SHOULD NOT EXCEED TWENTY (20, INCLUDING FIGURES AND TABLES) PAGES (OPTIMAL 7 TO 15), SHORT PAPER FOUR (4) AND OTHER TWO (2) WITHOUT TEXT FLOWING BY GRAPHICS AND TABLES.

Abstract (Times New Roman, Normal, 11): The text of the abstract is placed here. The abstract should be concise and should present the aim of the work, essential results and conclusion. It should be typed in font size 11, single-spaced. Except for the first line, the text should be indented from the left margin by 10 mm. The length should not exceed fifteen (15) lines (10 are recommended).

Izvleček (TNR, N, 11): Kratek izvleček namena članka ter ključnih rezultatov in ugotovitev. Razen prve vrstice naj bo tekst zamaknjen z levega roba za 10 mm. Dolžina naj ne presega petnajst (15) vrstic (10 je priporočeno).

Key words: a list of up to 5 key words (3 to 5) that will be useful for indexing or searching. Use the same styling as for abstract.

Ključne besede: seznam največ 5 ključnih besed (3–5) za pomoč pri indeksiranju ali iskanju. Uporabite enako obliko kot za izvleček.

Introduction (Times New Roman, Bold, 12)

Two lines below the keywords begin the introduction. Use Times New Roman, font size 12, Justify alignment.
There are two (2) admissible methods of citing references in text:

1. by stating the first author and the year of publication of the reference in the parenthesis at the appropriate place in the text and arranging the reference list in the alphabetic order of first authors; e.g.:
   "Detailed information about geohistorical development of this zone can be found in: Antonijević (1957), Grubić (1962), ..."
   "… the method was described previously (Hoefs, 1996)"
2. by consecutive Arabic numerals in square brackets, superscripted at the appropriate place in the text and arranging the reference list at the end of the text in the like manner; e.g.:
   "... while the portal was made in Zope[3] environment."

Materials and methods (Times New Roman, Bold, 12)

This section describes the available data and procedure of work and therefore provides enough information to allow the interpretation of the results, obtained by the used methods.

Results and discussion (Times New Roman, Bold, 12)

Tables, figures, pictures, and schemes should be incorporated in the text at the appropriate place and should fit on one page. Break larger schemes and tables into smaller parts to prevent extending over more than one page.

Conclusions (Times New Roman, Bold, 12)

This paragraph summarizes the results and draws conclusions.

Acknowledgements (Times New Roman, Bold, 12, Center - optional)
This work was supported by the ****.

References (Times New Roman, Bold, 12)

In regard to the method used in the text, the styling, punctuation and capitalization should conform to the following:

FIRST OPTION - in alphabetical order

Casati, P., Jadoul, F., Nicora, A., Marinelli, M., Fantini-Sestini, N. & Fois, E. (1981): Geologia della Valle del'Anisici e dei gruppi M. Popera - Tre Cime di Lavaredo (Dolomiti Orientali). *Riv. Ital. Paleont.*; Vol. 87, No. 3, pp. 391–400, Milano.

Folk, R. L. (1959): Practical petrographic classification of limestones. *Amer. Ass. Petrol. Geol. Bull.;* Vol. 43, No. 1, pp. 1–38, Tulsa.

SECOND OPTION - in numerical order

[1] Trček, B. (2001): *Solute transport monitoring in the unsaturated zone of the karst aquifer by natural tracers.* Ph. D. Thesis. Ljubljana: University of Ljubljana 2001; 125 p.

[2] Higashitani, K., Iseri, H., Okuhara, K., Hatade, S. (1995): Magnetic Effects on Zeta Potential and Diffusivity of Nonmagnetic Particles. *Journal of Colloid and Interface Science 172*, pp. 383–388.

Citing the Internet site:

CASREACT-Chemical reactions database [online]. Chemical Abstracts Service, 2000, updated 2.2.2000 [cited 3.2.2000]. Accessible on Internet: http://www.cas.org/CASFILES/casreact.html.

The length of full paper should not exceed twenty (20, including figures and tables) pages (optimal 7 to 15), short paper four (4) and other two (2) without text flowing by graphics and tables.

Text in Slovene (title, abstract and key words) can be written by the author(s) or will be provided by the referee or by the Editorial Board.

PREDLOGA ZA SLOVENSKE ČLANKE

Naslov članka (Times New Roman, 14, Center)

The title of the manuscript should be written in bold letters (Times New Roman, 14, Center)

Ime Priimek[1], …, Ime Priimek[X] (Times New Roman, 12, Center)

[X]Univerza…, Fakulteta…, Naslov…, Država… (Times New Roman, 11, Center)

*Korespondenčni avtor. E-mail: ... (Times New Roman, 11, Center)

Izvleček (TNR, N, 11): Kratek izvleček namena članka ter ključnih rezultatov in ugotovitev. Razen prve vrstice naj bo tekst zamaknjen z levega roba za 10 mm. Dolžina naj ne presega petnajst (15) vrstic (10 je priporočeno).

Abstract (Times New Roman, Normal, 11): The text of the abstract is placed here. The abstract should be concise and should present the aim of the work, essential results and conclusion. It should be typed in font size 11, single-spaced. Except for the first line, the text should be indented from the left margin by 10 mm. The length should not exceed fifteen (15) lines (10 are recommended).

Ključne besede: seznam največ 5 ključnih besed (3–5) za pomoč pri indeksiranju ali iskanju. Uporabite enako obliko kot za izvleček.
Key words: a list of up to 5 key words (3 to 5) that will be useful for indexing or searching. Use the same styling as for abstract.

Uvod (Times New Roman, Bold, 12)

Dve vrstici pod ključnimi besedami se začne Uvod. Uporabite pisavo TNR, velikost črk 12, z obojestransko poravnavo. Naslovi slik in tabel (vključno z besedilom v slikah) morajo biti v slovenskem jeziku.

Slika (Tabela) X. Pripadajoče besedilo k sliki (tabeli)

Obstajata dve sprejemljivi metodi navajanja referenc:

1. z navedbo prvega avtorja in letnice objave reference v oklepaju na ustreznem mestu v tekstu in z ureditvijo seznama referenc po abecednem zaporedju prvih avtorjev; npr.:

"Detailed information about geohistorical development of this zone can be found in: Antonijević (1957), Grubić (1962), ..."

"… the method was described previously (Hoefs, 1996)"

ali

2. z zaporednimi arabskimi številkami v oglatih oklepajih na ustreznem mestu v tekstu in z ureditvijo seznama referenc v številčnem zaporedju navajanja; npr.;

"... while the portal was made in Zope[3] environment."

Materiali in metode (Times New Roman, Bold, 12)

Ta del opisuje razpoložljive podatke, metode in način dela ter omogoča zadostno količino informacij, da lahko z opisanimi metodami delo ponovimo.

Rezultati in razprava (Times New Roman, Bold, 12)

Tabele, sheme in slike je treba vnesti (z ukazom Insert, ne Paste) v tekst na ustreznem mestu. Večje sheme in tabele je po treba ločiti na manjše dele, da ne presegajo ene strani.

Sklepi (Times New Roman, Bold, 12)

Povzetek rezultatov in sklepi.

Zahvale (Times New Roman, Bold, 12, Center - opcija)

Izvedbo tega dela je omogočilo ……

Viri (Times New Roman, Bold, 12)

Glede na uporabljeno metodo citiranja referenc v tekstu upoštevajte eno od naslednjih oblik:

PRVA MOŽNOST (priporočena) – v abecednem zaporedju

Casati, P., Jadoul, F., Nicora, A., Marinelli, M., Fantini-Sestini, N. & Fois, E. (1981): Geologia della Valle del'Anisici e dei gruppi M. Popera – Tre Cime di Lavaredo (Dolomiti Orientali). *Riv. Ital. Paleont.*; Vol. 87, No. 3, pp. 391–400, Milano.

Folk, R. L. (1959): Practical petrographic classification of limestones. *Amer. Ass. Petrol. Geol. Bull.;* Vol. 43, No. 1, pp. 1–38, Tulsa.

DRUGA MOŽNOST - v numeričnem zaporedju

[1] Trček, B. (2001): *Solute transport monitoring in the unsaturated zone of the karst aquifer by natural tracers.* Ph. D. Thesis. Ljubljana: University of Ljubljana 2001; 125 p.

[2] Higashitani, K., Iseri, H., Okuhara, K., Hatade, S. (1995): Magnetic Effects on Zeta Potential and Diffusivity of Nonmagnetic Particles. *Journal of Colloid and Interface Science 172*, pp. 383–388.

Citiranje Internetne strani:

CASREACT-Chemical reactions database [online]. Chemical Abstracts Service, 2000, obnovljeno 2.2.2000 [citirano 3.2.2000]. Dostopno na svetovnem spletu: http://www.cas.org/CASFILES/casreact.html.

Dolžina izvirnega znanstvenega članka ne sme presegati dvajset (20, vključno s slikami in tabelami), kratkega članka štiri (4) in ostalih prispevkov dve (2) strani.

Znanstveni in pregledni članki se objavijo samo v angleškem jeziku.

Skupina HSE

PREMOGOVNIK VELENJE

PREMOGOVNIK VELENJE

je pomemben in zanesljiv člen
v oskrbi Slovenije
z električno energijo.

Zavedamo se odgovornosti do
lastnikov, zaposlenih in okolja.

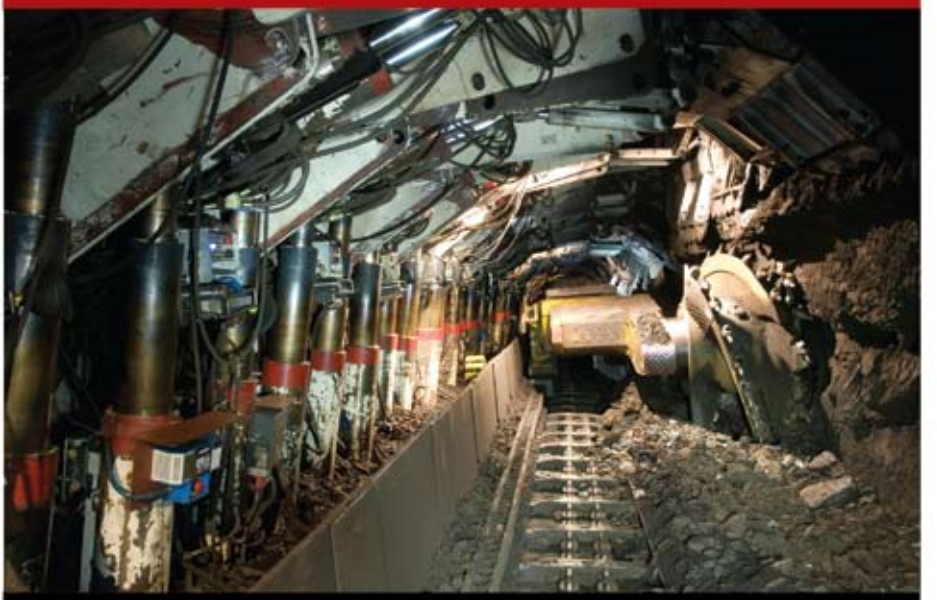

ČUT ZA PRIHODNOST


RTH

Če se premakne, boste izvedeli prvi

Leica Geosystems rešitve za opazovanje premikov

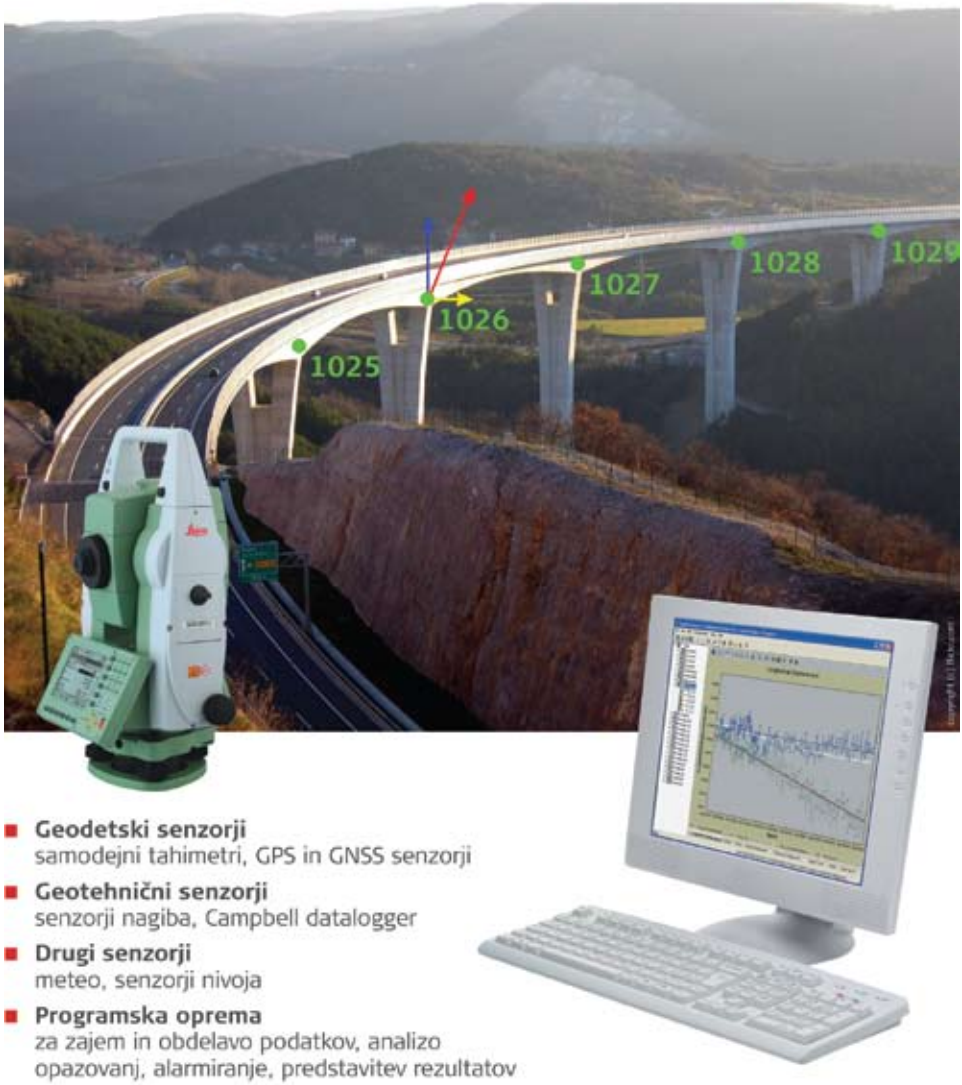

- **Geodetski senzorji**
  samodejni tahimetri, GPS in GNSS senzorji
- **Geotehnični senzorji**
  senzorji nagiba, Campbell datalogger
- **Drugi senzorji**
  meteo, senzorji nivoja
- **Programska oprema**
  za zajem in obdelavo podatkov, analizo opazovanj, alarmiranje, predstavitev rezultatov

geo servis

Geoservis, d.o.o.
Litijska cesta 45, 1000 Ljubljana
t. (01) 586 38 30, i. www.geoservis.si

Authorized Leica Geosystems Distributor

- when it has to be **right**

Leica Geosystems

Univerza v Ljubljani, Naravoslovnotehniška fakulteta

Oddelek za materiale in metalurgijo

Aškerčeva cesta 12
1000 Ljubljana

Telefon: (01) 470 46 08,
E-pošta: omm@ntf.uni-lj.si

internetni naslov:
http://www.ntf.uni-lj.si/